OXYGEN ABSORPTION in a COUNTERCURRENT PULSED BUBBLE COLUMN

By

MICHAEL F. TESSARO, B. Eng.

A Thesis

Submitted to the Faculty of Graduate Studies

in Partial Fulfilment of the Requirements

for the Degree

Master of Engineering

1973

MASTER OF ENGINEERING(1973) McMaster University
(Chemical Engineering) Hamilton, Ontario.

TITLE: Oxygen Transfer in a Countercurrent, Pulsed Bubble Column.

AUTHOR: Michael F. Tessaro, B.Eng.

SUPERVISOR: Dr. M.H.I. Baird

NUMBER OF PAGES: vii, 115

SCOPE: A 5.0 cm. diameter column was used for gas absorption. The column contained internal baffling and was operated in a countercurrent mode. Oxygen comprised the gaseous phase and tap water the liquid phase. The column was operated both with and without pulsations. The injection and exhaustion of compressed air to the system provided the pulsation mechanism. The mixing as well as the mass transfer characteristics were examined. A set of experiments independent of the mass transfer work was carried out in order to study mixing in the column. A refluxing mechanism is uncovered in the mixing experiments. Values for the axial dispersion coefficient, volumetric mass transfer coefficient and reflux ratio are reported over the range of the operating parameters.

Acknowledgments

The author is indebted to his supervisor, Dr. M.H.I. Baird, for his help and guidance throughout this work. Financial assistance received from McMaster University is gratefully acknowledged.

Also appreciation is expressed to members of the staff, graduate students and technical staff who had occasion to extend helpful suggestions and advice to the author throughout the course of this work.

Table of Contents

		Page
1.	Introduction	1
2.	Previous Work	5
3.	Mass Transfer Apparatus	6
4.	Tracer Work	17
5.	Mass Transfer Modelling	21
6.	Tracer Modelling	25
7.	Mass Transfer Results/Discussion	31
8.	Tracer Results/Discussion	54
9.	Conclusions/Recommendations	67
	References	69
	Appendices	72
	Plates	89
	Tabulated Results	102
	Nomenclature	114

Figures

		Page
1.	Two film theory	2
2.	Zero gas phase resistance	2
3.	Simplified diagram of apparatus	7
4.	Column outlet configuration	11
5.	Column sampling arrangement	11
6.	Column dimensions	12
7.	Central rod support fixture	13
8.	Baffle plate	13
9.	Pulsation generating system	15
10.	Tracer flow	18
11.	Tracer distributor	18
12.	Mass transfer in a differential increment	22
13.	Mass transfer with reflux	22
14.	Tracer mixing with reflux	27
15.	Strongly refluxed condition	30
16.	Dispersion coefficient vs. pulsation velocity	32
17.	Dispersion coefficient vs. superficial liquid velocity	34
18. . 20.	Absorption rate vs. pulsation velocity	35-37
21.	Absorption rate correlation	39
22.	Integral curve for NTU	41
23.	Lagrangian interpolation fit to oxygen concentration profiles	42
24. . 26.	Number of transfer units vs. superficial liquid velocity	44-46
27.	Effect of backmixing	47
28. . 30.	Efficiency vs. pulsation velocity	49-51

31.	Axial dispersion coefficient vs. superficial gas velocity	55
32. . 33.	Tracer concentration profiles	57-58
34. . 35.	Reflux patterns	59-60
36.	Reflux ratio vs. pulsation velocity	61
37.	Dispersion number vs. velocity ratio	63
38.	Oxygen flow meter calibration curve	74
39.	Dichromate concentration vs. absorbance	77

Plates

			Page
Plate N..... Equipment			9
	Pulsation Velocity(cm./sec.)	Superficial Gas Velocity(cm./sec.)	
Plate A	27.0	0.388	90
Plate B	27.0	0.650	91
Plate C	27.0	1.165	92
Plate D	39.0	0.388	93
Plate E	39.0	0.650	94
Plate G	39.0	1.165	95
Plate H	49.0	0.388	96
Plate I	49.0	0.650	97
Plate J	49.0	1.165	98
Plate K	0.0	0.388	99
Plate L	0.0	0.650	100
Plate M	0.0	1.165	101

1. Introduction

The application of external agitation to improve mass transfer between two phases is a well established and widely applied principle. Stirred tanks have been used for this both with liquid-liquid systems and gas-liquid systems. External agitation in columns however, has mainly been confined to liquid-liquid systems [17]. The present investigation concerns an agitated column using a gas-liquid system to carry out mass transfer. A brief survey of mass transfer theory as it concerns this investigation is presented below.

Throughout the years various models have been postulated trying to provide insight into the fundamental mechanisms of mass transfer. The penetration theory of Higbie [20] and the modification of this theory involving surface renewal by Danckwerts [9,10,11] both present k_L as being proportional to the square root of the diffusivity. A relatively simple model proposed by Whitman [38] is the two-film theory which has proven to be a useful and widely applied model. As pointed out by Levenspiel [23] , although the surface renewal theories are probably more correct from a physical point of view than the two-film theory and experimental fact would appear to support this contention, the fact remains that the two approaches give essentially the same results in design work.

In figure 1.1 the case of both liquid phase and gas phase resistance to mass transfer is depicted in the fashion of the two-film model. However in gas-liquid operations involving sparingly soluble or pure gases the rate of mass transfer is very likely to be controlled by the liquid film resistance. Figure 1.2 depicts this situation.

In this study water saturated oxygen made up the gaseous phase and all the resistance could safely be

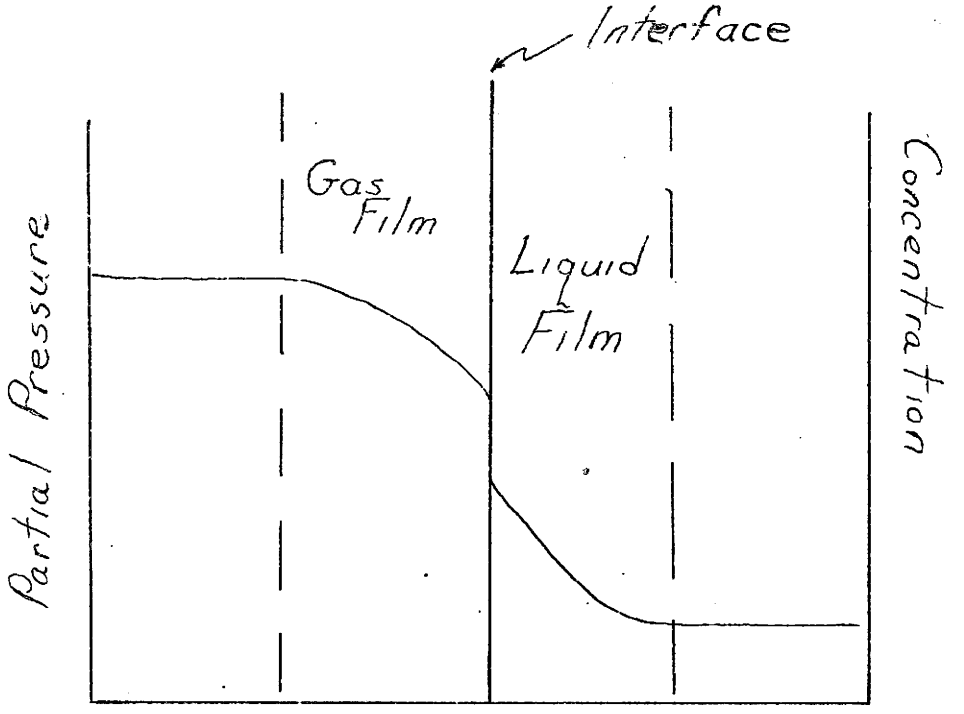

Figure 1.1

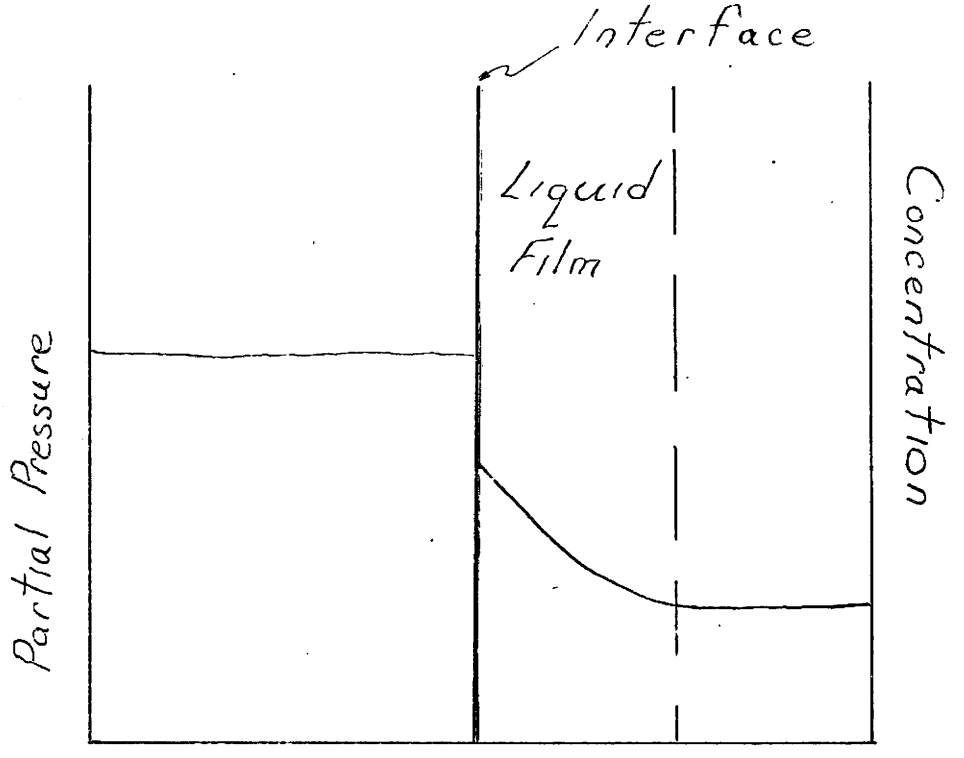

Figure 1.2

assumed to reside in the liquid (tap water) phase. From the two-film theory the rate of mass transfer per unit volume of dispersion is given by:

$$N = k_L a \, (c^* - c)$$

Obviously an increase in k_L , the film mass transfer coefficient and/or an increase in the specific interfacial area, a , will from the above expression increase the rate of mass transfer. The film mass transfer coefficient and the specific interfacial area are subject to conditions in the particular dispersed system at hand. It is thus convenient [6,14,32] to consider the product, $k_L a$,the volumetric mass transfer coefficient when assessing the performance of a gas-liquid contactor. The injection of energy (agitation) will cause the specific interfacial area to improve markedly in a fluid dispersion- the bubble size decreases and the holdup increases. The main type of agitated contactor used industrially for gas-liquid systems is the stirred tank which has been thoroughly investigated [5] . In this particular work the film mass transfer coefficient could also be expected to improve with the excellent shearing action provided by the baffles during pulsed operation of the column (see plate J) . Since a stirred tank is approximately equal to one equilibrium stage at best, it would seem reasonable that the advantages of countercurrent operation and external agitation should be combined for gas-liquid systems as has been done industrially in the case of liquid-liquid systems [22] .

The other term in the expression for the rate of mass transfer is the concentration driving force $(c^* - c)$. In a countercurrent contactor it is possible to maintain a large concentration driving force at all positions in

order to have a good rate of mass transfer throughout the column. The phenomenon of backmixing or recirculation will adversely affect the concentration gradients and reduce the efficiency of a countercurrent device by decreasing the concentration driving force below the optimal value which could be expected for plug flow [36] .

The object then of this work is to investigate the performance of a pulsed bubble column. This apparatus combines countercurrent operation with external agitation for a gas-liquid system. $K_L a$ values are calculated from the data obtained along with axial dispersion coefficients, E_L ,and reflux ratios, R . The latter two parameters were also looked at in separate mixing experiments as well as in the mass transfer work.

2. Previous Work

Several workers have investigated the effect of vibration or pulsation on gas absorption. Baird and Garstang [3] have provided a review of these studies. Generally it has been found that an improvement in the rate of mass transfer was possible. As far as the application of external agitation to a countercurrent gas-liquid contactor is concerned there has been very little work in this area, although there is a considerable amount of information available dealing with liquid-liquid systems.

Sullivan and Treybal [34] have used a multistage agitated tower, previously used for a liquid-liquid system, with a gas-liquid system. They evaluated E_L and H_{OL}. Haug [19] recently has produced a correlation for backmixing applicable to columns of the type used by Sullivan and Treybal. A good review of previous work concerning the various aspects (mass transfer, heat transfer, backmixing and design) of bubble columns is given by Mashelkar [25] .

The most recent investigation of a pulsed bubble column is that of Baird and Garstang [3] . Their system was operated in a batch fashion using oxygen as the dispersed phase and tap water as the continuous phase. They measured values of k_La and found them to be comparable to a high-efficiency gas-liquid contactor [14]; however, it was concluded that the power utilization was less efficient than that of a stirred tank contactor. The column used by Baird and Garstang was baffled in a fashion similar to this work. Most bubble columns in the literature have no baffles either being open or packed columns.

3. Mass Transfer Apparatus

A simplified diagram of the apparatus is shown in figure 3.1 . The column consisted of 2 inch diameter Q.V.F. glass pipe sections. Pure oxygen gas was taken from a gas cylinder to a pressure regulator, R, (40 psig) through a flow meter, F, and dispersed in the column by passing the gas through an air stone, S. The air stone was constructed of fused crystalline alumina grains and was cylindrical in shape, measuring 1 inch long and having a diameter of 9/16 inches.

The normal height of water above the air stone during a run would be approximately 8.5 feet. Various means are available for generating pulsations into gas-liquid systems. A good review of the various methods in the literature is given by Garstang [15] . The method used by Garstang and also used in this work was Baird's [2] method of introducing compressed air and subsequent exhausting.

The column was a smooth U-shape (figure 3.1) with one side of the U being used to conduct the mass transfer operation and the other side used to generate the pulsations. Air from the laboratory supply (100 psig) was taken to a regulator, R, and normally reduced to around 10 psig; from the regulator the line went to a solenoid valve. The photo relay, P,(Sigma Industries Inc.-Model 8RCO2A) is activated when water is at such a level so as to focus light from the light bulb (60 watts) on it. When the photo relay is activated the solenoid valve closes to atmosphere and opens to the air supply. High pressure air then enters the column forcing the level of the liquid to travel downwards and thereby raising the level of liquid on the other side of the U. As the water passes the photo relay-light bulb level, focus is broken and the solenoid valve now closes to the high pressure air opening to atmosphere. The height of liquid on the other side of the U exhausts

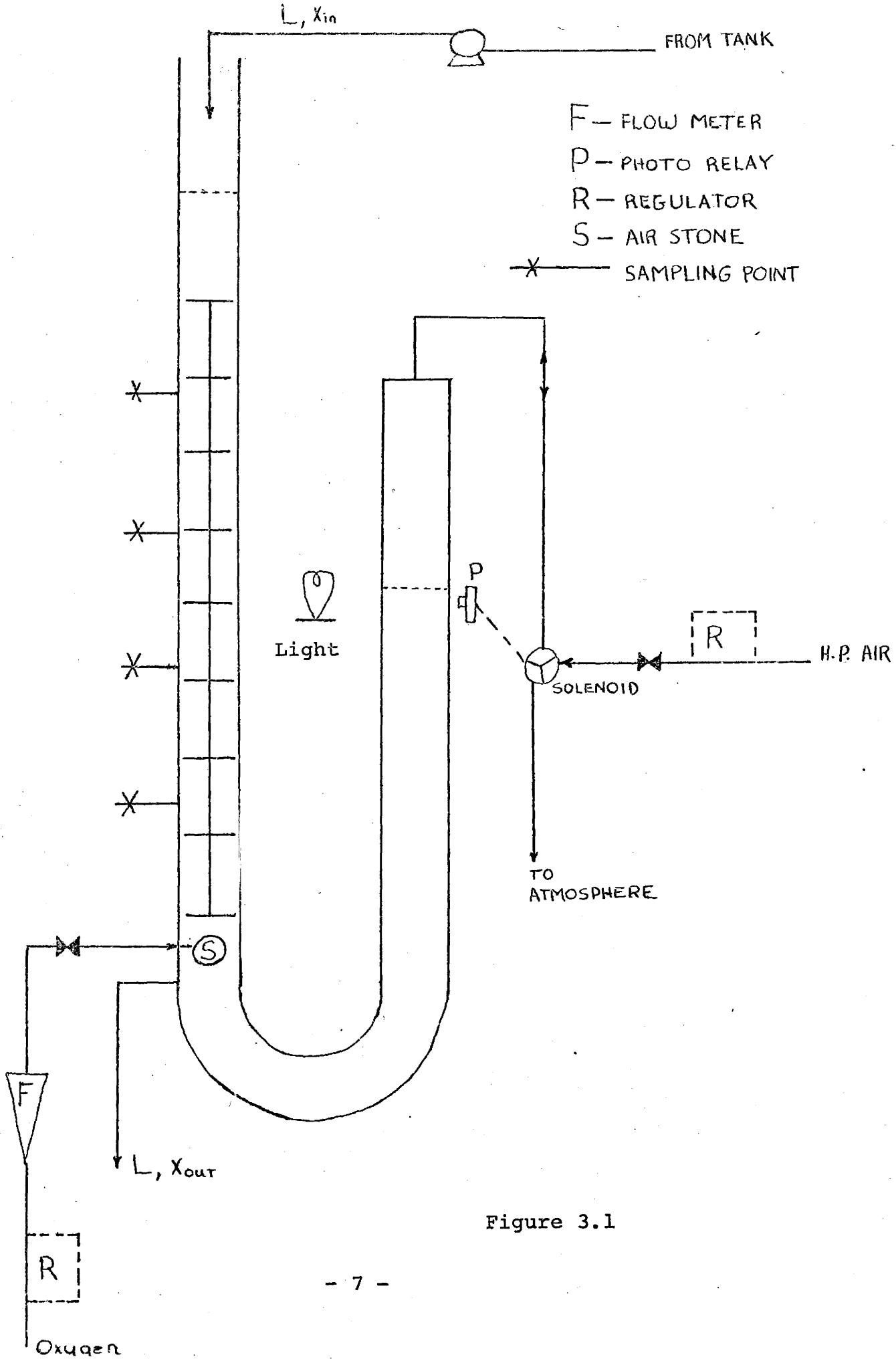
L, Xin
FROM TANK
F — FLOW METER
P — PHOTO RELAY
R — REGULATOR
S — AIR STONE
SAMPLING POINT
Light
P
R
H.P. AIR
SOLENOID
TO ATMOSPHERE
S
F
L, Xout
R
Oxygen

Figure 3.1

the air and when the level of water has risen back to the photo relay-light bulb level the cycle recommences. In this way the pulsations are applied to the system at its natural frequency. The motion of the liquid back and forth over the baffles as shown by plate J . The superficial liquid velocity in the photographs was 1.6 cm./sec. . Plates K,L,M show conditions in the column with no pulsation. The bubbles are quite oblate and their motion up the column is oscillatory. Clearly the bubbles in plate K (U_G =0.388 cm./sec.) are for the most part noticeably smaller than those of plate M (U_G =1.165 cm./sec.) . Generally this is the case that as the gas flow rate increases the bubbles tend to become larger no doubt through increased coalesence; however, from the photos it can be seen that the application of pulsation helps to keep the bubble size more uniform as the gas flow rate increases than is the case for no pulsation. Another interesting feature can be observed in plates A,D,H (U_G =0.388 cm./sec.) . Here the effect of pulsation on holdup can clearly be seen- the superficial gas velocity is the same in each case however the velocity of pulsation is increasing (27,39,49 cm./sec.)

Liquid was held in a holding tank on the floor above the apparatus. The arrangement is shown in plate N. Both a Delasco Peristaltic pump (HY-15D) and a Robbins and Meyers Moyno pump were used to move water into the column. In the tracer experiments both pumps were used simultaneously - the Moyno was used for pumping the tracer and the Delasco for the water. A Haak temperature control unit was placed in the holding tank in an effort to maintain a water temperature of 25^{o}C (±1). Air was bubbled through the water in the tank between runs;bubbles rose from the centre bottom of the tank. This served to bring the dissolved oxygen level of the feed water to air saturation as well as creating circulation currents which helped in keeping

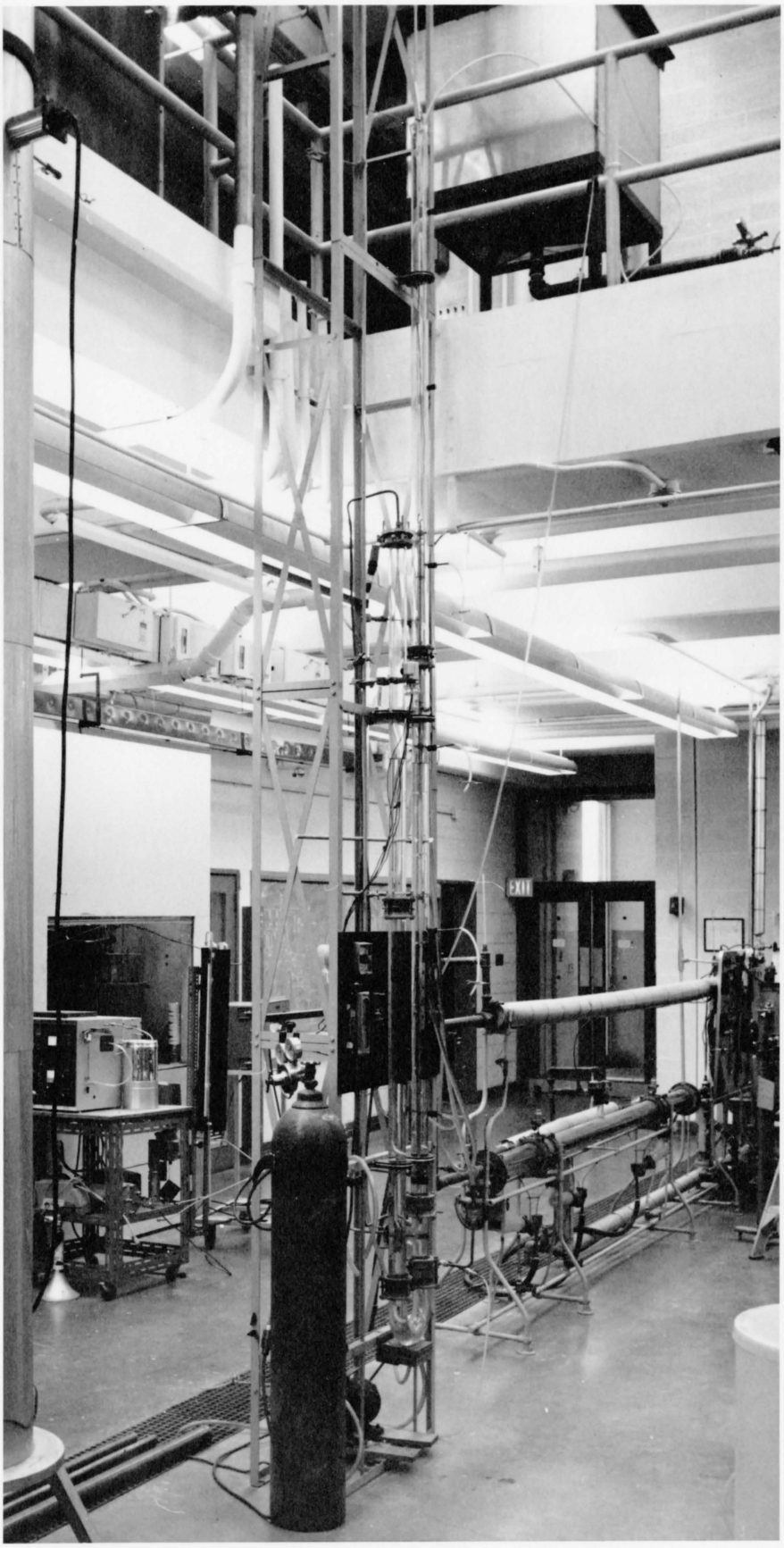

Plate N

a uniform temperature throughout the tank.

Just below the air stone water was removed from the column. For this purpose a plexi-glass plug (figure 3.2) was bored out to a 2 inch diameter; a hole was drilled in the side which was then tapped and fitted with a 1/2 inch Swagelock pipe-tube fitting. Also at this drawoff point was an overflow branch to provide a measure of control on the height of liquid in the column. Referring to figure 3.4 the various dimensions are shown for the mass transfer side of the U. In figure 3.5 the details (not to scale) are shown for the baffle plates and support fixtures. The arrangement at a sampling point is shown in figure 3.3 . At the sampling point the diameter of the copper tubing is a 1/4 inch as is the Tygon plastic tubing stretched over it.The support collars for the central rod were bored and tapped as shown in figure 3.5. The collars were positioned on the rod and held in place by screws. To support the rod in the centre of the column flexible plastic tubing was forced over each protruding screw and the four plastic supports were adjusted in length so as to rub hard against the walls of the column. The plastic was of sufficient thickness so as to position the rod and hold it in place. As shown in figure 3.4 four of these supports were used. The baffle plate shown in figure 3.5 was 1/4 inches thick and tapped so that it could be held to the central rod with a recessed brass screw. The material of the central rod was stainless steel; it was 84 inches long having an outer diameter of 3/8 inches and a wall thickness of 1/16 inches.

Samples taken from the sampling points were analysed for dissolved oxygen using the Winkler titration; specifically the Pomeroy [29] modification was used as this has been shown by Montgomery [27] to be one of the superior Winkler modifications. Before sampling care was taken to remove air from the sampling lines. Liquid was passed through the sample

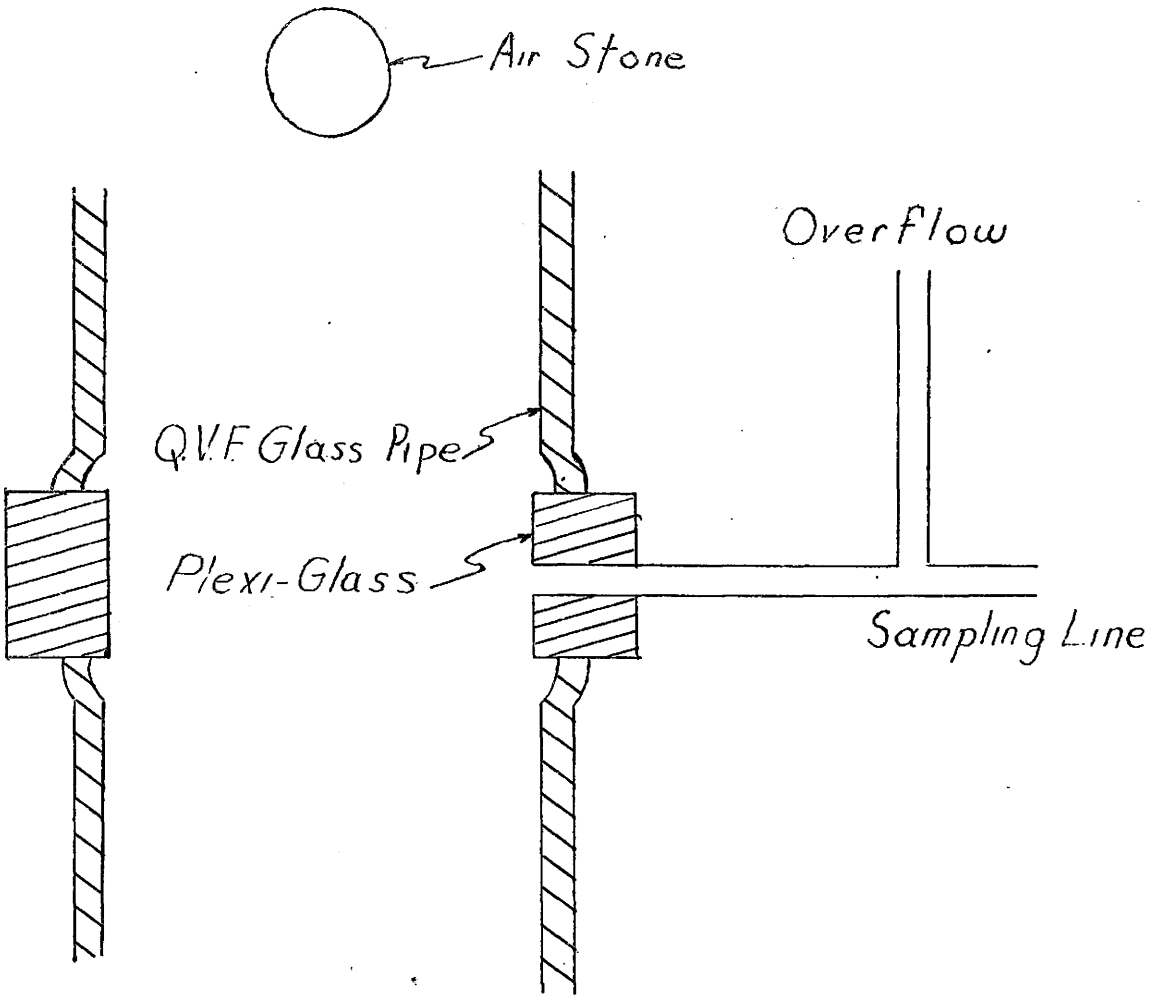

Figure 3.2

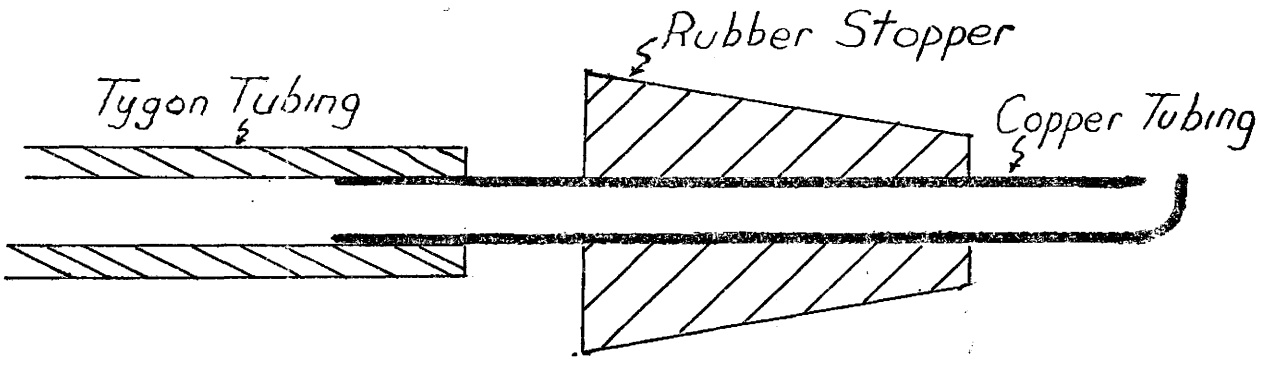

Figure 3.3

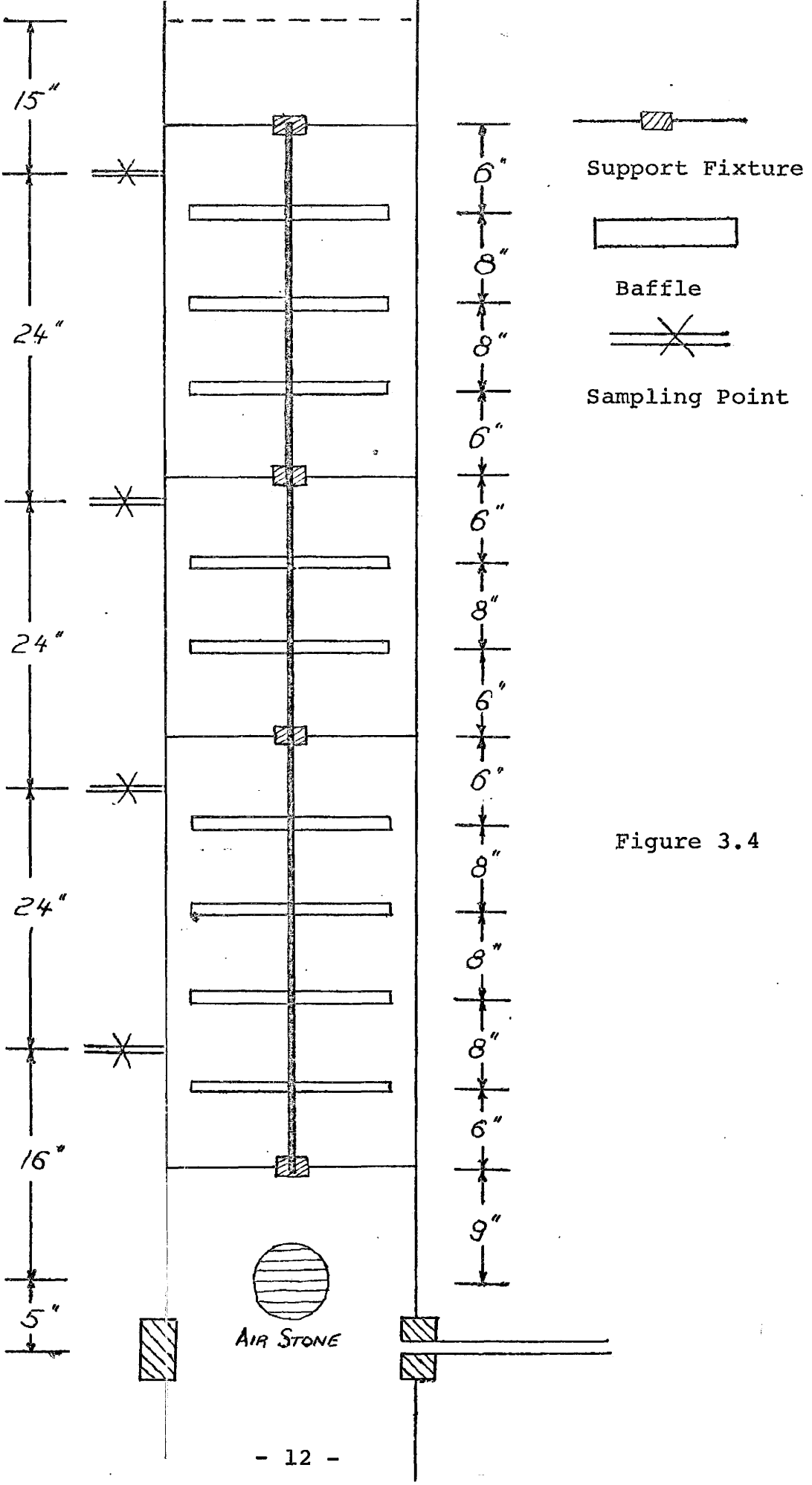
15"
24"
24"
24"
16"
5"
6"
8"
8"
6"
6"
8"
6"
6"
8"
8"
8"
6"
9"
Support Fixture
Baffle
Sampling Point
AIR STONE

Figure 3.4

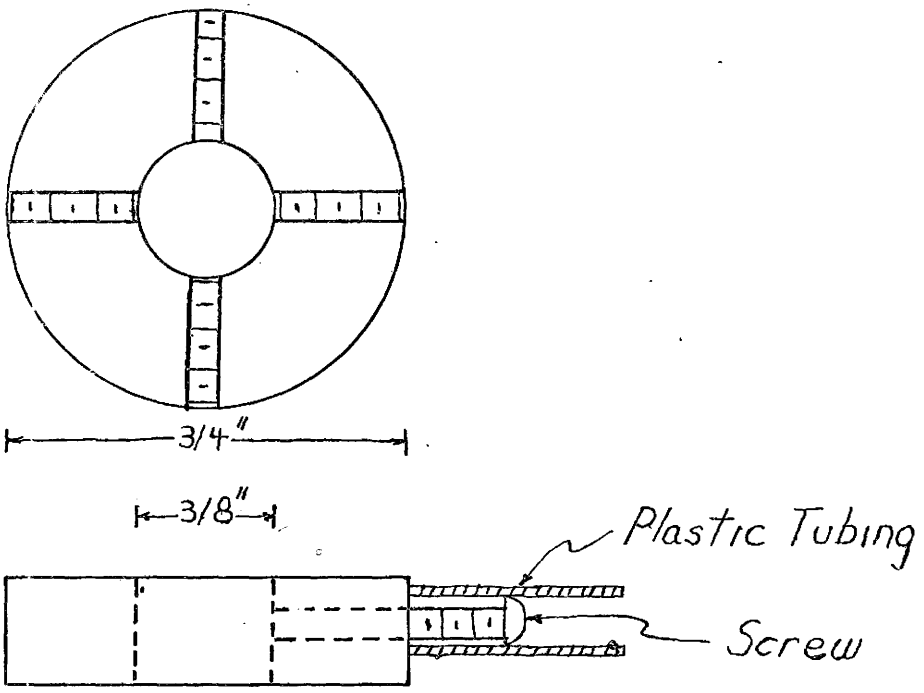

Support Fixture

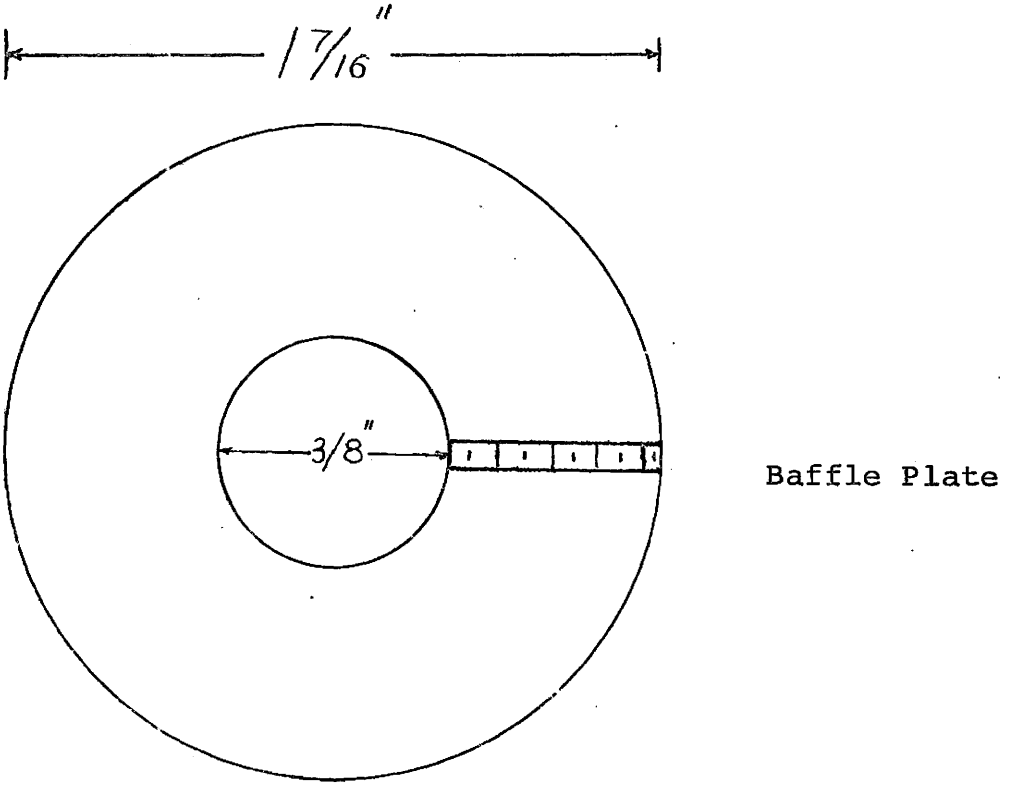

Baffle Plate

Figure 3.5

line at such a rate so as not to entrain bubbles from the column with it. This control was achieved by using a needle valve on the sampling line. The chemical analysis for dissolved oxygen is discussed in appendix 3 . Outlines of sampling techniques and precautions to be taken were consulted and adhered to [27,40]. The upturned copper tubing of the sampling arrangement further hindered the entry of bubbles into the sampling line.

Under pulsation the liquid level moved up and down in a sinusoidal fashion. The time taken for the upward stroke of the liquid level was approximately equal to the time taken for the downward stroke. The amplitude of pulsation , A, is defined as one half the stroke. The frequency was measured in cycles per second. As mentioned previously the frequency obtained was a natural frequency by the positioning of the photo relay-light bulb level as well as the height of water above the air stone. Another factor which increased both frequency and amplitude was the utilization of a vacuum pump on the exhaust side of the solenoid. The frequency then varied over a range of 0.90 c.p.s. to 1.25 c.p.s. . Referring to figure 3.6 :

$$y = A \sin(wt)$$

$$w = 2\pi f \qquad f \text{ - frequency}$$

$$A = \text{stroke}/2$$

$$dy/dt = Aw \cos(wt)$$

$$(dy/dt)_{max} = wA$$

In this fashion the pulsation velocity is defined. The usual method in making adjustments to the amplitude was to vary the pressure of the supply air to the column. When using a vacuum pump a bleed was placed on the line to atmosphere to allow some variation in the effect created

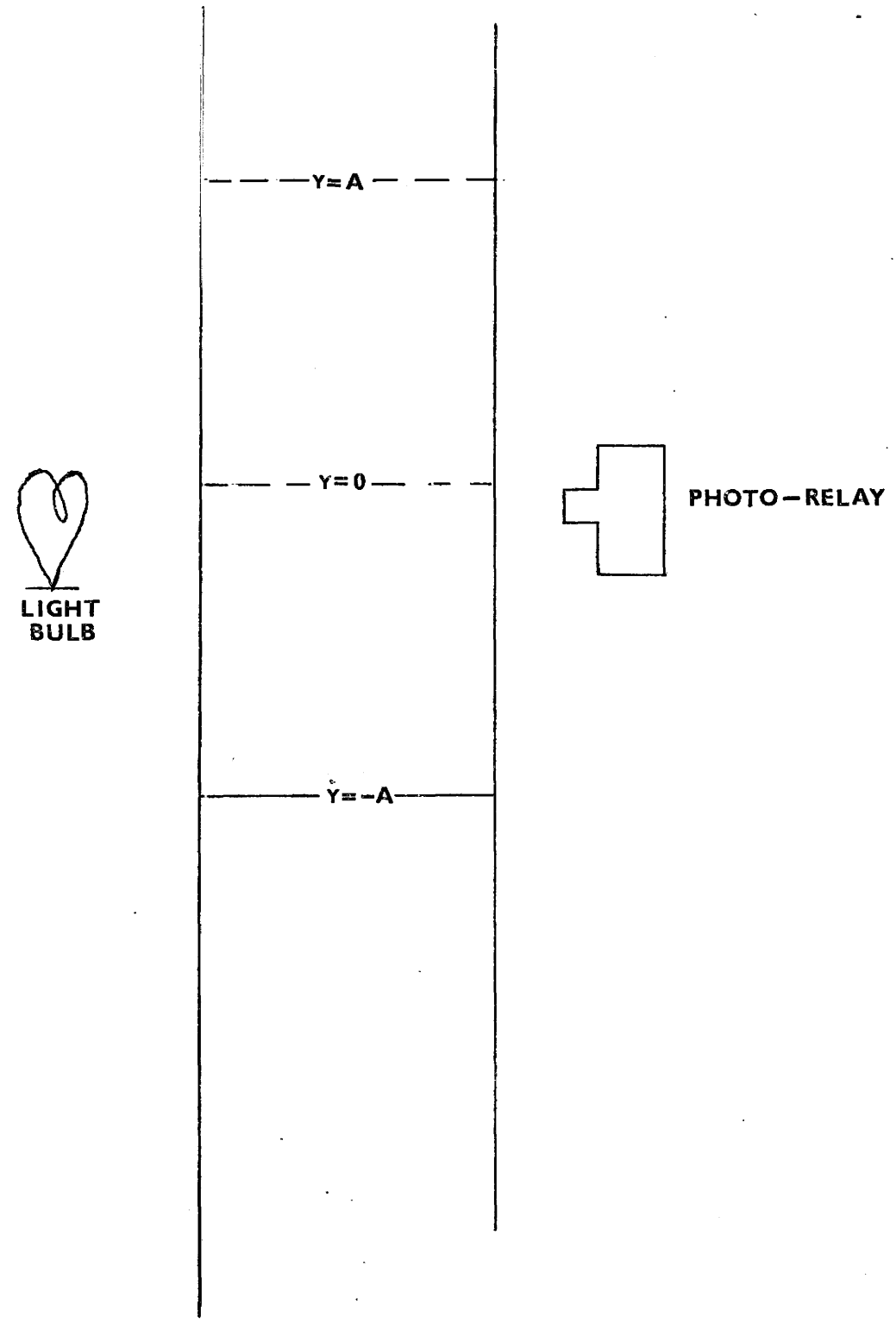

Figure 3.6

by the vacuum pump. After the column had been operating at the adjusted level for a few minutes the liquid level in the pulsation side of the column was closely observed with the high and low levels of the stroke being marked with a grease pencil and checked by following several cycles. The distance between the pencil marks was then measured using a tape ruler graduated in 16 ths. of inches; this measurement gave the stroke of the pulsation. The frequency was measured using a stop watch to measure the time required for 20 cycles. With the knowlege of the stroke and frequency the velocity of pulsation was calculated.

4. Tracer Work

The method used here was a steady-state method. The principles [30] of this method are outlined below with reference to figure 4.1 .

Since at any cross-section the net rate of transport of the tracer is zero:

$$E_L \, dc/dh = U_L c \qquad (4.1)$$

Applying the following boundary condition:

$$c = c_o \quad @ \quad h = H$$

The solution to 4.1 is:

$$c/c_o = \exp(U_L/E_L * (h-H)) \qquad (4.2)$$

Defining $z = h-H$

$$c/c_o = \exp(U_L/E_L * z) \qquad (4.3)$$

The inherent assumptions of equation 4.3 are: the axial dispersion coefficient is independent of position and that radial concentration variations are absent or negligible.

For the tracer experiments a 1/4 inch semi-circular piece of copper tubing was positioned at the first sampling point above the air stone. The copper tube was blocked at one end while tracer flowed in from the other end; facing downwards in the direction of the liquid flow were four 1/8 inch diameter holes spaced 1/2 inch apart. The length of the outside of the arc was 3 inches (figure 4.2). The tracer was held in a tank on the floor above and delivered by the Moyno pump. The tracer itself was potassium dichromate usually in a strength of around 0.015 molar so as to provide an outlet concentration from the bottom of the column of

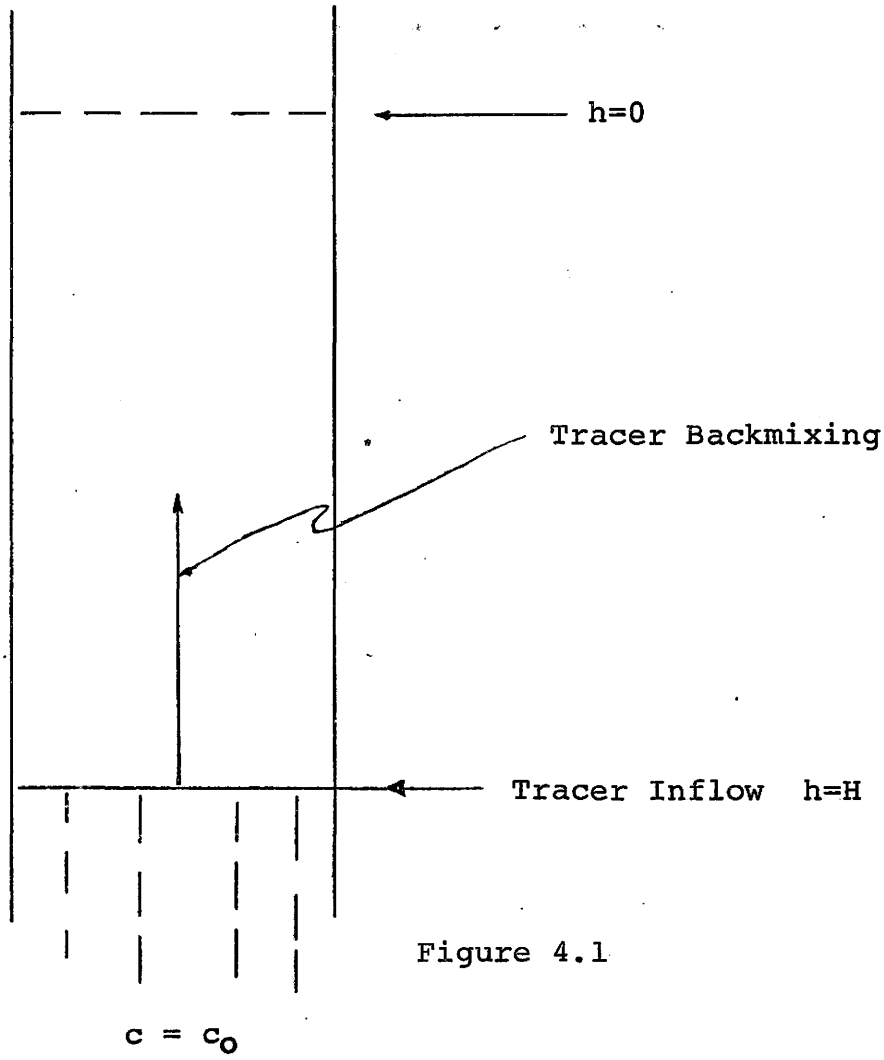

Figure 4.1

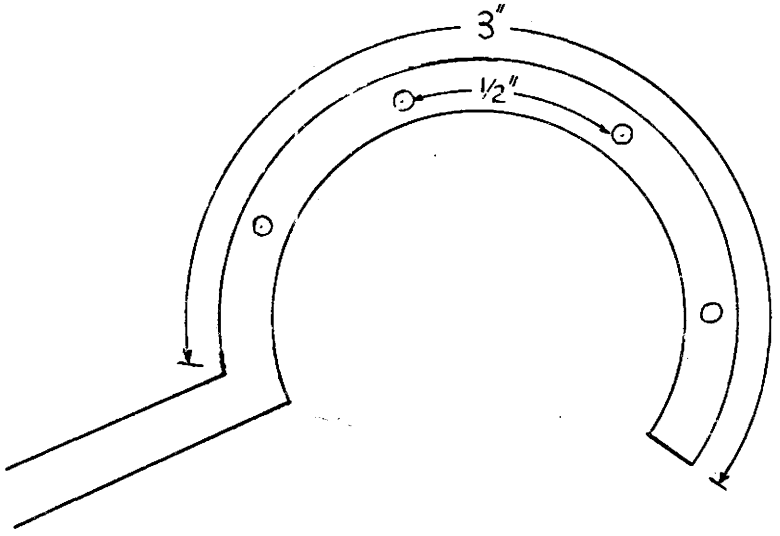

Tracer Distributor

Figure 4.2

around 0.009 molar. Once all the conditions of pulsation, gas flow, liquid flow and tracer flow had been applied to the column a period of about 15 minutes was allowed to let the column reach steady-state. Outlined below is an example run which was used to determine the time to reach steady-state.

Table 4.1

Time(min.)	Transmission(%)
5	72.0
10	53.2
15	56.1
18	54.6
21	54.6
24	57.4

Samples were drawn off using the same setup as with the mass transfer. By controlling the flow of sample using a needle valve the sample withdrawn was effectively averaged over the length of the stroke. About 20 mls. of liquid were drawm off into an Erlenmeyer flask . The samples were then analysed using a Bausch & Lomb Spectronic 20. Details of the optical analysis are given in the appendix.

One of the assumptions in the tracer and mass transfer modelling is the absence of radial gradients. Certainly under pulsation the intense mixing at each baffle plate makes the assumption of no radial dependence seem quite reasonable. To further check into this possibility runs under various conditions were carried out with samples being taken from 3 radial positions at the sampling point closest to the injection point. This position was chosen because if there were any significant radial effects they should have been strongest nearest the point of injection; the positions were 1/4 inch apart. The radial variations of concentration were not found to be significant; a typical run is outlined below- the conditions were: U_G =0.388 cm./sec.,

U_L =1.0 cm./sec., wA =0.0 cm./sec. .

Table 4.2

Radial Position	Transmission(%)
#1	79.5
#2	78.5
#3	79.5

In comparison with axial variations the small radial fluctuations were of no significance. Eissa [31] while studying radial concentration gradients in his column also employed the steady-state method. He found that radial gradients of any significance persisted only about a column's diameter distance form the point of injection and concluded that they were of little significance compared to the axial gradients

5. Mass Transfer Modelling

In considering the mass transfer an axial dispersion model was chosen. The axial dispersion model has been used by a number of workers studying bubble columns [1,25,30,33-35]. Using the dispersion model the following mathematical relationships were previously developed (refer to figure 5.1)

Assuming E_L, U_L, and k_La to be independent of position:

$$-E_L \, d^2x/dh^2 + U_L \, dx/dh = k_La(x^* - x) \qquad (5.1)$$

Now the equilibrium relationship can be expressed as a function of position:

$$x^* = sh + c_Q \qquad (5.2)$$

Substituting into 5.1:

$$-E_L \, d^2x/dh^2 + U_L \, dx/dh = k_La(sh + c_Q - x) \qquad (5.3)$$

Substituting $z = h/H$:

$$- d^2x/dz^2 + HU_L/E_L * dx/dz = k_LaH/E_L \, (sHz + c_Q - x) \qquad (5.4)$$

The following boundary conditions were applied :

B.C. #1 $\quad U_L x_i = U_L x - E_L \, dx/dh \quad @ \; h=0, \; z=0$

B.C. #2 $\quad dx/dh = dx/dz = 0 \quad @ \; h=H, \; z=1$

This second boundary condition follows from the physical impossibility of a step change in concentration at the column outlet.

A discussion of modelling for backmixing and the application of boundary conditions is given by Hartland and Mecklenburgh [18]. The analytical methods for solving 5.4

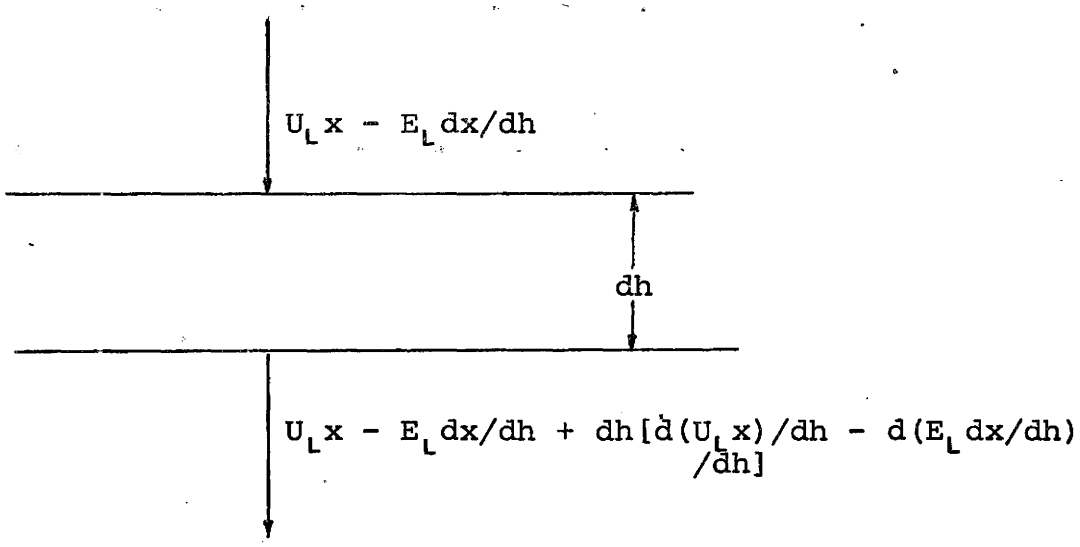

Figure 5.1

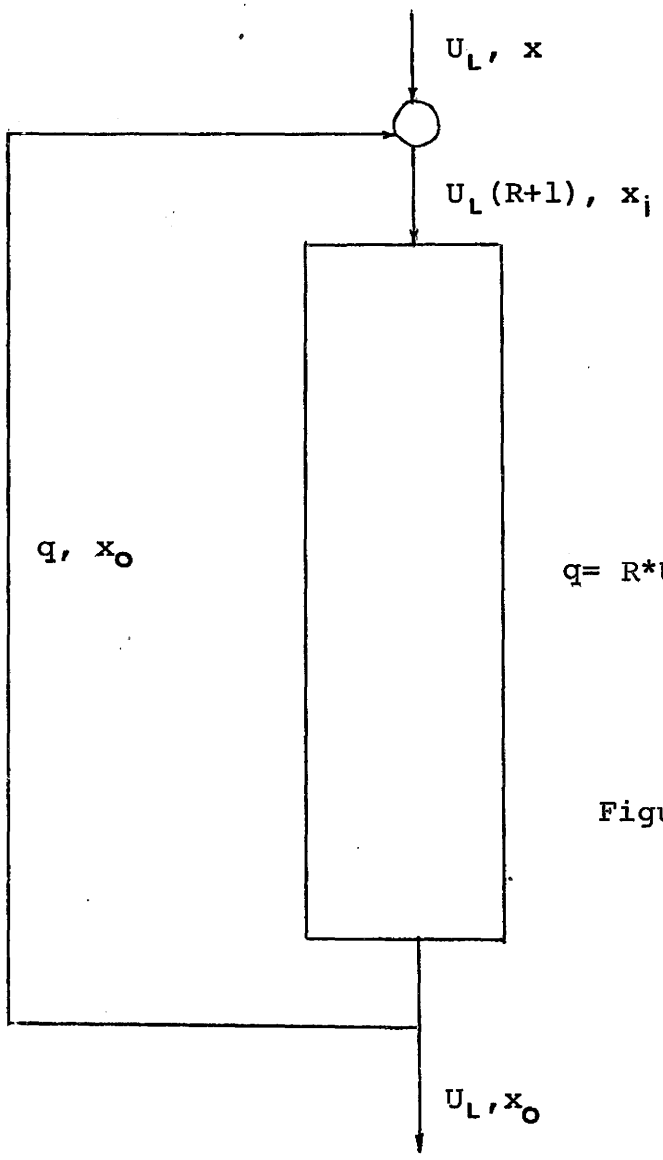

Figure 5.2

are standard techniques [39]. The complementary function is:

$$x_C = C_1 \exp(m_1 \times z) + C_2 \exp(m_2 \times z) \quad (5.5)$$

where $m_1 = HU_L/2E_L * (1 + \sqrt{1+4k_L aE_L/U_L})$

$m_2 = HU_L/2E_L * (1 - \sqrt{1+4k_L aE_L/U_L})$

for the particular integral :

$$x_P = c_Q - sU_L/k_L a + sHz \quad (5.6)$$

the solution being :

$$x = x_C + x_P$$
$$= C_1 \exp(m_1 z) + C_2 \exp(m_2 z) + c_Q - sU_L/k_L a + sHz \quad (5.7)$$

Applying the boundary conditions :

$$C_1 (m_1 \exp(m_1)) + C_2 (m_2 \exp(m_2)) = -sH \quad (5.8)$$

$$C_1 (1-m_1 E_L/HU_L) + C_2 (1-m_2 E_L/HU_L) = x_i + sE_L/U_L - c_Q + sU_L/k_L a \quad (5.9)$$

There now exist two equations in two unknowns, C_1 and C_2, which can be solved for.

Now the mixing experiments indicated that a reflux mechanism due to a circulation effect was occurring under certain conditions during the operation of the bubble column. Introducing a reflux ratio parameter into the above model (figure 5.2) results in an expression which reduces exactly to the above expression if the reflux ratio, R, is set to zero. The solution is :

$$x = C_1 \exp(m_1 z) + C_2 \exp(m_2 z) + c_Q - sU_L(R+1)/k_L a + sHz \quad (5.10)$$

Of course the boundary conditions and hence C_1 , C_2 , m_1 , and m_2 are also functions of the reflux ratio, R.

Since 5 sampling positions were available, there were 5 values of x at 5 values of z the independent variable. A reflux model was used by Gillespie and Carberry [16] for modelling a chemical reactor in order to predict conversion for varying degrees of mixing. They used a plug flow reactor with recycle. The questions that might now be asked are : What are the values of these various parameters that are best going to account for the actual measured profiles? Will the values of the reflux parameter found in the mass transfer work support the observations of the reflux phenomenon in the tracer experiments? It is quite readily observeable that the parameters in the mass transfer model are non-linear; thus, the technique for estimating the most likely values of the parameters will have to be a non-linear technique. Available from the Program Library of the McMaster Computing Centre was the program NLWOOD. This is a non-linear least squares curve fitting program using Marquardt's Maximum Neighbourhood method [24].

One of the important assumptions of the least squares method is that the variance of the dependent variable not depend on the value of the independent variable in the appendix this property is examined using Bartlett's test and found to be satisfactory at the 95% level of confidence.

6. Tracer Modelling

A great many techniques have been used for the investigation of the mixing characteristics within chemical process equipment. Most commonly unsteady-state methods such as step and pulse response techniques have been used. Frequency response techniques as well as steady-state profiles resulting from step inputs have also been used. A review of the various methods, modelling approaches, and parameter estimation techniques is given by Wilson [37]. The steady-state method used in this work has been employed by a number of other investigators using bubble columns [1,30,33-35].

The normal course of expected events for a mixing experiment of this nature is as follows : the column would be filled with water, the pulsation velocity applied, gas and liquid flow rates adjusted, and tracer flow started. Then the pulsation velocity would be adjusted as close as possible to the desired value. According to the axial dispersion mechanism the tracer would start to work its way up the column against the liquid flow direction slowly colouring from the injection point to the top of the column. The column would be darkest at the injection point and lightest at the top.

This does indeed describe the course of events for many of the experimental runs; however, in certain cases a definite reflux would be observed. Colour would appear at the top of the column before having worked back from the injection point any significant distance.Finally the column would appear to take a uniform or near uniform colour in cases where this reflux phenomenon occurred. There was no reason to assume that the normal backmixing mechanism was not operative in these instances but that it tended to be dominated by the reflux condition. It is felt that the most

probable explanation for this reflux effect was some asymmetry in the baffling arrangement of the column. On one occasion wA=0.0 cm./sec., U_L=1.0 cm./sec., and U_G=0.388 cm./sec. the reflux effect was occurring. In an attempt to clarify the situation the baffle column was removed and reflux could not be induced in the apparatus; however, after replacing the baffles the reflux action reappeared.

In light of these effects an axial dispersion model with reflux was used (figure 6.1).

$$R = q/U_L \quad (6.1)$$

$$c_i = Rc_o/R+1 \quad (6.2)$$

Applying the dispersion model and using the boundary condition

$$dc/dh = 0 \quad @\ h= -H$$

$$U_L(R+1)c = E_L dc/dh + K \quad (6.3)$$

Using $c = c_o$ @ h=0 as the other boundary condition :

$$\exp(U_L(R+1)h/E_L)*(1-R/R+1) + R/R+1 = c/c_o \quad (6.4)$$

With R=0 this solution reverts exactly back to the same solution which would have been obtained had no reflux been included.

In passing radiation through an absorbing medium the beam of radiation will diminish in power proportional to the number of absorbing molecules in its path. The quantitative statement of this relationship is the Beer-Lambert law : Successive increments in the number of identical absorbing molecules in the path of a beam of monochromatic radiation absorb equal fractions of the radiant energy traversing them.

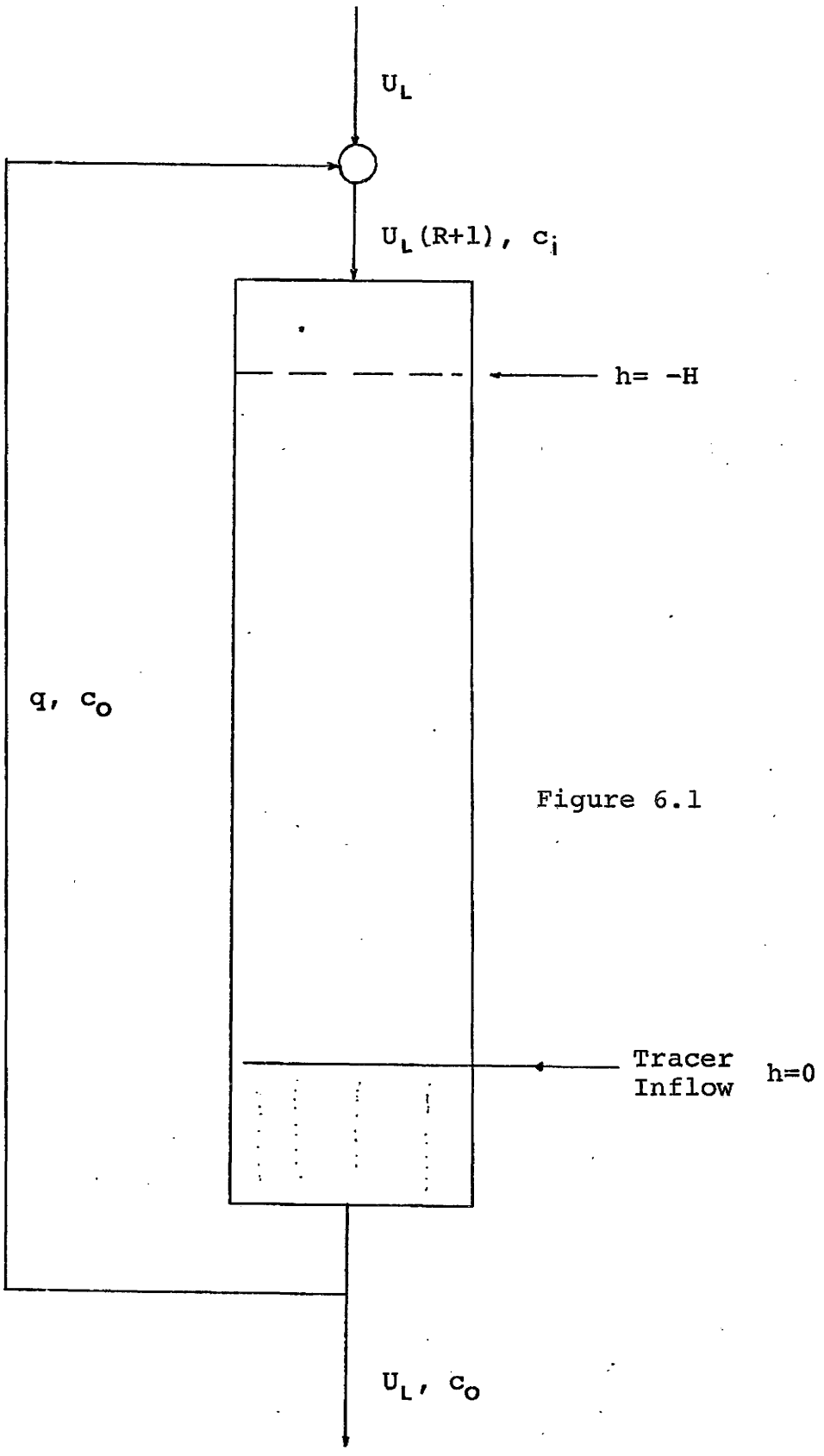

Figure 6.1

$$dT/dn = -bTp \qquad (6.5)$$

$$T/T_0 = \exp(-bNp) \qquad (6.6)$$

T - transmittance
b - constant (includes path length)
Np - number of molecules effective in absorbing radiation (concentration)

The logarithm of T/T is called the absorbance and it is this property which follows a linear relationship with concentration in the event the Beer-Lambert law applies; since the law did apply for the potassium dichromate solutions (see appendix) in the concentration range used the ratio of concentrations was then taken as equal to the ratio of absorbances.

The program NLWOOD was applied to the tracer data in order to obtain an unbiased estimate as to the parameters involved. Applying Bartlett's test to the tracer data indicated that the assumption of homoscedacticity for this data was not valid. An iterative linear least squares (weighted) technique was used to estimate the parameters of equation 6.4 . The weights (see appendix) used for this technique [41] were the reciprocal of the variances at the independent variable positions as estimated from repeated experimental runs using the same conditions. An estimate of the value of R/R+1 was available as a result of applying NLWOOD to the data; hence, a new variable, y, was defined :

$$c/c_0 - R/R+1 = y = \exp(U_L(R+1)h/E_L) * (1 - R/R+1) \qquad (6.7)$$

Taking logarithms of equation 6.7 results in a linear

relationship between log y and h . Iterating on values of R and performing the linear least squares until the residual sum of squares was a mimimum was done. In this way then the most likely value of the parameters and the confidences associated with them were calculated.In cases where the plot of $\log(c/c_o)$ vs. h resembled figure 6.2 the iterative procedure broke down. In these cases the reflux condition was quite dominant and the results of applying NLWOOD to cases of this type is instructive. The program would tend to suppress the value of E_L while the value of R would be such that R/R+1 would tend towards the average value of the points and the maximum possible value of E_L would be obtained . By hand simply taking 1% of the average value at the first position as being attributable to the axial dispersion coefficient term at the first sampling position resulted in the same results. Using the average value of c/c_o as being equal to R/R+1 and calculating R this way in these highly refluxed cases gave the same results again as obtained by NLWOOD. Smaller values of E_L would however also be acceptable since the exponential contribution only determines the manner in which the profile drops to the average value which is determined by the reflux conditions.

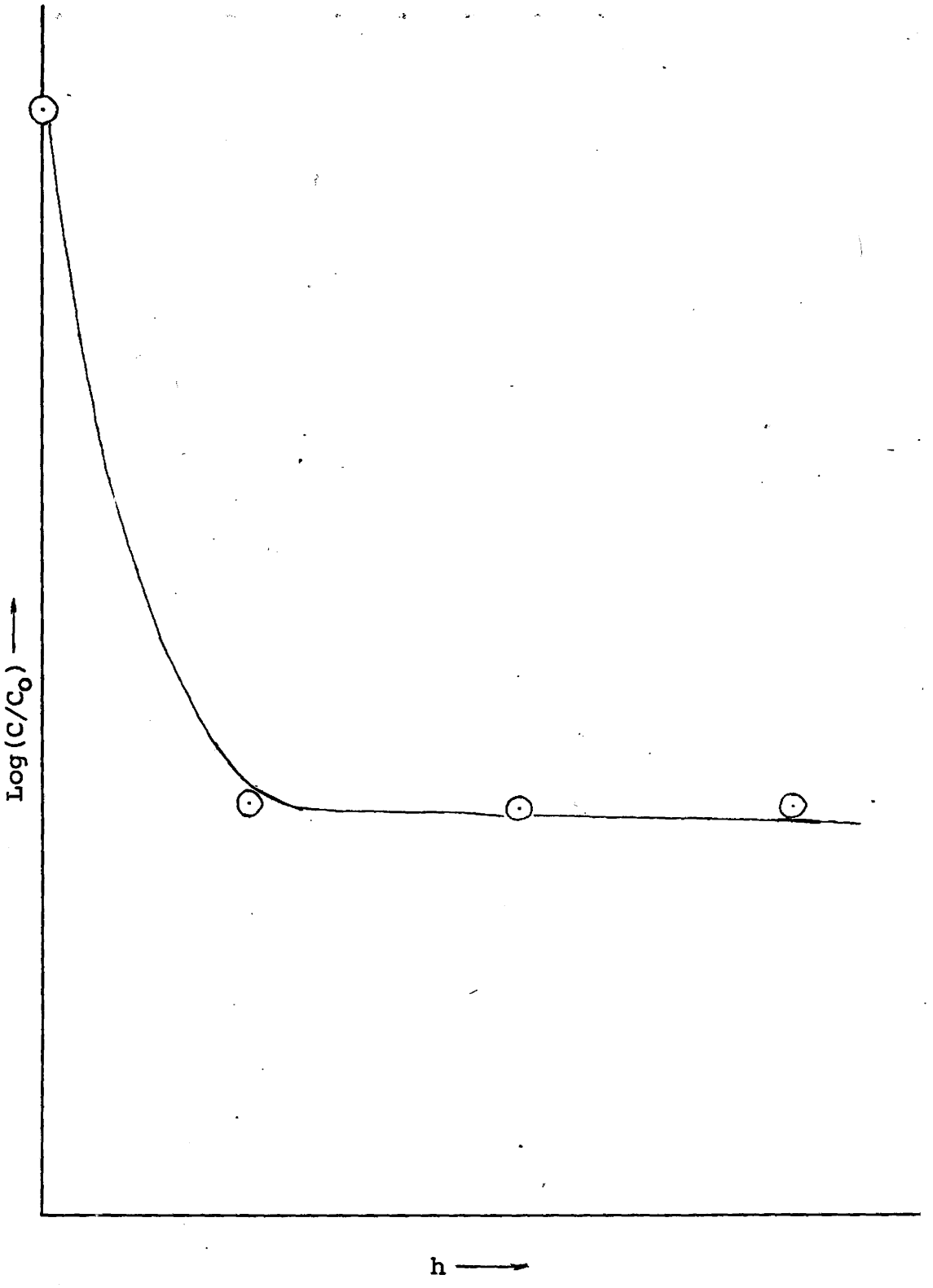

Figure 6.2

7. Mass Transfer Results/Discussion

Both the reflux and non-reflux(dispersion only) models were applied to the mass transfer data. Generally speaking the values of E from fitting the mass transfer data are higher than those obtained from the tracer experiments. However the relationship of E_L to the operating parameters is not really elucidated by the mass transfer data; the reasons for this are discussed further on. Figure 7.1 shows a plot of E_L vs wA at U_G =0.388 cm./sec. . The depression of E_L with reflux is observable. The reflux points on the plot are points where the reflux model applied in that the values of the reflux ratio were non-zero and reasonable. The reflux with axial dispersion model found application in twenty of the forty-three mass transfer runs. In cases where the indication was that reflux was possible the residual sum of squares for the reflux-dispersion case was never any worse than for the axial dispersion alone case and usually there was an improvement, sometimes as much as five times in the residual sum of squares.

In view of the strong reflux indicated by the tracer work under certain conditions the model was further modified and applied to the data by assuming a plug flow model with reflux only. Thirteen runs showed this modification to apply. Where it did apply the reflux-dispersion model also applied with both showing an improvement over the axial dispersion model alone.The proportion of relux to non-reflux cases shows a reasonably good agreement with the tracer work as does the comparison of the conditions under which reflux occurs. The number of possible strong reflux cases compared to the total number of reflux cases is also compatible with the results of the tracer work.

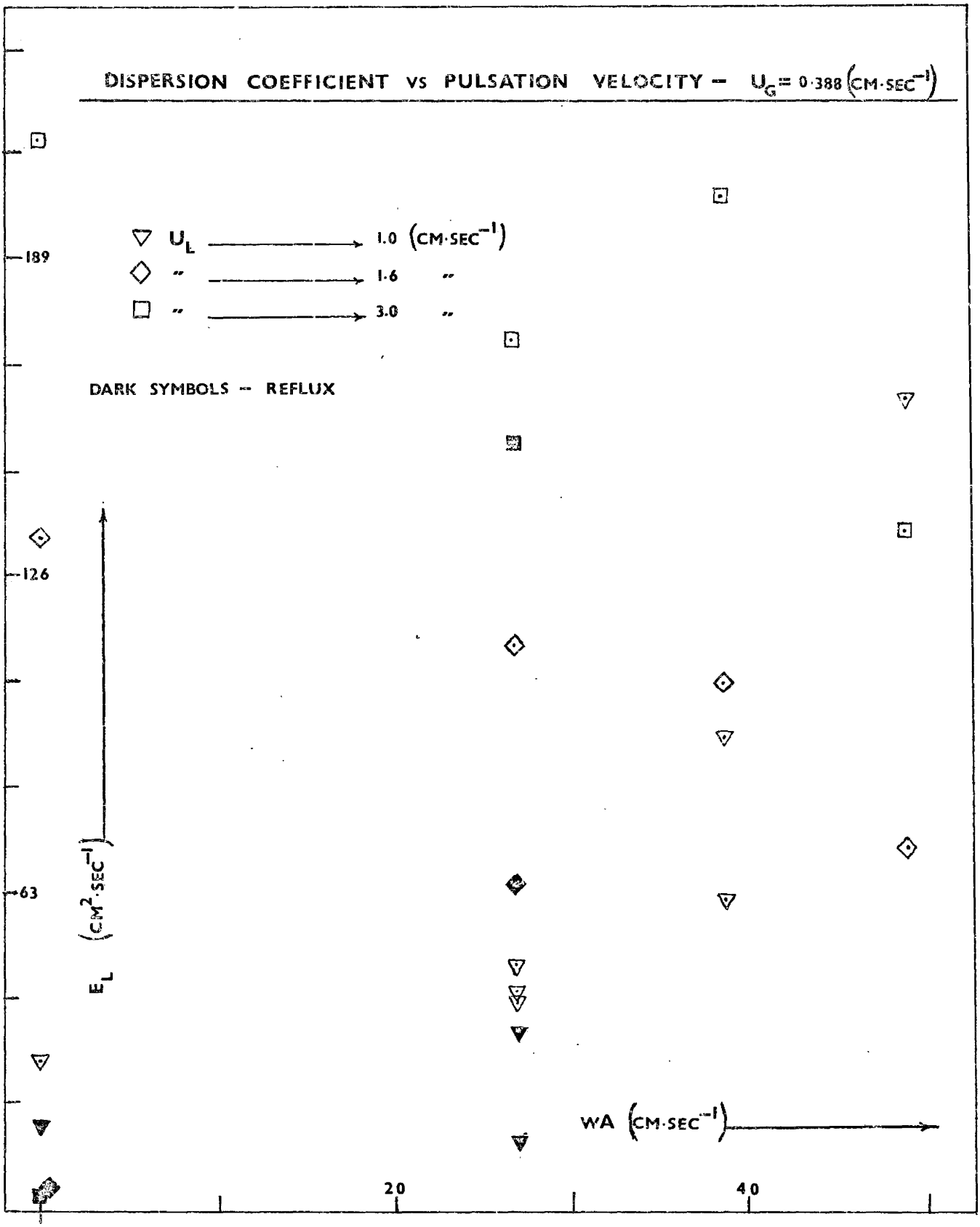
DISPERSION COEFFICIENT vs PULSATION VELOCITY – $U_G = 0.388 (CM \cdot SEC^{-1})$
U_L ——— 1.0 $(CM \cdot SEC^{-1})$
" ——— 1.6 "
" ——— 3.0 "
DARK SYMBOLS – REFLUX
189
126
63
E_L $(CM^2 \cdot SEC^{-1})$
WA $(CM \cdot SEC^{-1})$
20
40

Figure 7.1

Although the value of E_L was affected by the value of the reflux ratio, the value of k_La showed virtually no change. Neither k_L nor a could realistically be expected to change as a result of a change in the fluid mixing mechanism provided the energy input to the system remained constant. The rate of mass transfer is determining k_La as measured.

The mixing effects of E_L and refluxing of course do influence $(x^* - x)$ and it is this effect which is detrimental to the operation of a countercurrent contactor. From figure 7.2 there would appear to be an effect of liquid flow rate on E_L but as mentioned earlier one cannot draw firm conclusions based on the mass transfer data as regards E_L .

The relation of k_La to the operating parameters is shown in figures 7.3,7.4, and 7.5 . For a given liquid flow rate on each figure the value of k_La improves with increasing pulsation velocity. The two exceptions are U_L= 1.0 cm./sec. in figures 7.4 and 7.5 here it would appear there is a maximum at wA=39.0 cm./sec. . With the exception of the two odd points there is a steady rise in k_La with an increase in superficial gas velocity. The values of k_La obtained in this work agree quite well with the values obtained by Baird and Garstang [3]. There generally appears to be an improvement in k_La with increasing liquid flow rate. Baird and Garstang used a larger column (3 inch) with more baffles (12 baffles, 2 inches in diameter, 1/4 inches thick)which means that their power input to achieve the same velocity of pulsation could then be expected to be proportionately greater. As their equipment operated in a batch-wise fashion possibly the effect of liquid flow rate on k_La might be the extra energy to the system in the form of the flowing liquid. Also the increased liquid flow rate would tend to diminish the axial graduents for a given E_L.

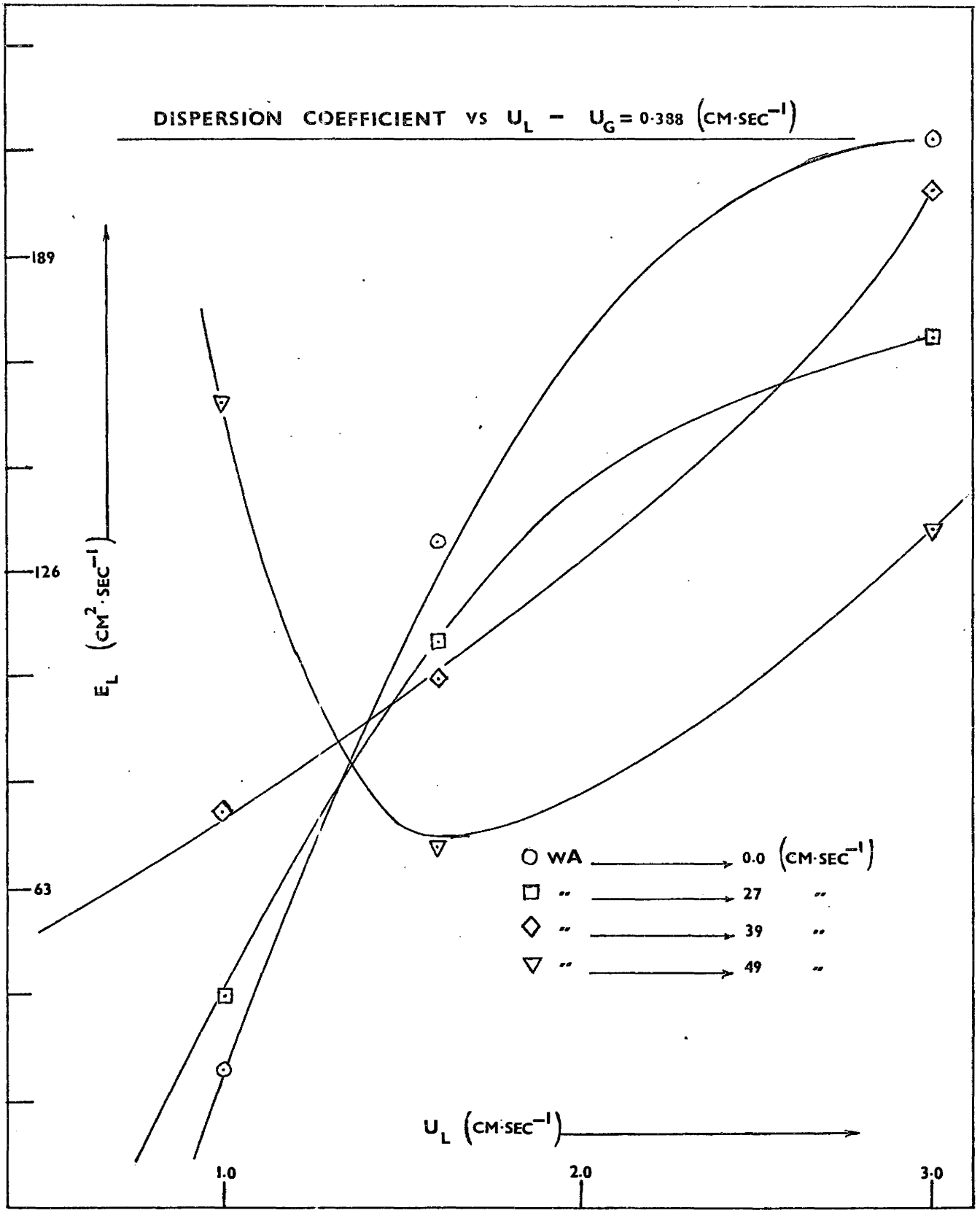
DISPERSION COEFFICIENT VS U_L – U_G = 0·388 (CM·SEC^{-1})
189
126
63
E_L (CM^2·SEC^{-1})
O WA → 0.0 (CM·SEC^{-1})
□ " → 27 "
◇ " → 39 "
▽ " → 49 "
U_L (CM·SEC^{-1})
1.0
2.0
3.0

Figure 7.2

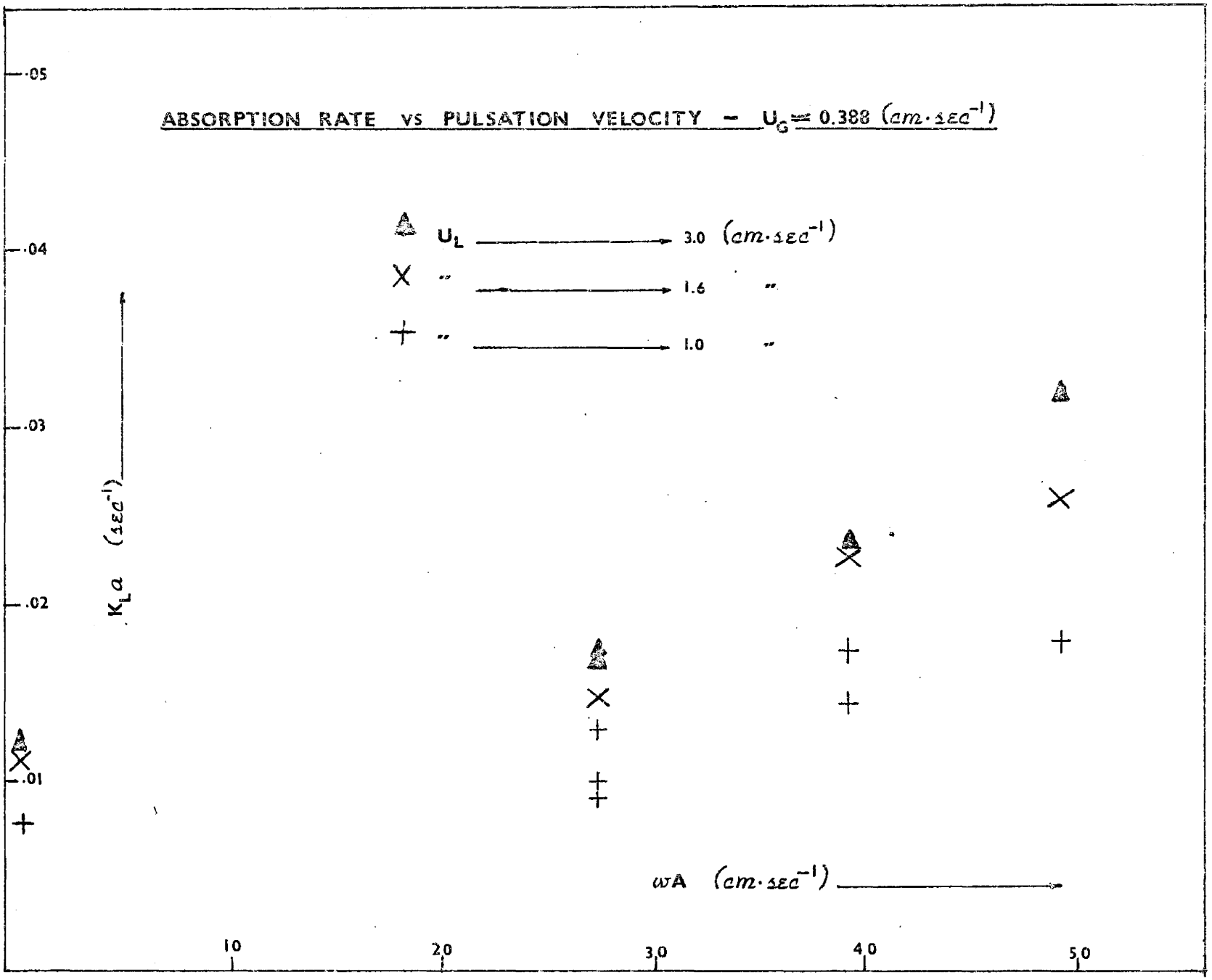
ABSORPTION RATE VS PULSATION VELOCITY – $U_G = 0.388$ (cm·sec^{-1})
U_L 3.0 (cm·sec^{-1})
" 1.6 "
" 1.0 "
$K_L a$ (sec^{-1})
.05
.04
.03
.02
.01
ωA (cm·sec^{-1})
10
20
30
40
50

Figure 7.3

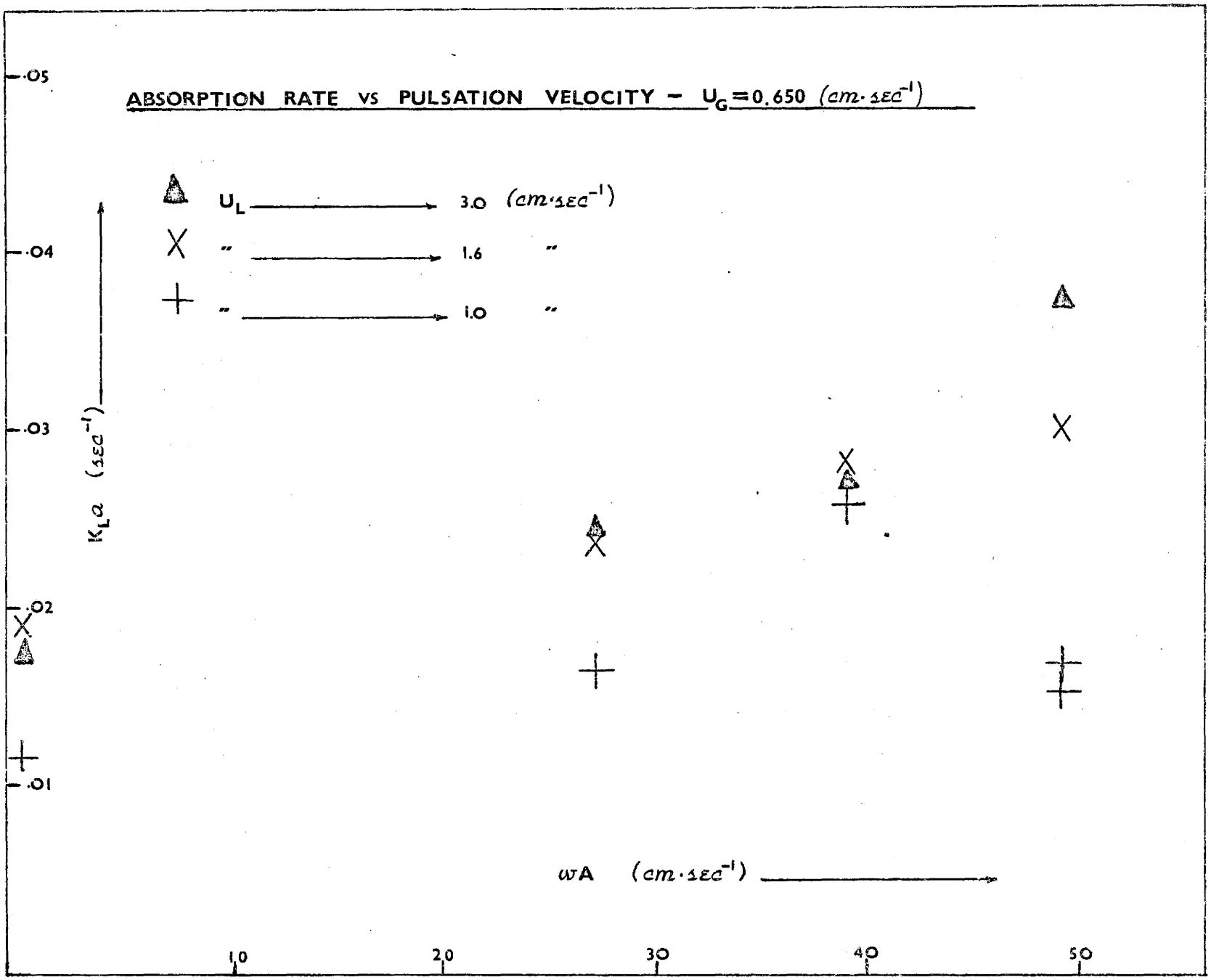
ABSORPTION RATE VS PULSATION VELOCITY – U_G=0.650 (cm·sec^{-1})
U_L ——— 3.0 (cm·sec^{-1})
" ——— 1.6 "
" ——— 1.0 "
$K_L a$ (sec^{-1})
.05
.04
.03
.02
.01
ωA (cm·sec^{-1})
10
20
30
40
50

Figure 7.4

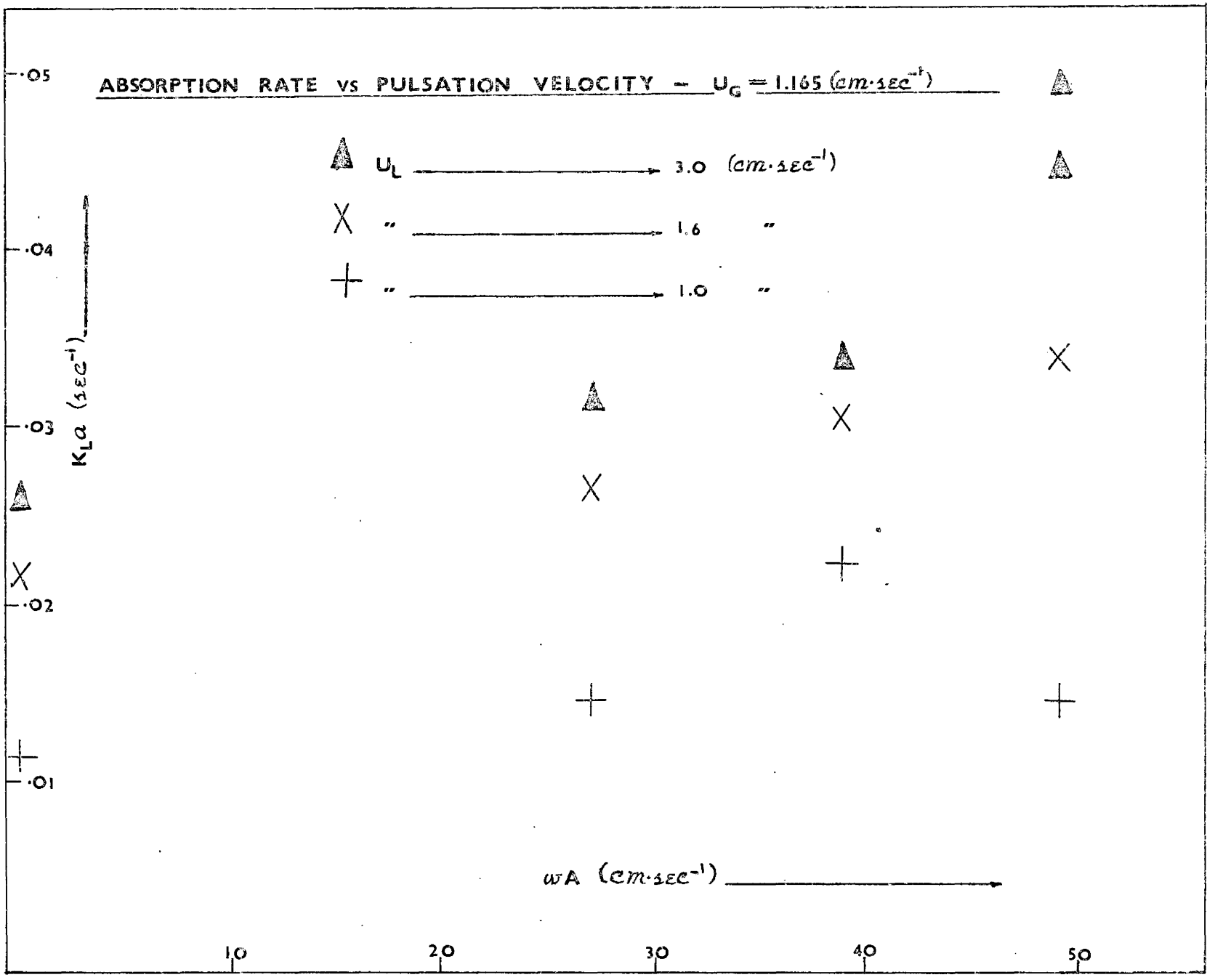
ABSORPTION RATE VS PULSATION VELOCITY – $U_G = 1.165$ (cm·sec^{-1})
U_L ——— 3.0 (cm·sec^{-1})
" ——— 1.6 "
" ——— 1.0 "
$K_L a$ (sec^{-1})
·05
·04
·03
·02
·01
wA (cm·sec^{-1})
10
20
30
40
50

Figure 7.5

The relationship of k_La and pulsation velocity as presented by Baird and Garstang [3] is approximately linear; here the relationship appears to be non-linear in nature. Garstang [15] points out that his k_La values are comparable to those of Gal-Or [14] who used a high efficiency gas-liquid contacting stage. Since the k_La values of this work support those of Garstang the same remarks apply here as well. Baird and Garstang measured power dissapation levels and presented a correlation for k_La depending on the total specific power dissipation and the gas flow rate.

$$k_La = 0.116 * J_T^{0.42} * U_G^{0.50} \qquad (7.1)$$

Using the data of this work and a model of the form :

$$k_La = b * U_G^C * U_L^D * (1 + e * wA) \qquad (7.2)$$

This resulted in :

$$k_La = 0.013 * U_G^{0.39} * U_L^{0.50} (1 + 0.016wA) \qquad (7.3)$$

The actual values of k_La obtained are plotted against the values predicted by equation 7.3 in figure 7.6. The dependence of k_La on U_G shows a reasonable agreement with the correlation of Baird and Garstang.

A common parameter used in describing the operation of a differential countercurrent contacting device is the number of transfer units (NTU_L). The NTU_L for each mass transfer run could be calculated from the profiles obtained. Outlined below are the relationships.

$$dh = (Q/k_LaS) * dx/(x^* - x) = H \qquad (7.4)$$

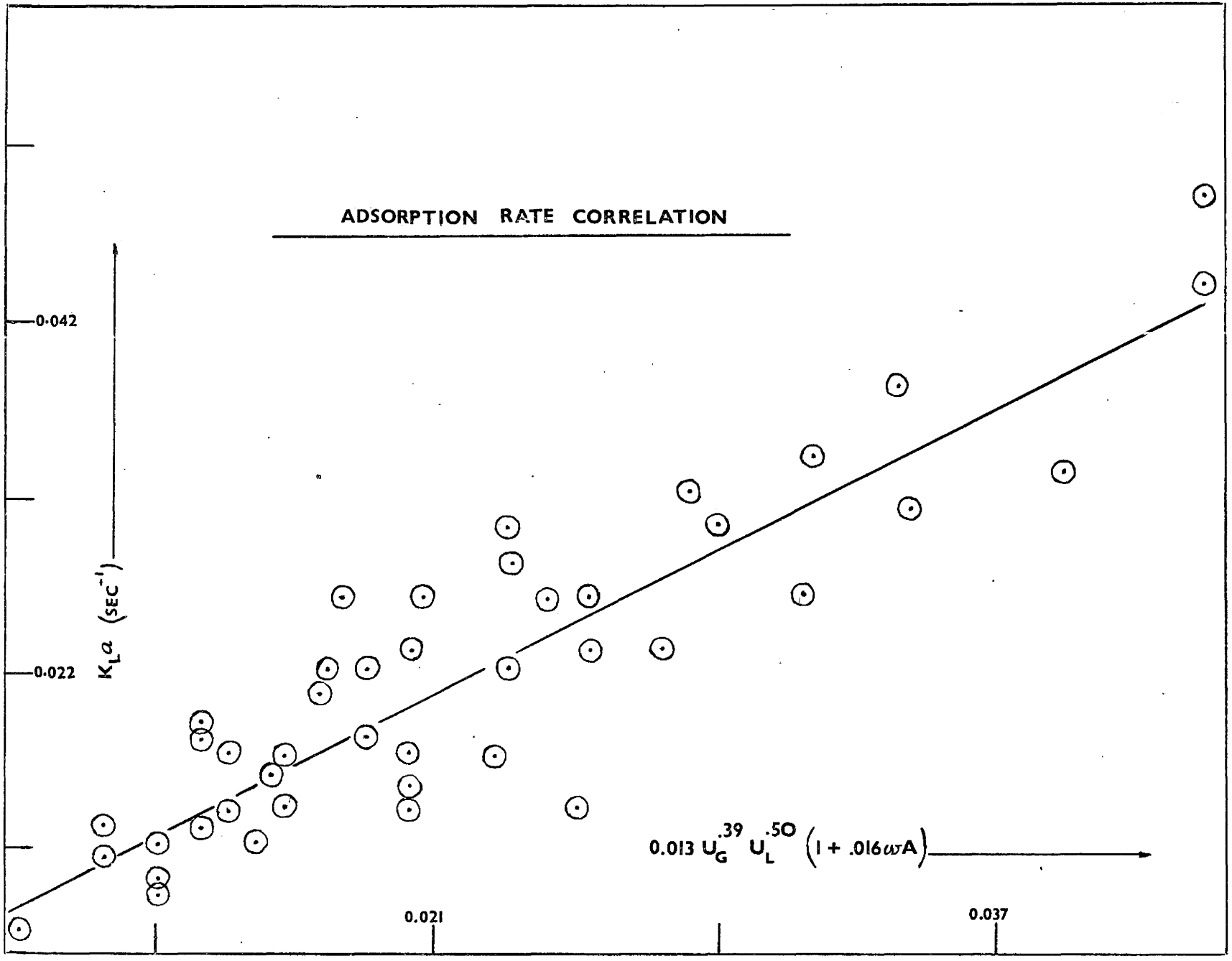
ADSORPTION RATE CORRELATION
0.042
0.022
$K_L a$ (SEC^{-1})
$0.013\ U_G^{.39}\ U_L^{.50}\ (1 + .016\omega A)$
0.021
0.037

Figure 7.6

The Number of Transfer Units (NTU_L) is defined as :

$$NTU_L = dx/(x^* - x) \quad (7.5)$$

Having the equilibrium and concentration profiles allows an evaluation of NTU_L . The equilibrium relationship was :

$$x = sHz + c_Q \quad (7.6)$$

A smooth curve was drawn through the plotted data points and a degree two Lagrange interpolation formula was found to fit the curve nicely. The value of the concentration predicted by the interpolation formula at z=0 was checked in several cases against model predictions of the concentration at the same point and found to be in good agreement.

With the corresponding concentration and equilibrium values the function $1/(x^* - x)$ could be evaluated and plotted against the concentration. Figure 7.7 shows such a plot. A base line was drawn along the bottom of the curve and the rectangular part of the total area evaluated exactly. The area between the curve and the baseline was determined using a planimeter. The planimeter technique was calibrated by using a known area and obtaining three readings on it and using the average value for calibrating purposes. A reading of 26±1 would represent the largest deviation experienced in the calibration procedure. Then three readings on the area between the curve and the baseline would be obtained. Here a representative reading might be 140±3 . A plot showing the interpolation formula fit to the concentration profile is shown in figure 7.8. All results for both the mass transfer and mixing work are tabulated in the back of the appendices.

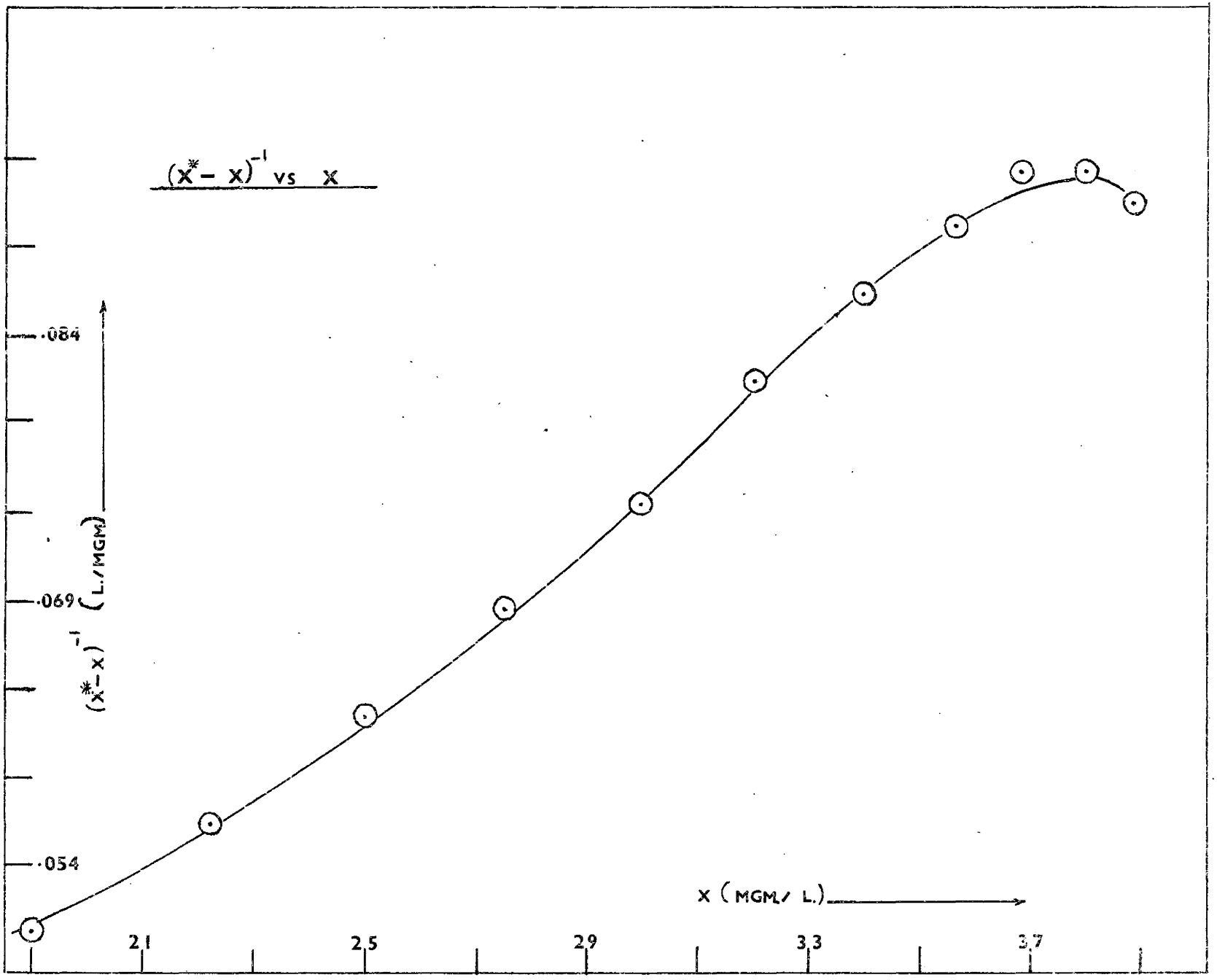

Figure 7.7

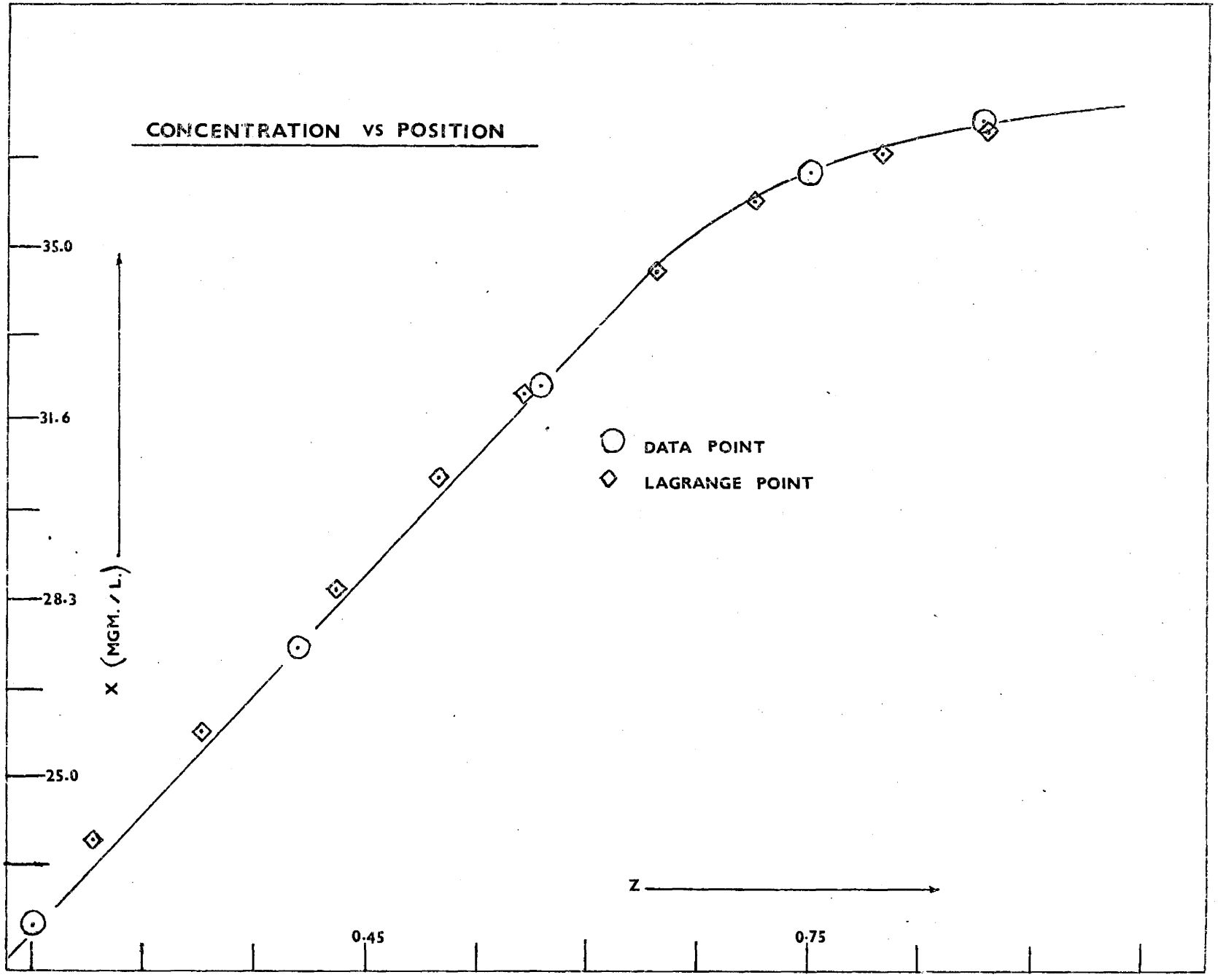
CONCENTRATION VS POSITION
35.0
31.6
28.3
25.0
X (MGM. / L.)
DATA POINT
LAGRANGE POINT
Z
0.45
0.75

Figure 7.8

Figures 7.9, 7.10, and 7.11 show plots of NTU_L versus U_L for various gas rates and pulsation velocities. Looking at these plots it can be seen that generally the pulsed cases are an improvement over the unpulsed cases with exceptions appearing to be at U_G = 1.165 cm./sec. (U_L = 1.0, 1.6 cm./sec.) under these two conditions the unpulsed cases appear to hold their own with the pulsed ones. At any particular given gas rate the best NTU_L seems to be at U_L = 1.0 cm./sec. and decreasing with increasing flow. The average NTU_L for the various gas flow rates are :

U_G = 0.388 cm./sec. $(NTU_L)avg.$ = 1.82
U_G = 0.650 " $(NTU_L)avg.$ = 2.23
U_G = 1.165 " $(NTU_L)avg.$ = 2.18

The number of transfer units over the three gas rates has a reasonably constant value.

The ideal situation in a countercurrent contactor is plug flow. When deviations from plug flow are experienced the mean driving force for mass transfer is reduced in a manner shown in figure 7.12 . Since the ideal situation is plug flow some feel for the efficiency of the column can be attained if the height of column required for the same degree of mass transfer were known for the plug flow case. For the plug flow case :

$$k_L a\,[x^* - x]\,dh = U_L\,dx \qquad (7.7)$$

$$dx/dh = k_L a/U_L * (c_Q + sh - x) \qquad (7.8)$$

Using the integrating factor $\exp(k_L ah/U_L)$ and the boundary condition $x = x_i$ at $h = 0$ the solution is :

$$x = c_Q + sU_L/k_L a * (k_L ah/U_L - 1) + (x_i - c_Q + sU_L/k_L a) * \exp(-k_L ah/U_L) \qquad (7.9)$$

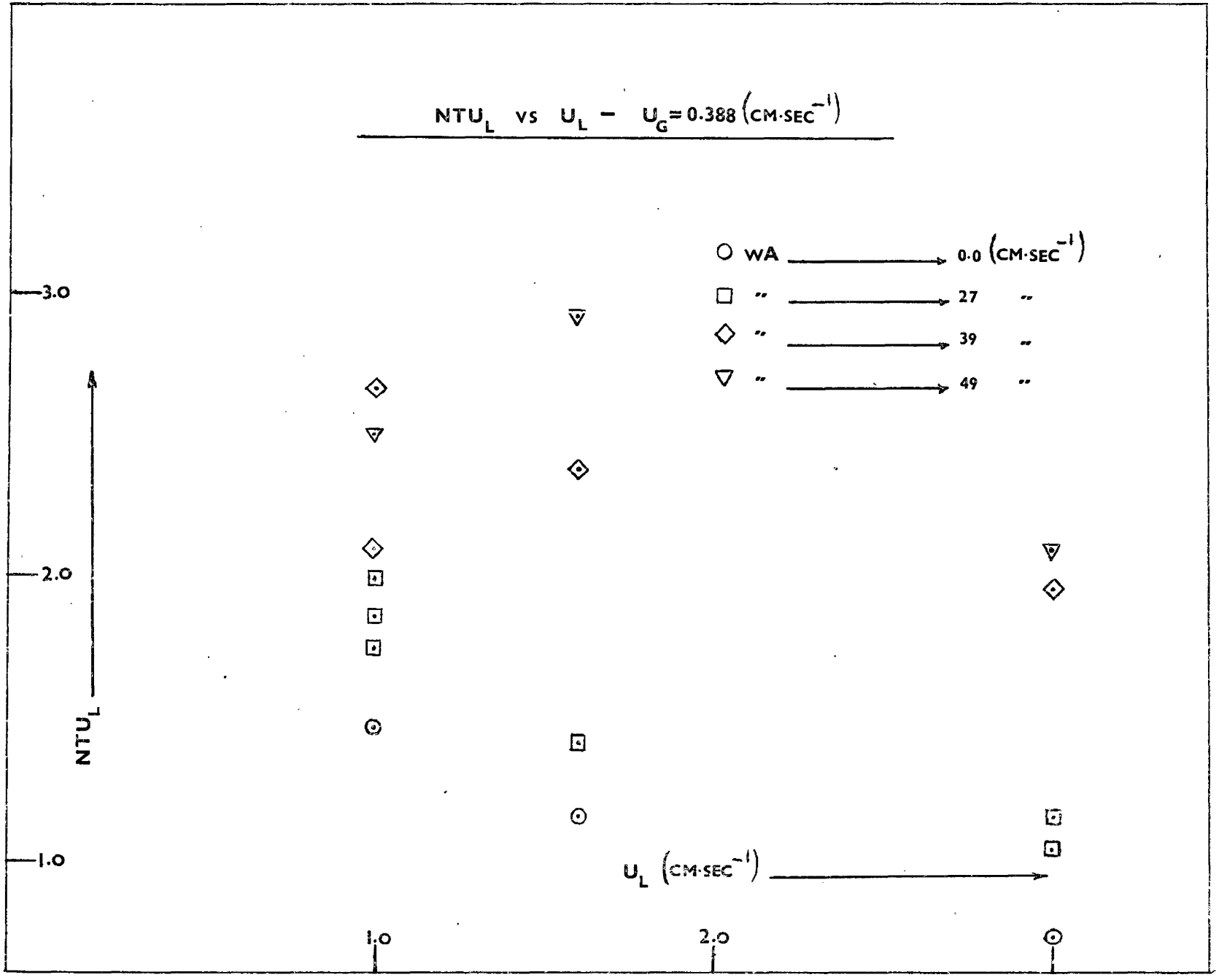
NTU_L vs U_L – U_G = 0.388 (CM·SEC⁻¹)
WA → 0.0 (CM·SEC⁻¹)
" → 27 "
" → 39 "
" → 49 "
3.0
2.0
1.0
NTU_L
U_L (CM·SEC⁻¹)
1.0
2.0

Figure 7.9

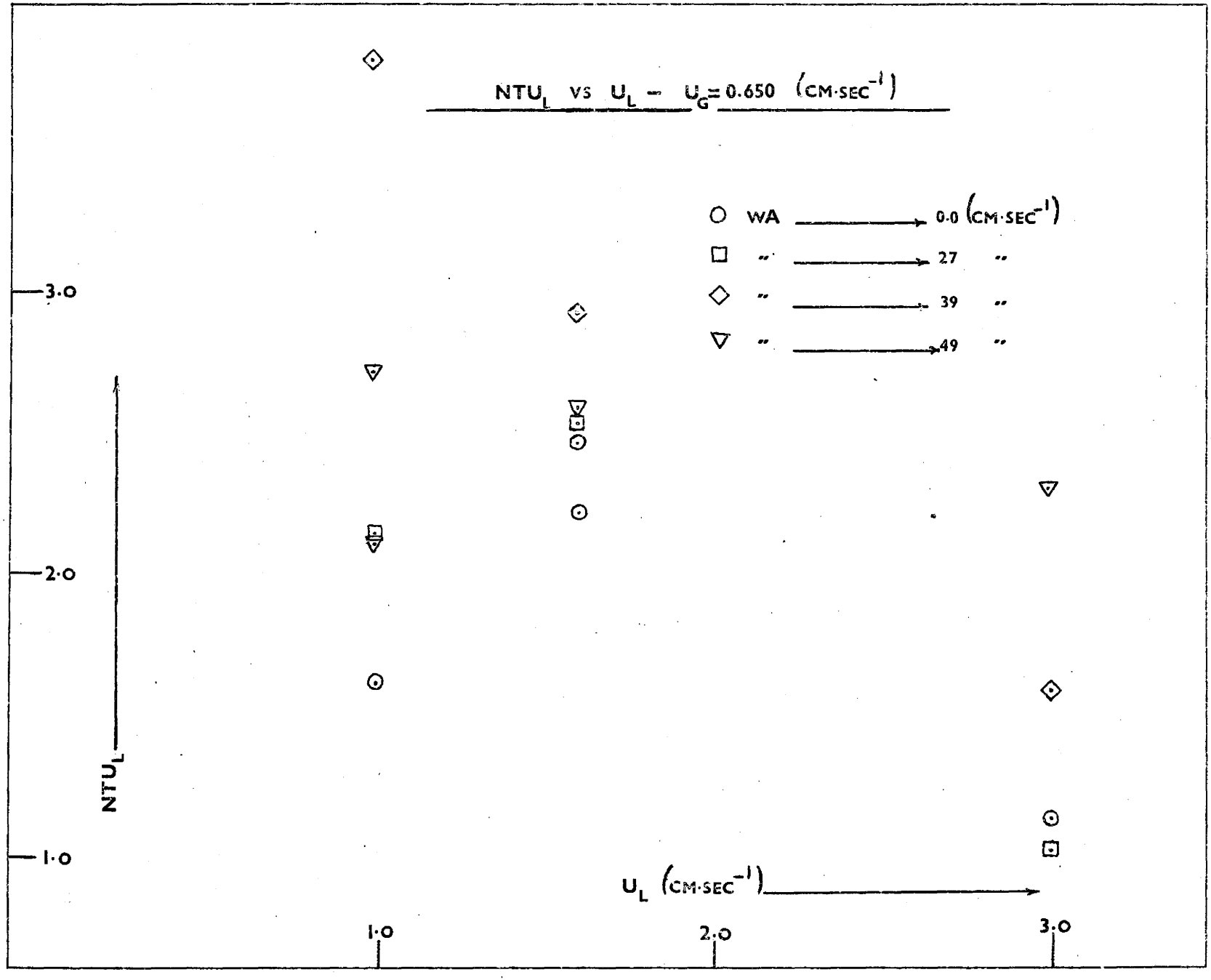
NTU_L vs U_L — U_G = 0.650 (CM·SEC⁻¹)
WA → 0.0 (CM·SEC⁻¹)
" → 27 "
" → 39 "
" → 49 "
3·0
2·0
1·0
NTU_L
U_L (CM·SEC⁻¹)
1·0
2·0
3·0

Figure 7.10

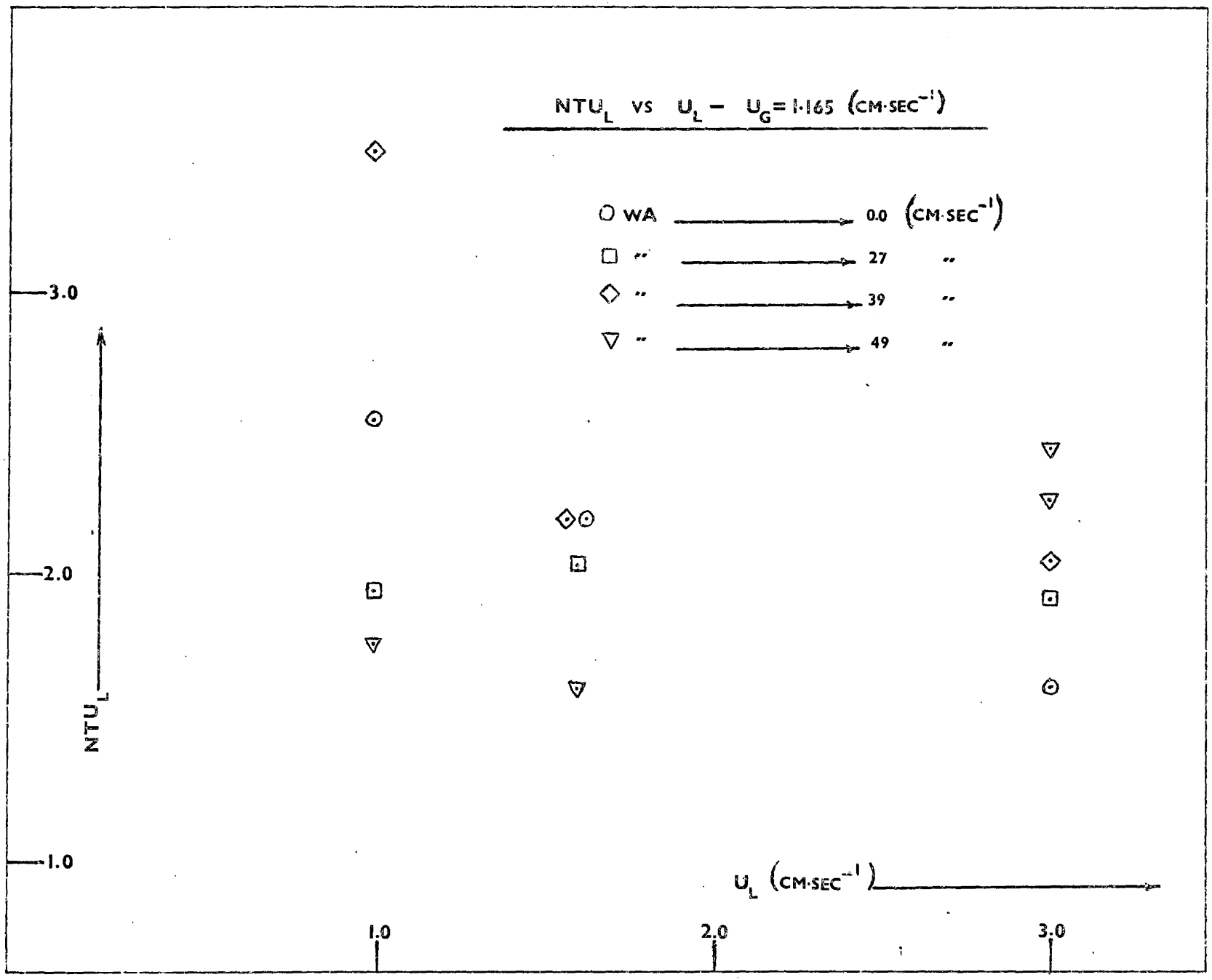
NTU_L vs U_L – U_G = 1·165 (CM·SEC⁻¹)
O WA 0.0 (CM·SEC⁻¹)
□ " 27 "
◇ " 39 "
▽ " 49 "
3.0
2.0
1.0
NTU_L
U_L (CM·SEC⁻¹)
1.0
2.0
3.0

Figure 7.11

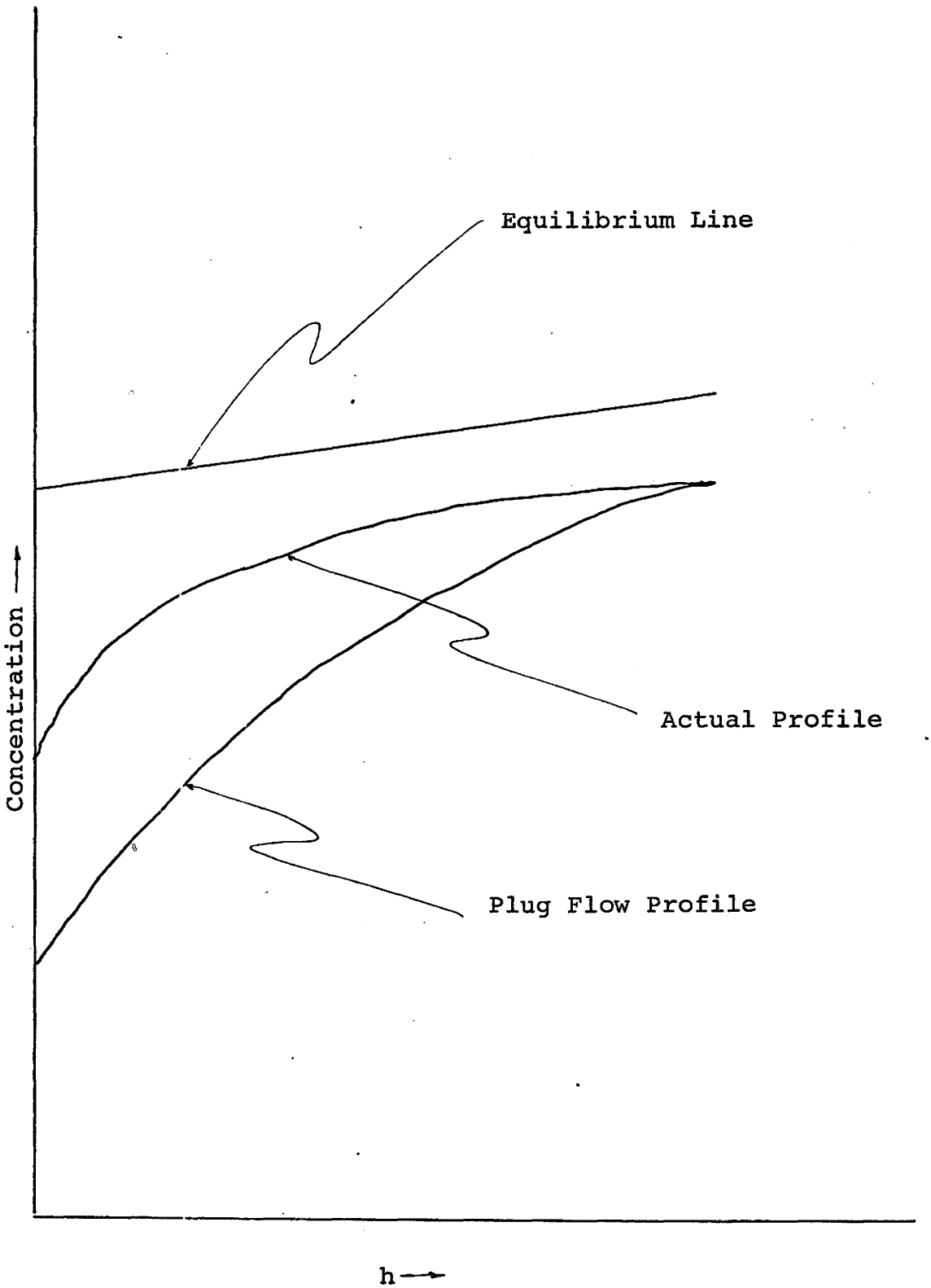
Equilibrium Line
Actual Profile
Plug Flow Profile
Concentration
h

Figure 7.12

Using the k_La arrived at for each run a computer program was written which iterated on the height until the outlet concentration equalled the outlet concentration of the particular run in question. The efficiency was then defined as :

$$E = \text{Height (plug flow)} / \text{Height (actual)} \quad (7.10)$$

The efficiency as defined is plotted in figues 7.13, 7.14, and 7.15 . As the gas flow rate increases the efficiency decreases; this can also be seen from the average values :

U_G= 0.388 cm./sec. -- 83.3% (1.2 plug flow columns)
U_G= 0.650 " -- 77.8% (1.29 " " ")
U_G= 1.165 " -- 71.5% (1.4 " " ")

Generally the effect of pulsation is to decrease the efficiency, no doubt through increased backmixing, although in several cases, particularly U_G= 0.388 cm./sec.(U_L= 1.6 cm./sec.) the effect is not great. The unpulsed cases appear to have slightly higher efficiencies no doubt due to the contribution to the backmixing made by the pulsations. There is no clear effect from the liquid flow rate although U_L=3.0 cm./sec. generally has the higher efficiencies over the three gas rates followed by U_L= 1.0 cm./sec. and then U_L= 1.6 cm./sec. .

In the previous discussion of the axial dispersion coefficient it was observed that some of the values appeared rather high; however, it can be said that the sensitivity to this parameter in the mass transfer work was not very good. The 95% level of confidence limits on this parameter show a wide spread. The lower end of these limits for the values that do appear high falls well into the region of support for the tracer work.

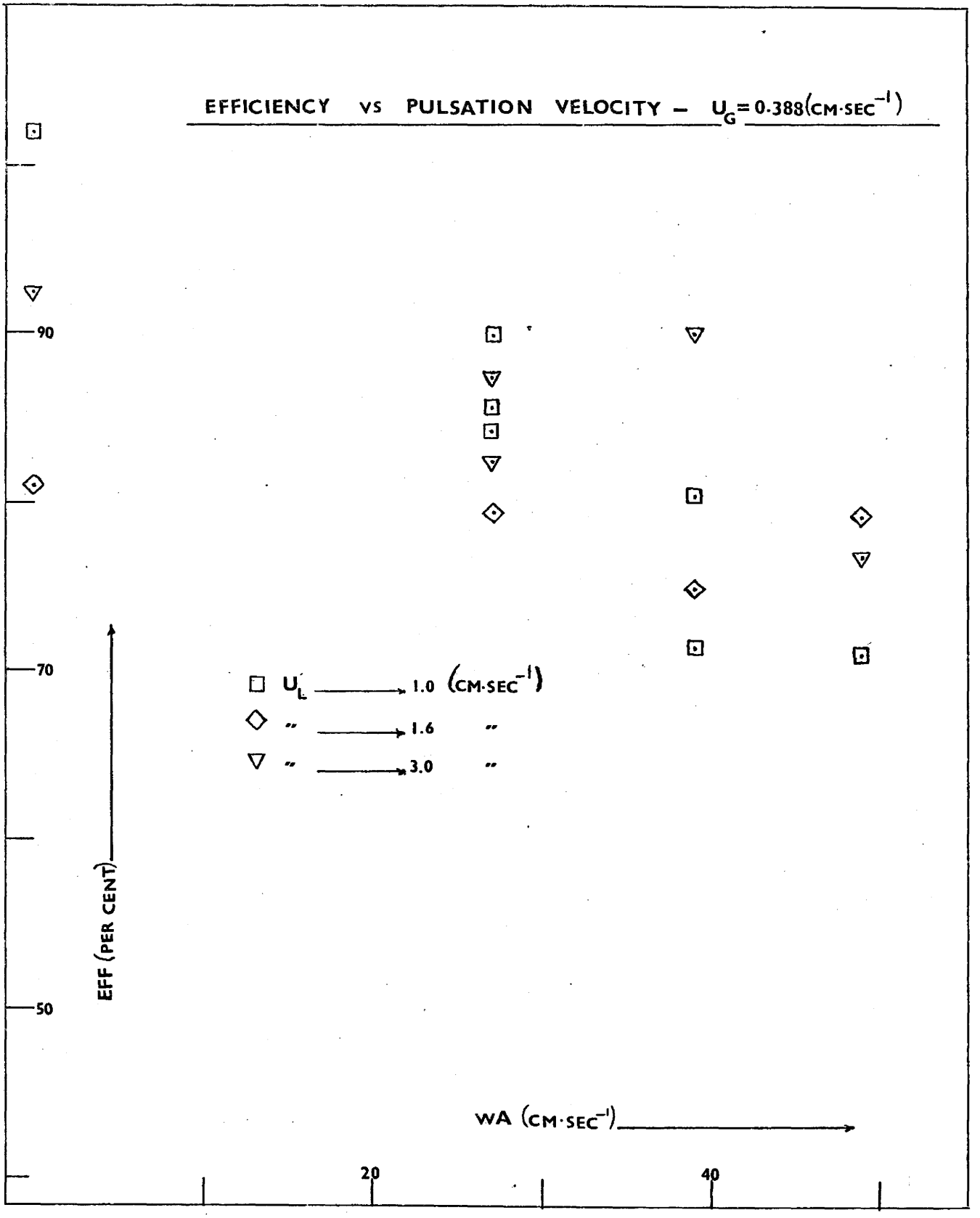
EFFICIENCY VS PULSATION VELOCITY – $U_G = 0.388 (CM \cdot SEC^{-1})$
90
70
50
EFF (PER CENT)
U_L ⟶ 1.0 $(CM \cdot SEC^{-1})$
" ⟶ 1.6 "
" ⟶ 3.0 "
WA $(CM \cdot SEC^{-1})$ ⟶
20
40

Figure 7.13

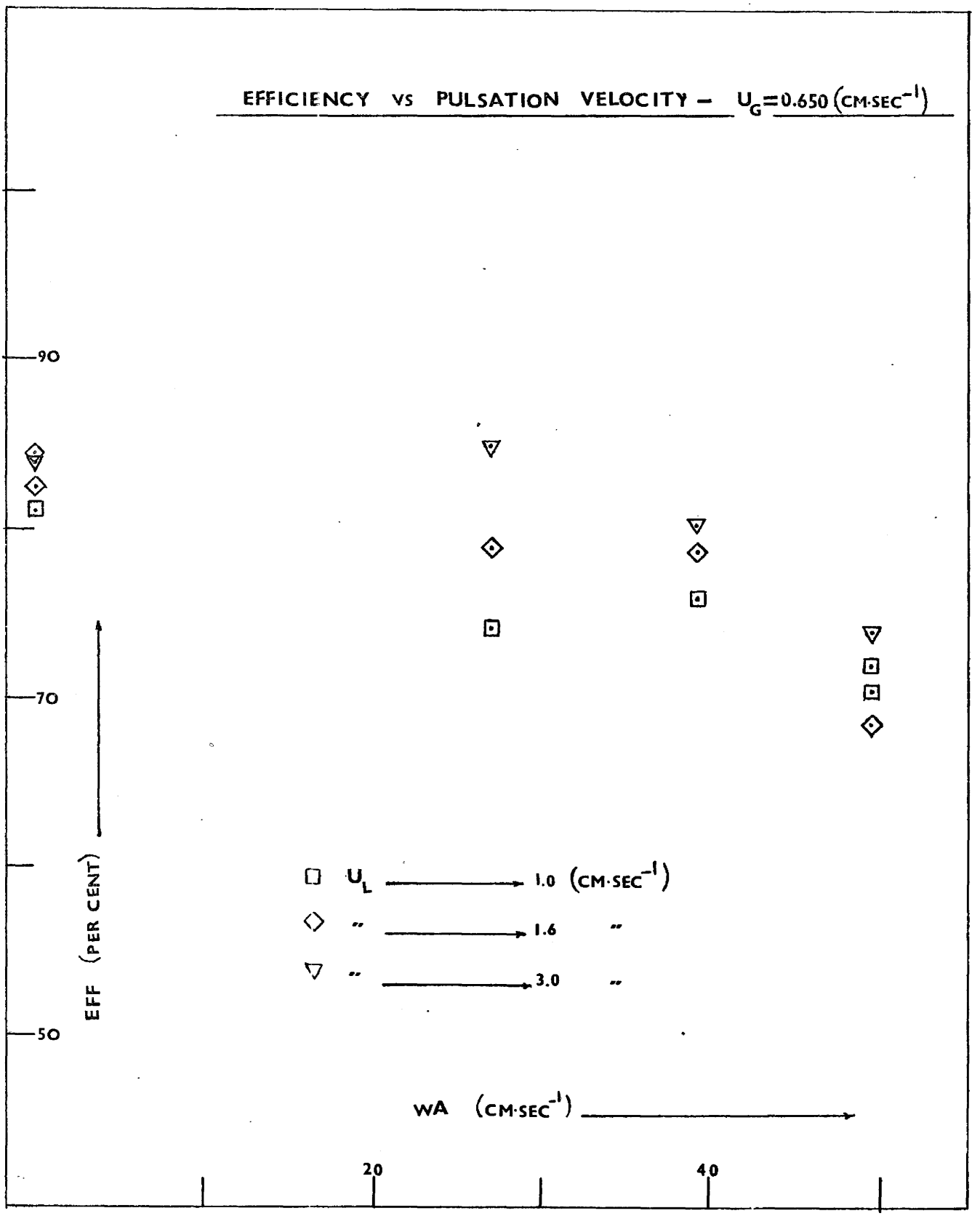
EFFICIENCY VS PULSATION VELOCITY – U_G=0.650 (CM·SEC^{-1})
90
70
50
EFF (PER CENT)
U_L ——→ 1.0 (CM·SEC^{-1})
" ——→ 1.6 "
" ——→ 3.0 "
WA (CM·SEC^{-1}) ——→
20
40

Figure 7.14

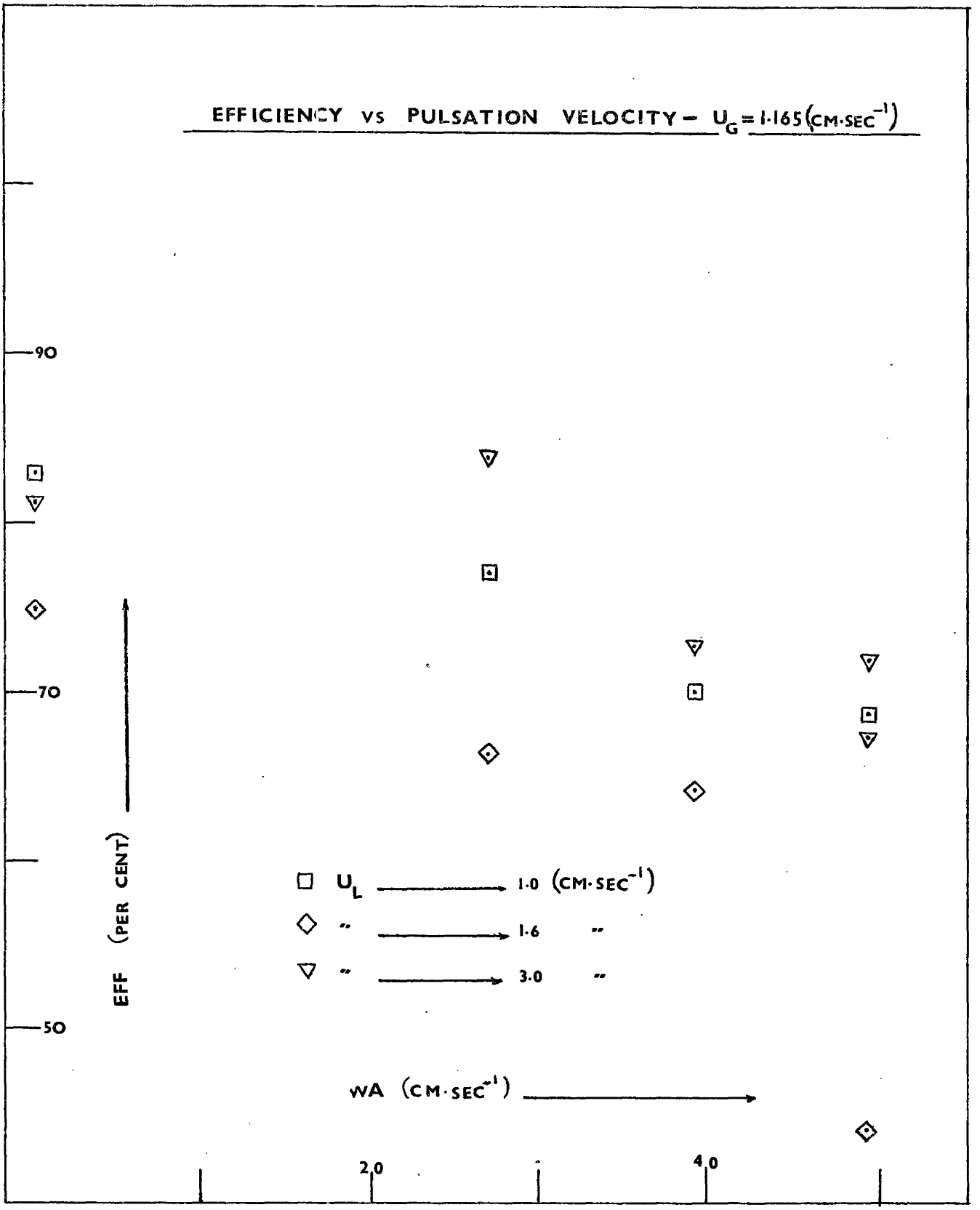
EFFICIENCY vs PULSATION VELOCITY – $U_G = 1.165 (CM \cdot SEC^{-1})$
90
70
50
EFF (PER CENT)
U_L ——— 1.0 $(CM \cdot SEC^{-1})$
" ——— 1.6 "
" ——— 3.0 "
WA $(CM \cdot SEC^{-1})$ ———
2.0
4.0

Figure 7.15

Looking through the mass transfer results shows this quite well. The results in the tracer work show much tighter confidence limits on the axial dispersion coefficient reflecting a more realistic value of this parameter. In fact drawing any firm conclusions as regards the axial dispersion coefficient data provided by the mass transfer work is not justifiable. However, although there are high values of the axial dispersion coefficient there are also plenty of other values that support the tracer experiments and generally the confidence limits are tighter here than for the higher value cases. The supporting values also show a lower residual sum of squares which of course effects the confidence limit spread. In the few cases of a high value of E_L plus a reasonably low residual sum of squares and low spread in the confidence limits the possibility of reflux is indicated with an improvement in the residual sum of squares.The reflux conditions as indicated by the mass transfer work tend to support the findings of the tracer work.

Of the forty-three mass transfer runs there are only two that show an inflated axial dispersion coefficient with a low residual sum of squares and tight confidence limits that give no indication of possible reflux. The values of the reflux parameter in both the mass transfer work and the mixing experiments are in fair agreement. The spread of the confidence limits in the reflux parameter are quite high as the addition of another parameter and loss of a degree of freedom tended to offset the improvement realized in the residual sum of squares when one of the reflux models was found to apply to the data.

Referring again to the effect of liquid flow rate on the axial dispersion coefficient one would have to conclude that although the mass transfer work indicated, (figure 7.2) as mentioned earlier, a dependence; the above

discussion of the high variance and coincidence of reflux surrounding this parameter really makes the tracer work's conclusion of little or no effect of liquid flow rate seem to be the valid conclusion.

8. Tracer Results/Discussion

In reviewing the results of the tracer experiments one of the objectives was to examine the factors affecting the reflux phenomenon. Also a number of investigators [1,4, 21,35] have found the axial dispersion coefficient to be independent of liquid flow rate. Chen [7] has developed a dependence using the relative velocity as a variable. In the tracer experiments done in this work it was found that no appreciable amount of tracer found its way to the sampling stations at the highest superficial liquid velocity used in the mass transfer work, U_L= 3.0 cm./sec. . At a superficial liquid velocity of 1.6 cm./sec. and a pulsation velocity of 55.0 cm./sec. the tracer concentration still remained virtually zero at the highest(farthest from the injection point) sampling point. Most runs were carried out at a superficial liquid velocity of 0.705 cm./sec. with several runs at 1.0 cm./sec. .

There did not appear to be any obvious dependence on the superficial liquid velocity at the rates used; figure 8.1 presents values of the axial dispersion coefficient in relation to the operating parameters with the presence or absence of reflux indicated. The varying of the liquid flow rate caused no observable change in the nature of the back-mixing mechanisms nor in the values obtained for the axial dispersion coefficient. Increasing the pulsation velocity generally had the effect of increasing the value of the axial dispersion coefficient. The backmixing contribution made by the application of pulsation to the system is clearly shown in figure 8.1 at U_G= 0.0 cm./sec. .

The various workers using the steady-state method invariably found good linear relationships in semi-log plots of c/c_o versus position. Often a semi-log plot of the experimental results obtained in this work would show a tailing off at low values of c/c_o ; it was felt that this

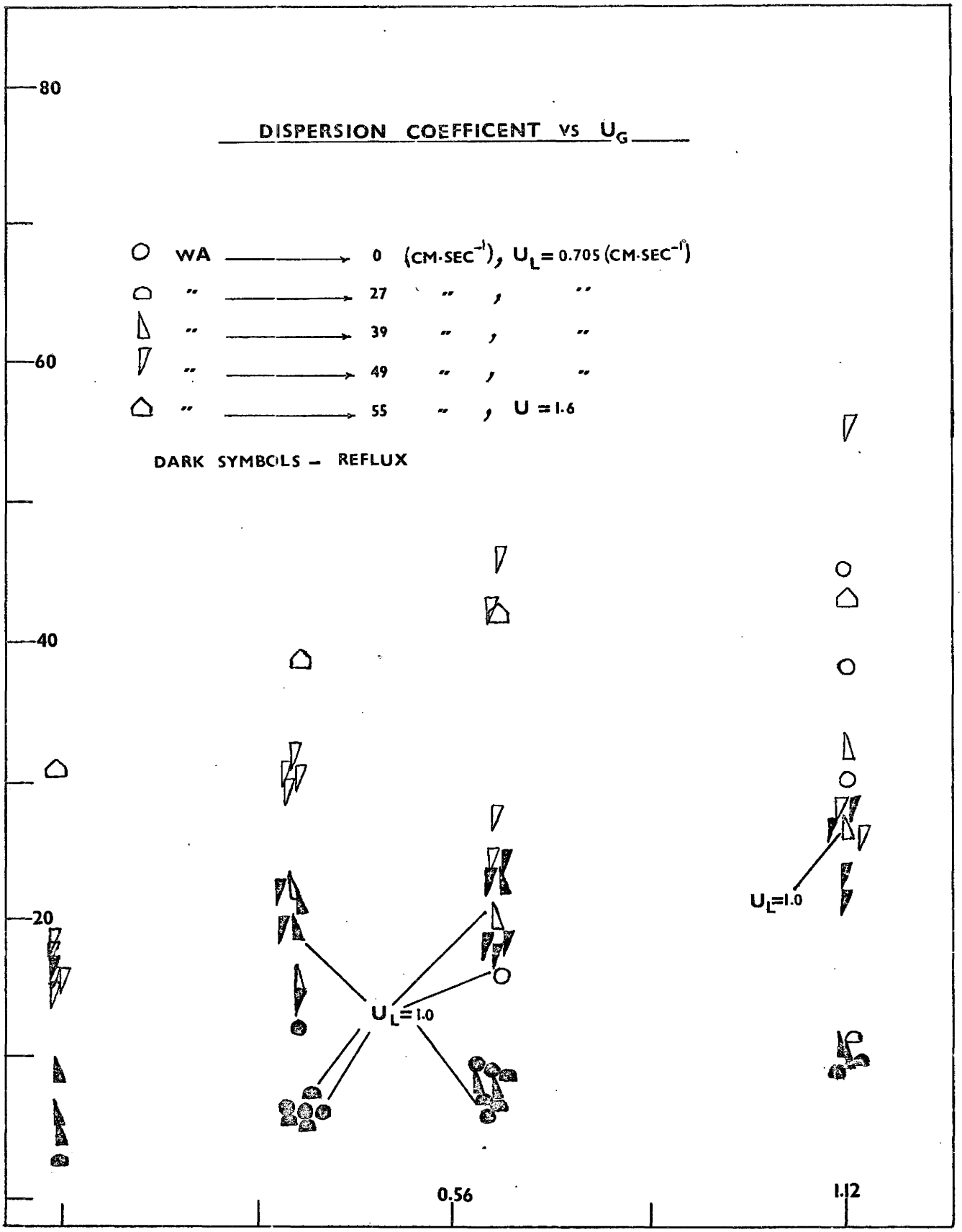
80
60
40
20
DISPERSION COEFFICENT VS U_G
WA ——→ 0 (CM·SEC^{-1}), U_L = 0.705 (CM·SEC^{-1})
" ——→ 27 " , "
" ——→ 39 " , "
" ——→ 49 " , "
" ——→ 55 " , U = 1.6
DARK SYMBOLS – REFLUX
U_L=1.0
U_L=1.0
0.56
1.12

Figure 8.1

tailing off was the result of refluxing. Figure 8.2 is a plot of experimentally obtained data exhibiting this effect. Figure 8.3 on the other hand shows a good linear relationship obtained from the experimental data. Looking at figures 8.4 and 8.5 the areas affected by the reflux phenomenon may be noted both for the tracer work and in the mass transfer work. The reflux condition would appear to be a rather complicated event with no clear cut conditions required for its appearance but rather with general broad areas seeming prone to refluxing, others escaping it and still others appearing to be in a border or probability region.

When the reflux model was applied to the mass transfer data it was thought that similar trends in the areas subject to refluxing might show themselves. Figures 8.4 and 8.5 show reasonably good agreement with respect to the reflux pattern indicated. It is therefore concluded that during the mass transfer work the column was refluxing under conditions sensitive to the reflux phenomenon. Values of the reflux ratio are plotted in relation to the operating parameters in figure 8.6 . In figure 8.1 the trend is for the axial dispersion coefficient to increase with an increase in either superficial gas velocity or pulsation velocity. It is interesting to observe that even with no gas flowing both modes of backmixing are generated by the application of pulsation alone. This is no doubt due to the interaction between the baffle plates and the support collars possibly aided by some asymmetry in the configuration of the column's internals. The effect of reflux on the value of the axial dispersion coefficient can also be seen in figure 8.1; the appearance of reflux tends to depress the values obtained for the axial dispersion coefficient.

The normal method of correlating the axial dispersion coefficient is against the superficial gas velocity or it is included in an assorted variety of Peclet or Dispersion

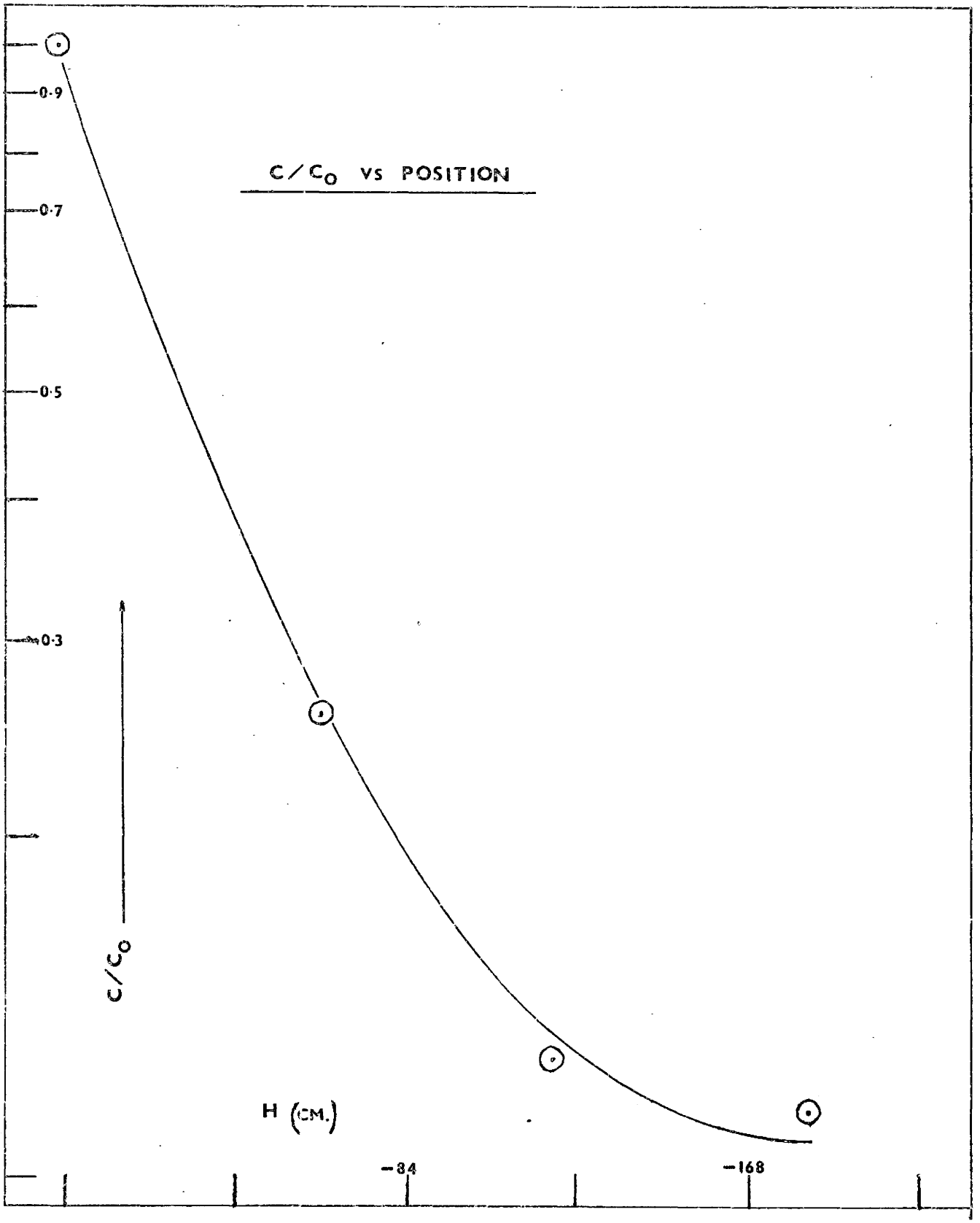

Figure 8.2

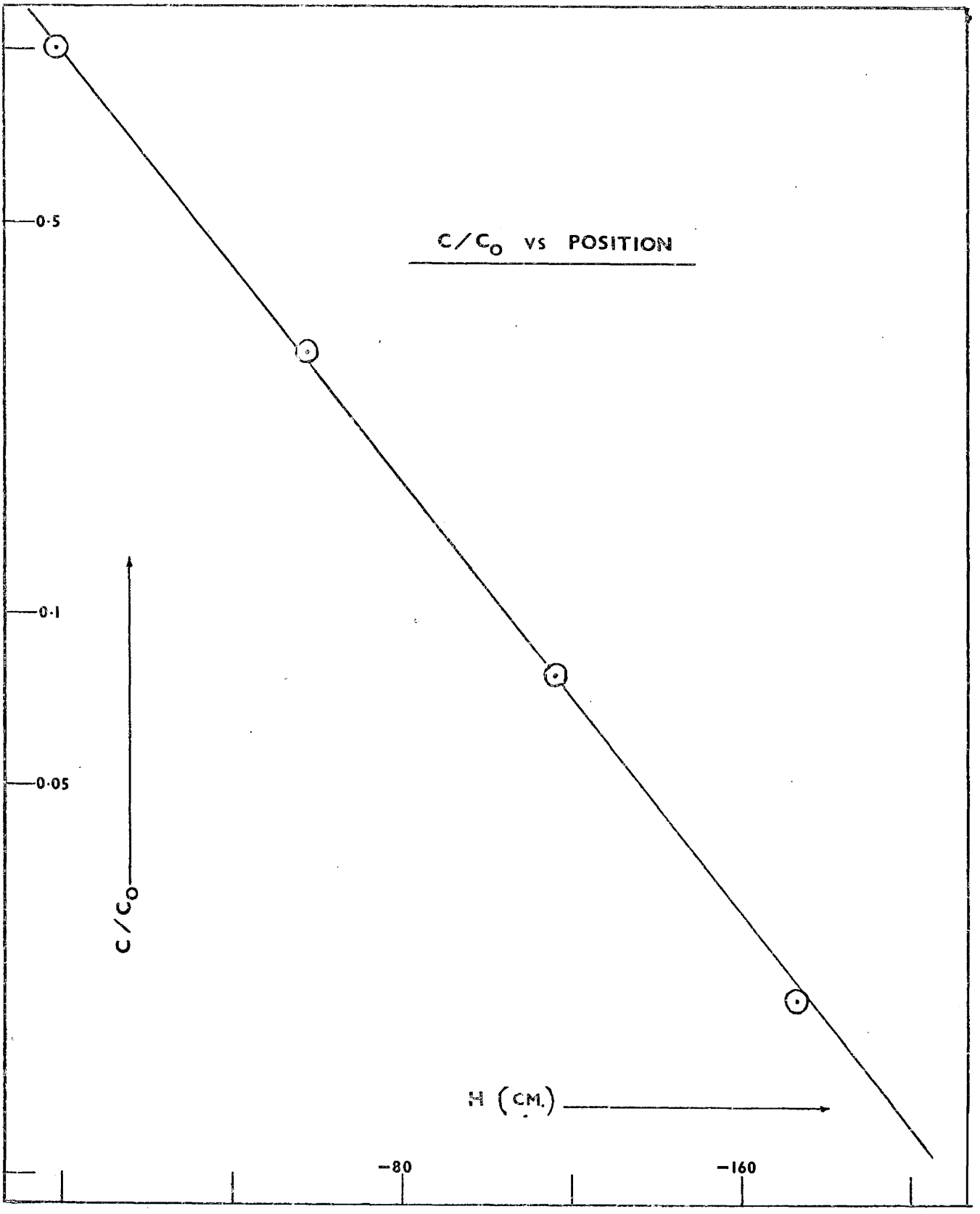

Figure 8.3

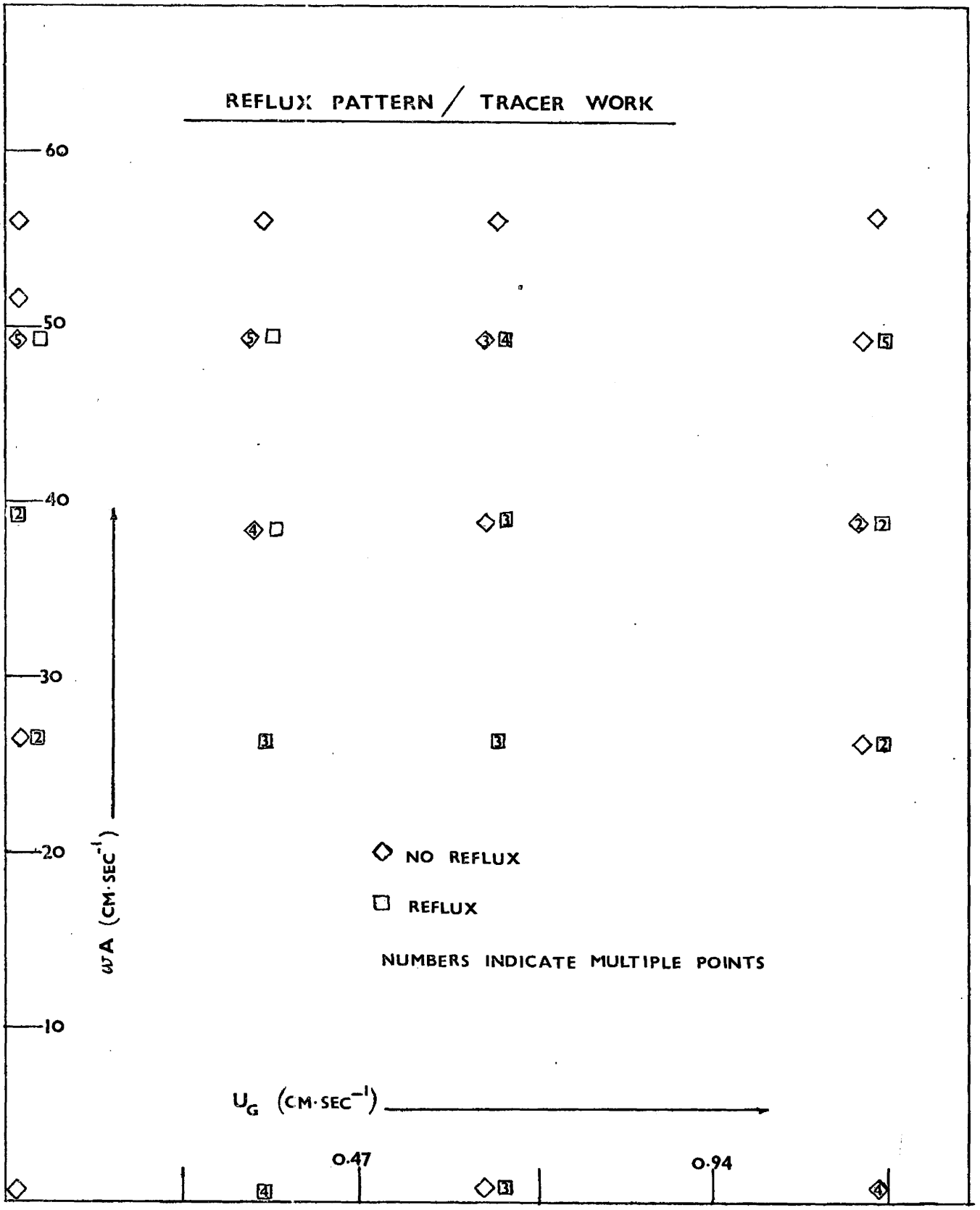
REFLUX PATTERN / TRACER WORK
60
50
40
30
20
10
ωA (CM·SEC⁻¹)
NO REFLUX
REFLUX
NUMBERS INDICATE MULTIPLE POINTS
U_G (CM·SEC⁻¹)
0.47
0.94

Figure 8.4

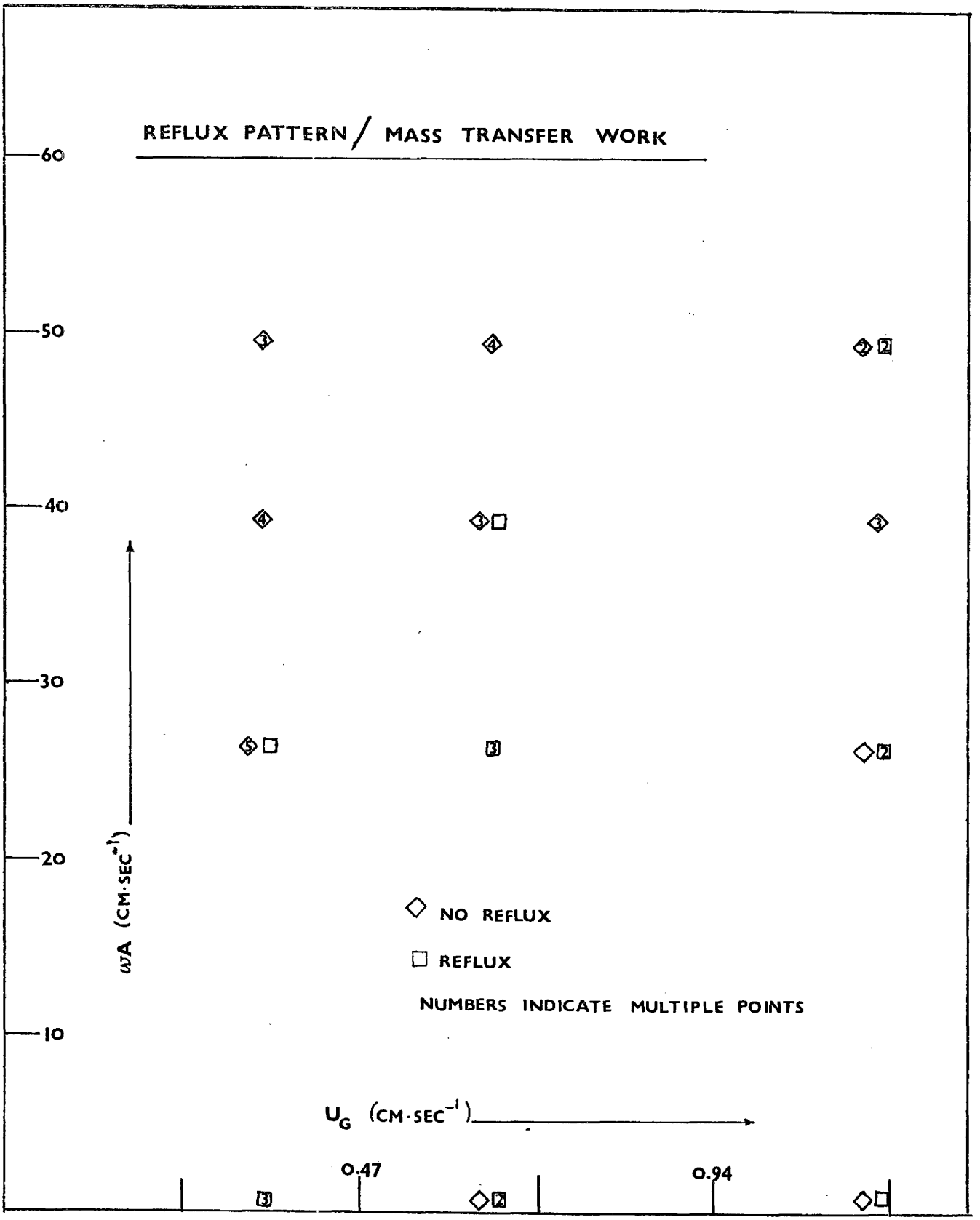
REFLUX PATTERN / MASS TRANSFER WORK
60
50
40
30
20
10
ωA (CM·SEC⁻¹)
NO REFLUX
REFLUX
NUMBERS INDICATE MULTIPLE POINTS
U_G (CM·SEC⁻¹)
0.47
0.94

Figure 8.5

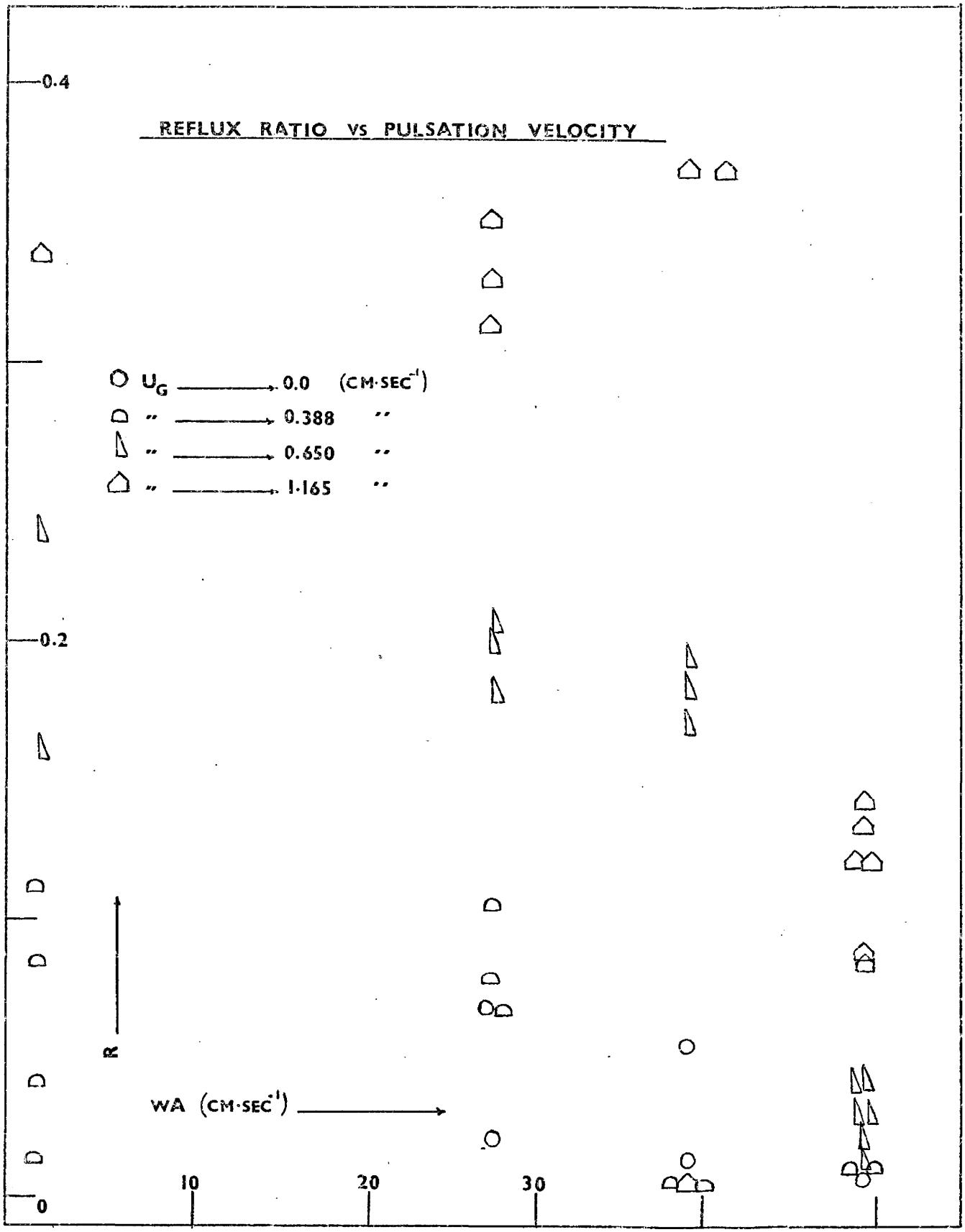
REFLUX RATIO VS PULSATION VELOCITY
0.4
0.2
0
U_G ——→ 0.0 (CM·SEC^{-1})
" ——→ 0.388 "
" ——→ 0.650 "
" ——→ 1.165 "
R
WA (CM·SEC^{-1}) ——→
10
20
30

Figure 8.6

numbers and then correlated against the superficial gas velocity. In figure 8.7 a Dispersion number is correlated against the ratio of the superficial gas velocity and the superficial liquid velocity. Two linear relationships are indicated. The lower line,

$$E_L/D_T U_L = 0.74(U_G/U_L) + 1.56 \quad (8.1)$$

passes through the strongly refluxed points (figure 6.2). The reflux points group quite well about the other line:

$$E_L/D_T U_L = 1.30(U_G/U_L) + 4.78 \quad (8.2)$$

The non-reflux points show considerable more scatter about this line (8.2) ; however, if the confidence limits (95% level) are examined,the ten non-reflux points which show the dispersion number to be greater than 8.0 (these ten show the largest deviation from the indicated linear relationship of the non-relux points) also show the largest percentage spread in their confidence limits: 43.3% versus 15.1% for the sixteen other non-reflux points which tend to group about the linear relationship indicated. The high percentage spread in the confidence limits plus the higher numerical value of the off-points would place them well within the linear region indicated by the other more reliable data points on the low side of their confidence limits. The absence of the pulsation velocity in this correlation might be questioned; however, Vermeulen et al. [36] reported that similar correlations using Peclet numbers held for pulsed as well as unpulsed columns in the liquid-liquid systems with which he was working. From figure 8.1 it can be seen that the bulk of the values for the axial dispersion coefficient are grouped between 6 and 30 cm^2./sec. . These values for the axial dispersion coefficient may be compared

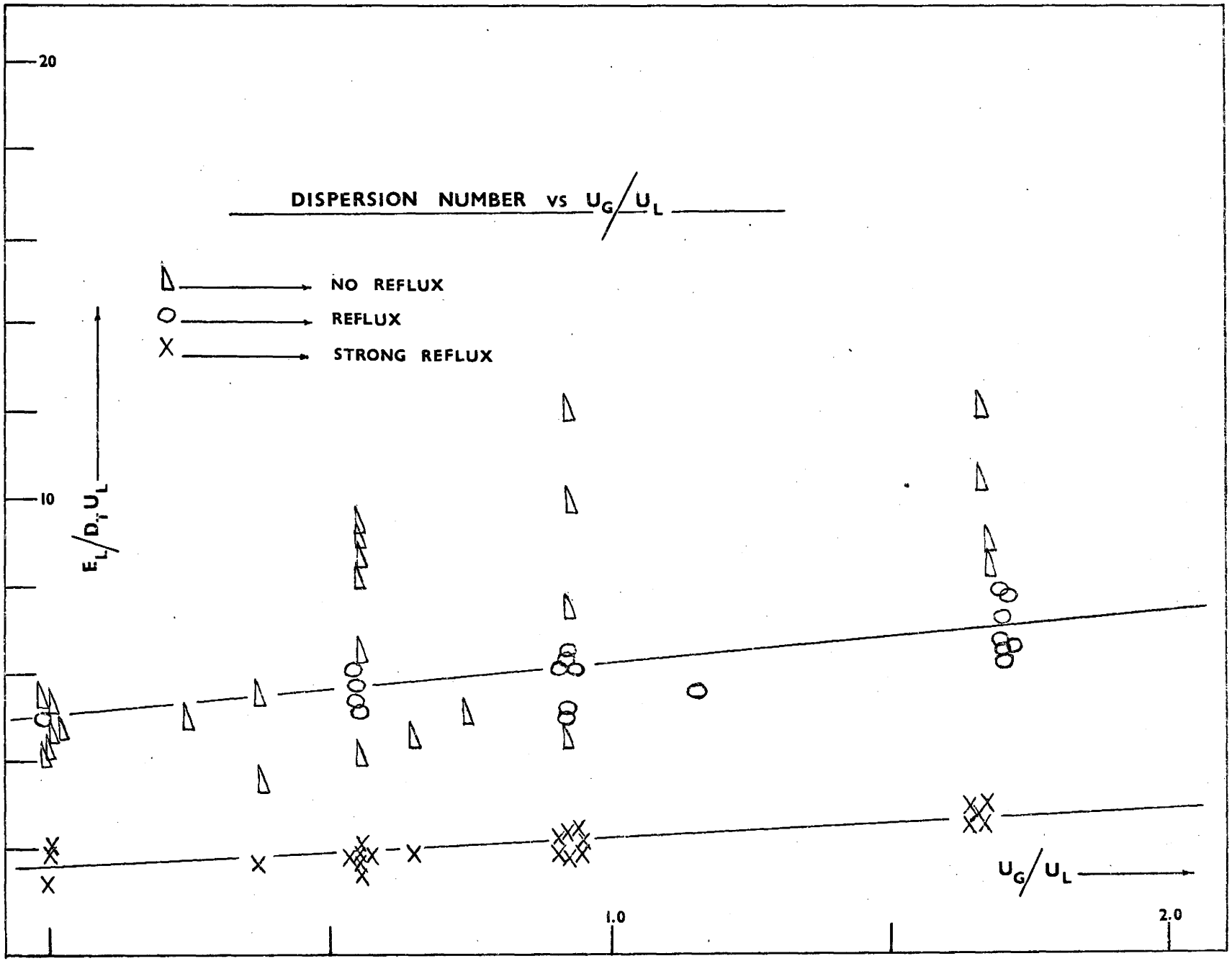
DISPERSION NUMBER vs U_G/U_L
NO REFLUX
REFLUX
STRONG REFLUX
$E_L/D_T U_L$
20
10
1.0
2.0
U_G/U_L

Figure 8.7

to values obtained by others.

Reith et al. [30] operated a conventional unbaffled bubble column of the same diameter as the one used here. For comparable superficial gas velocities they report values of the axial dispersion coefficient from 25-30 $cm^2./$ sec. . These values are slightly higher than the values obtained in this work for no pulsation; however , the overall picture is reasonably in line with the work of Reith. Reith found the onset of slug flow to occur at a superficial gas velocity of 5.0 cm./sec. . In this column the onset of slug flow occurred at a superficial gas velocity of approximately 2.5 cm./sec. ; the lower velocity here was no doubt due to the column's internals. Reith pointed out that the eddy diffusion model is not applicable to slug flow in small columns; they also showed that column diameter was an important factor influencing the value of the axial dispersion coefficient. Thus any comparison of the values obtained here with those of other workers using columns not of the same or nearly the same column diameter would not be very instructive.

Argo and Cova [1] using a cocurrent column of 1.8 inches diameter conducted mixing experiments both with baffling and without. The baffled cases show values for the axial dispersion coefficient that are somewhat lower than those of the unbaffled cases; this coincides with the fact that the values here found for the cases where the pulsation velocity was zero are somewhat lower than the values found by Reith et al. for comparable superficial gas velocities. Reith used no baffles. It would seem that the obstruction represented in the column's internals has an effect similar to that of decreasing the column's diameter i.e. values obtained for the axial dispersion coefficient are lower and the onset of slug flow occurs at a lower superficial gas velocity. Argo and Cova report values of

around 13.0 cm^2./sec. at comparable gas flow rates. They found that the superficial liquid velocity had no noticeable effect on the values obtained for the axial dispersion coefficient. Argo and Cova also found the axial dispersion coefficient to increase with increasing column diameter. Both Reith et al. and Argo & Cova presented Peclet number correlations.

Tadaki and Maeda [35] using a 5.0 cm. column reported values for the axial dispersion coefficient from 15-50 cm^2./sec. . They concluded that the axial dispersion coefficient increased with increasing gas flow rate; they observed no effect of the liquid flow rate. Generally this has been the case - liquid flow rate has not had an effect on the values obtained for the axial dispersion coefficient. However in the case of packed bubble columns Chen [7] and Chen & Douglas [8] report an effect of liquid flow rate on the axial dispersion coefficient. Chen explains the dependence is derived from the relative velocities of the two phases and that the packings used by him have been shown to reduce the rise velocity of bubbles by as much as one third the unimpeded rise velocity. Siemes & Weiss [33] and Ohki & Inoue [28] both examined mixing in batch systems. Ohki used a 4.0 cm. column and found values of the axial dispersion coefficient ranging from 10-30 cm^2./sec. over superficial gas velocities of 2-4 cm./sec. .

Eissa and El-Halwagi [13] operated a 5.0 cm. column in a countercurrent fashion. At the low end of their (high end of this work) gas flow rate range Eissa reports values of the axial dispersion coefficient ranging from 25-32 cm^2./sec. over the range of liquid flow rates used. Eissa et al. claim an effect of liquid flow rate; however at the lower end of the superficial gas velocity range this effect of liquid flow rate is quite small. Its signifigance

increases as the gas flow rate increases. Eissa and El-Halwagi also investigated the radial concentration profiles in their column in order to determine the value of the radial dispersion coefficient. They found radial gradients of any signifigance to persist for about a column diameter above and below the tracer injection point. They concluded that radial mixing effects were quite minor compared to the axial mixing effects. Reith et al. found no signifigant radial variations and Argo & Cova reported signifigant radial concentration gradients at only one condition which they attributed to their physical setup. In this work no signifigant radial concentration variations were found at the sampling position nearest the tracer injection point.

Sullivan and Treybal [34] using a multistage agitated column found values for the axial dispersion coefficient of 10-17 cm^2/sec. and used a dispersion number correlation to present their mixing results. Their column was 6 inches in diameter and had 12 compartments each 3.28 inches high. In light of previous work in this area the values of the axial dispersion coefficient obtained in this work represent no obvious departure from the literature reported values.

9. Conclusions/Recommendations

It is clear that there was a signifigant improvement in $k_L a$ due to the application of external agitation in the form of pulsations. A fair degree of backmixing could also be attributed to the same pulsations. The effect of increasing the gas flow rate is to progressively deteriorate the efficiency of the apparatus by increasing the backmixing. At the lowest gas flow rate a 20%(average) increase in column height was used over that required for the same degree of mass transfer for the plug flow case; this efficiency fell to a 40% increase for the highest gas flow rate used. If there was an effect of liquid flow rate on the axial dispersion coefficient it was not clear and the dominant factors affecting the value of the axial dispersion coefficient were pulsation velocity, superficial gas velocity and the reflux phenomenon. Although the efficiency dropped with increasing pulsation velocity the number of transfer units experienced a slight increase. Pulsation was then a rather mixed blessing; the number of transfer units and $k_L a$ increased while the efficiency decreased.

Mashelkar [25] has reported that investigations into the sectionalizing of bubble columns have shown that a reduction in the degree of backmixing can be realized in this fashion. Perhaps placing mesh across the cross section of the column at regular intervals would be an improved design. It would accomplish two things: it would tend to sectionalize the column and hopefully then reduce the backmixing; also, the placing of mesh at right angles to the flow direction should allow for a sturdy symmetrical configuration without any undue difficulties. The interesting points here would be the effects of spacing, mesh size, and mesh thickness on $k_L a$, and E_L . No doubt an optimal configuration study could be done correlating the various parameters mentioned as well as the power consumption.

Mesh of a suitable size should provide an excellent shear surface for the bubbles in the presence of pulsation. Also the mesh could perhaps be used as a porous packing which would likely raise the power consumption but also tend to decrease the backmixing [25]. Thus the pulsed bubble column when operated in a countercurrent fashion retained the level of performance in terms of k_La shown in previous [3,15] studies. It did suffer from the effects of backmixing but no more so than unpulsed bubble columns reported in the literature.

References

1. Argo W.B., Cova D.R.; Ind. Engng. Chem.-P.D.D., 4(1965)352

2. Baird M.H.I.; A.I.Ch.E.-Int. Chem. Eng., Symposium Ser. 6, pg. 53, London Instn. Chem. Engnrs. (1965)

3. Baird M.H.I., Garstang J.H.; Chem. Engng. Sci., 27(1972) 823

4. Bischoff K.B., Phillips J.B.; Ind. Engng. Chem.-P.D.D. 5(1966)416

5. Buchanan R.H., Teplitsky D.R., Oedjve D.; Ind. Engng. Chem.-P.D.D., 2(1963)173

6. Calderbank P.H.; Trans. Instn. Chem. Engnrs., 37(1959) 173

7. Chen B.; Can. J. Chem. Engng., 50(1972)436

8. Chen B., Douglas W.J.M.; Can. J. Chem. Engng., 47(1969) 113

9. Danckwerts P.V.; Trans. Faraday Soc., 46(1950)300

10. Danckwerts P.V.; A.I.Ch.E.J., 1(1955)456

11. Danckwerts P.V.; Ind. Engng. Chem., 43(1951)1460

12. Eissa H., El-Halwagi M., Saad M.; Chim. Ind. Gen. Chimq. 103(1970)1132

13. Eissa H., El-Halwagi M.; Chim. Ind. Gen. Chimq., 104(1971) 2080

14. Gal-Or B., Hauk J.P., Hoelscher H.E.; Int. J. Heat and Mass Transfer, 10(1967)1559

15. Garstang J.H.; Ph.D. Thesis, Univ. of Edinburgh (1970)

16. Gillespie B., Carberry J.J.; Ind. Engng. Chem.-Funda., 5(1966)164

17. Hanson C.; Chem. Engng., 75(1968)18

18. Hartland S., Mecklenburgh J.C.; Chem. Engng. Sci., 21 (1966)1209

19. Haug H.F.; A.I.Ch.E.J., 17(1971)586

20. Higbie R.; Trans. A.I.Ch.E., 31(1935)365

21. Hoogendoorn C.J., Lips J.; Can. J. Chem. Engng., 43 (1965)125

22. Jamrack W.D.; "Rare Metal Extraction by Chemical Engineering Techniques", Pergamon Press, London(1963)

23. Levenspiel O.; "Chemical Reaction Engineering", J. Wiley and Sons (1967)

24. Marquardt D.W.; J. Soc. Ind. Appl. Math., 11(1963)431

25. Mashelkar R.A.; Br. Chem. Engng., 15(1970)1299

26. Mellon M.G.; "Analytical Absorption Spectrscopy", J. Wiley and Sons (1950)

27. Montgomery H.A.C., Thom N.S., Cockburn A.; J. Appl. Chem., 14(1964)280

28. Ohki Y., Inoue H.; Chem. Engng. Sci., 25(1970)1

29. Pomeroy R., Kirschman H.D.; Ind. Engng. Chem.-Anal., 17(1945)715

30. Reith T., Renken S., Israel B.A.; Chem. Engng. Sci., 23(1968)619

31. Sawyer C.N.; "Chemistry for Sanitary Engineers", McGraw-Hill (1960)

32. Sideman S., Hortascu O., Fulton J.W.; Ind. Engng. Chem, 58(1966)38

33. Siemes W., Weiss W.; Chemie Ind. Tech., 29(1957)727

34. Sullivan G.A., Treybal R.E.; Chem. Engng. J.,1(1970)302

35. Tadaki T., Maeda S.; Chem. Engng.(Japan), 2(1964)195

36. Vermeulen T., Moon J.S., Hennico A., Miyauchi T.; Chem. Engng. Prog., 62(1966)95

37. Wilson A.W.; Ph.D. Thesis, McMaster University (1971)

38. Whitman W.G.; Chem. and Met. Engng., 29(1923)127

39. Wylie C.R.; "Advanced Engineering Mathematics", McGraw-Hill (1960)

40. "Standard Methods for the Examination of Water and Wastewater", Amer. Publ. Health Assoc. Inc., 1790 Broadway, New York 19, N.Y. (1960)

41. Draper N.R., Smith J.R.; "Applied Regression Analysis", J. Wiley and Sons (1967)

APPENDICES

Appendix 1-Flow Rate Calibrations

The flow meter used for the oxygen gas was calibrated in the following manner. Oxygen leaving the gas cylinder was reduced to 40 psig through a regulator, then flowed to the flow meter and through a needle valve. Tygon tubing was affixed to the copper tubing leading from the valve. To measure the gas flow rate, the gas was simply collected into a litre sized graduated cylinder over water; a stop watch was used to measure the collection time and the volume collected was easily read off the graduated cylinder.

After collecting the level of water in the cylinder and in the collection vessel holding the water were equalized so as to obtain a reading corrected to atmospheric conditions. In table A the results of the calibration are shown corrected to 754 mm Hg saturated atmospheric pressure and 21.5 C. The results are also plotted in figure A.

Table A

Flow Meter Setting	Litres	Time(sec.)	Ft /Hr(Avg.)
2	0.940	158.5	
	0.945	162.2	
	0.940	156.5	
	0.960	160.9	0.754
4	0.960	94.2	
	0.895	88.5	
	0.950	93.3	
	0.930	90.6	
	0.925	90.0	1.298
7	0.785	40.2	
	0.905	43.7	
	0.900	43.0	
	0.875	42.0	
	0.910	43.9	2.612
10	0.908	30.8	
	0.927	31.3	
	0.930	31.1	
	1.840	62.7	

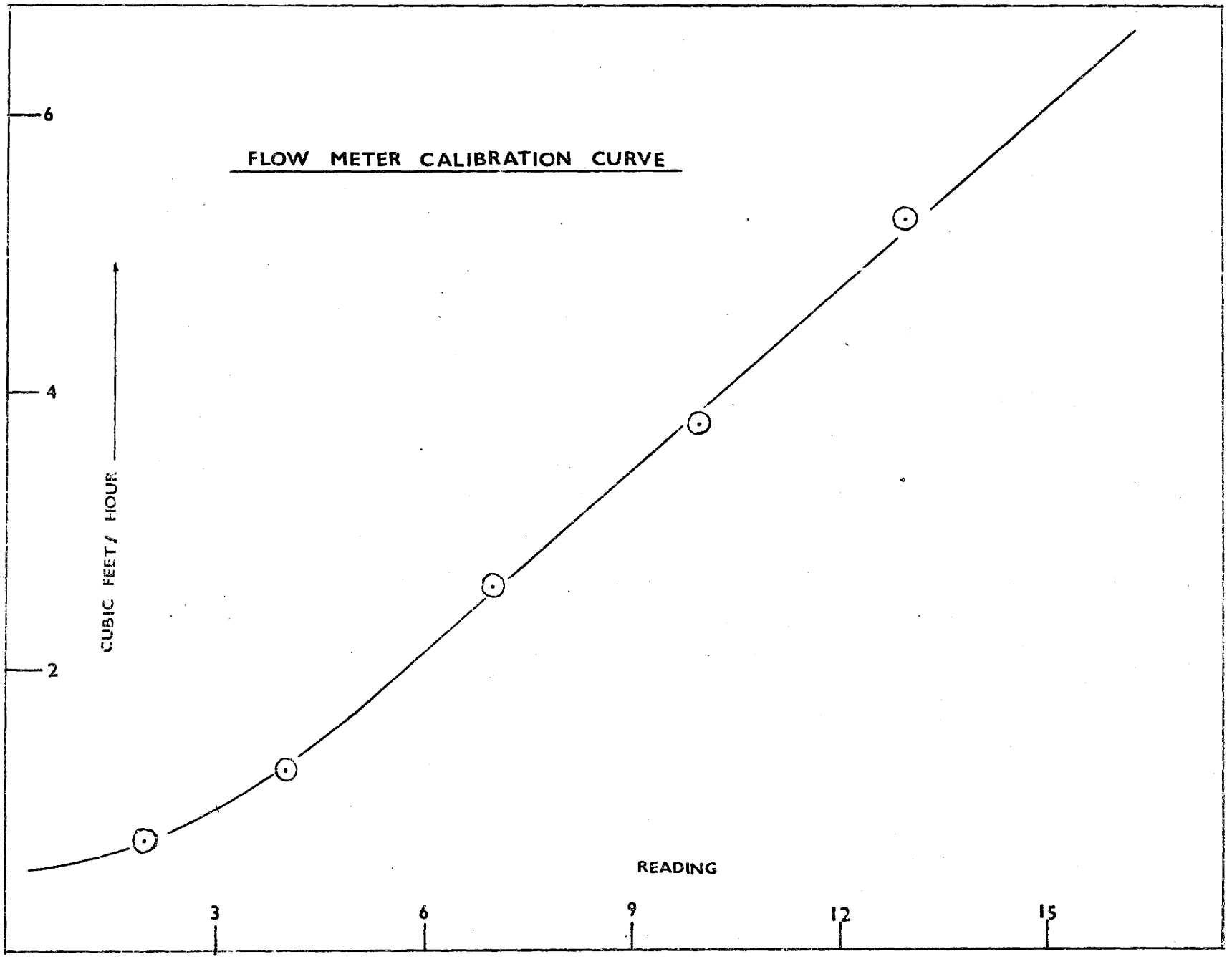
FLOW METER CALIBRATION CURVE
6
4
2
CUBIC FEET / HOUR
READING
3
6
9
12
15

Figure A

Table A (cont'd.)

Flow Meter Setting	Litres	Time (sec.)	Ft /Hr (Avg)
10	0.925	31.2	3.763
13	0.916	22.4	
	0.905	21.8	
	1.870	45.2	
	1.850	44.7	
	1.850	45.1	
	1.860	45.6	5.233

The water flow rate was checked before runs using a stop watch and a litre cylinder; the variable speed pumps could then be adjusted for the flow rate desired.

Appendix 2-Tracer Analysis

The material chosen as the tracer was potassium dichromate. It was felt that being an inorganic material its surface effects in the two phase system would be less than many of the common organic tracer materials. Adsorptive transport of the material by the bubbles was considered to be negligible. In the concentration used the density difference was low, only about 0.6%. The instrument used as a detector for this part of the work was a Bausch & Lomb Spectronic 20. The specifications reported by the manufacturer show photometric accuracy 2.5% of full scale and photometric reproduceability 1% of full scale.

The wavelength chosen was 491 millimicrons and the concentration of the tracer was 0.009 molar and lower. Figure A shows the plot of Absorbance vs concentration; absorbance being defined as the logarithm of the inverse of the transmission. For calibrating the instrument, solutions of known strength were made up using tap water since tap water was being used in the column. The results of the calibration are presented in table A and a plot of absorbance vs concentration is shown in figure A.

Table A

Cell	Solution	Transmission(%)	1/Transmission
#1	0.01 molar	8.5	11.75
#2	0.008 "	12.0	8.34
#3	0.0067 "	18.0	5.55
#4	0.005 "	27.0	3.70
#5	0.004 "	36.0	2.77
#6	0.0033 "	44.1	2.27
#7	0.0025 "	54.0	1.85
#8	0.0017 "	69.0	1.45
#9	tap water	100.0	1.00

Figure A indicates that the Beer-Lambert law is followed by the solutions of potassium dichromate in tap water.

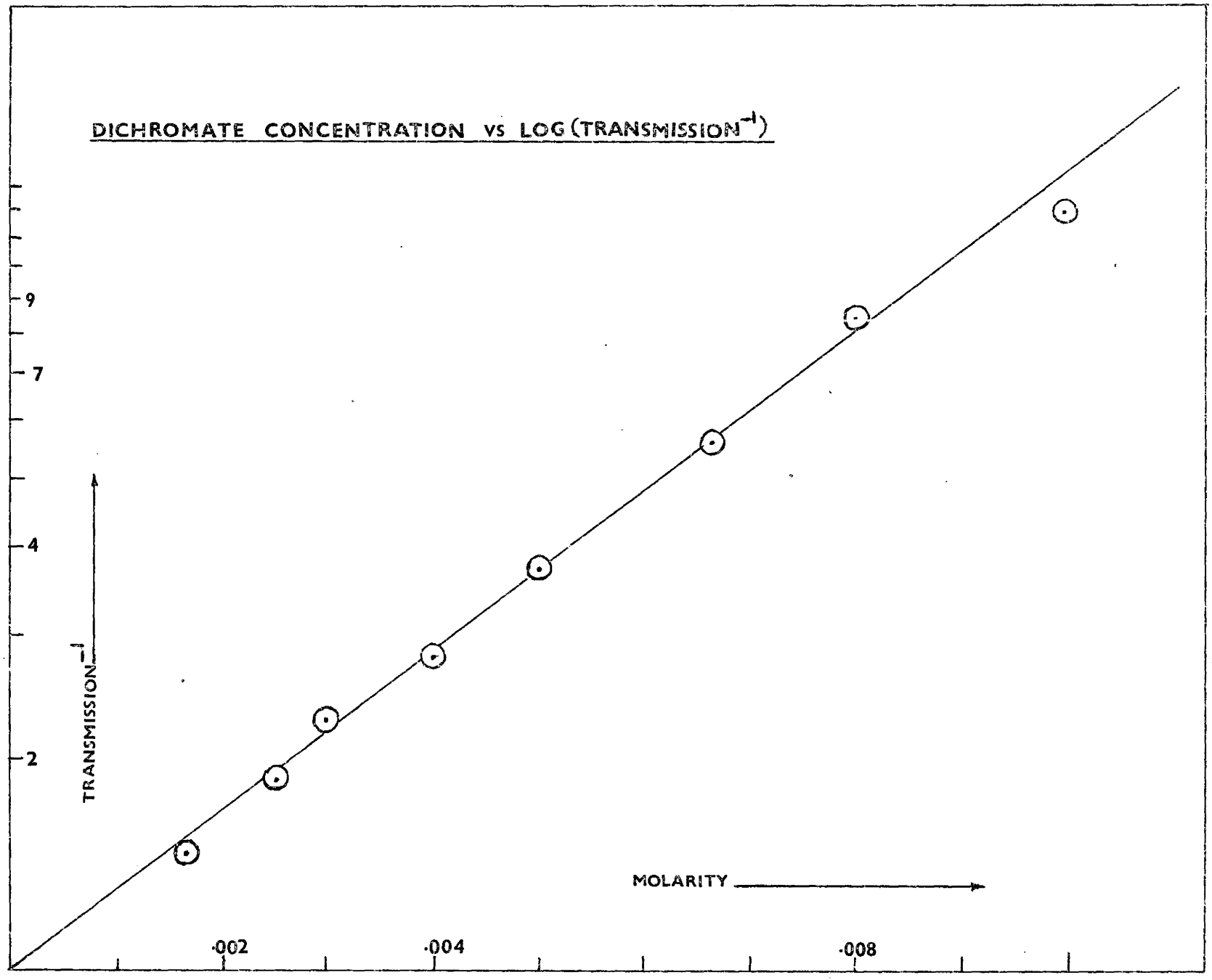
DICHROMATE CONCENTRATION vs LOG (TRANSMISSION^{-1})
9
7
4
2
TRANSMISSION^{-1}
MOLARITY
·002
·004
·008

Figure A

Thus the absorbance is directly proportional to the concentration of tracer.

During the course of the work the optical cells were checked several times against each other. A typical result is shown in table B for a solution of 0.005 molar potassium dichromate placed in cells 1-9 .

Table B

Cell	Transmission (%)
#1	27.0
#2	27.0
#3	27.0
#4	27.0
#5	27.0
#6	27.2
#7	26.5
#8	27.0
#9	27.0

As can be seen from table B the checks showed the cells to be within 1/2% or better. The 491 millimicrons provided the largest spread compared to the other wavelengths available on the machine. As far as temperature effects are concerned, Mellon [26] mentions that chromate ion at 436 millimicrons shows only a 0.1% change in absorbance per centigrade degree; 2,4-dinitrophenalate ion considered to be very sensitive, shows a 1% per centigrade degree change shift towards red. Since the temperature of this work was 25^{o}C$\pm$1 it is felt that any variations in temperature of this magnitude were not signifigant.

Appendix 3-Chemical Analysis

The chemical analysis for the measurement of dissolved oxygen is now outlined. The sampling vessels were 50 ml. volumetric flasks with ground-glass, tapered stoppers. The alkalai-iodide solution was prepared by dissolving 400 grams of sodium hydroxide pellets in 560 mls. of boiled distilled water still hot from the boiling and also adding 900 grams of sodium iodide. This is about 7 times the normal amount of iodide used. According to Montgomery [27] the higher iodide content provides increased accuracy by eliminating losses from iodine volatilisation; sharpening the end-point, and providing a precipitate that dissolves rapidly and completely. During the course of this work the dissolving of the precipitates was always accomplished without difficulty and the end-points normally were quite sharp. The manganous sulphate solution consisted of 364 grams of $MnSO4.H2O$ per litre. A 15% solution of sodium azide was the third reagent.

An outline of the chemistry of the Winkler analysis is given by Sawyer [31]. The analysis utilizes the fact that oxygen will oxidize $Mn+2$ to a higher state of valence under alkalai conditions and that manganese in higher states of valance is capable of iodide ion to free iodine under acidic conditions.

$$Mn+2 + 2OH- = Mn(OH)2 \quad \text{white ppt.}$$

or if oxygen is present :

$$Mn+2 + 2OH- + O = MnO2 + H2O$$

brown hydrated oxide

now under acidic conditions :

$$MnO2 + 2I- + 4H+ = Mn+2 + I2 + 2H2O$$

The iodine liberated is available for titration with thiosulphate. As a preservative 1 gram of sodium hydroxide was added to each litre of sodium thiosulphate solution when it was made up. The sodium azide is used to surpress any possible nitrogen interference in the technique. The factor which appears to limit the level of dissolved oxygen that can be determined by this method is the concentration of Mn+2 ion as the iodide is available in extremely large excess.

moles Mn+2 per litre - 364/169

moles Mn+2 in 0.4 mls. - 0.00086

From the previous relationship 1 mole of Mn+2 utilizes 1 mole (16 grams) of oxygen [O]. Consider a 50 mgm./l. solution of oxygen and a sample size of 54 mls. .

moles oxygen - 0.05 * 0.054/16.0
- 0.000169

Thus the excess of Mn+2 ion is about 5 times and the experimental levels are adequately covered by a solution of this strength. The maximum levels encountered in the experimental work were around 46 mgm./l. .

The actual sampling procedure was as follows : The sampling line was inserted into the volumetric flask so that the tube was slightly above the bottom of the flask. Approximately 2 volumes were allowed to flow and then the sampling line was slowly withdrawn. Prior to sampling the line was purged by allowing a slow flow through the line for a couple of minutes before sampling.

Using a propipette and 3-0.5 ml. pipettes, one for each of the three reagents, 0.5 mls. of manganous sulphate solution were withdrawn and 0.4 mls. ran into the sample with the pipette inserted about 1/2 inch under the liquid surface. Next 0.1 mls. of sodium azide were added at the surface; followed by 0.4 mls. of the alkalai reagent added at the surface as well. The flask was then carefully stoppered so as to exclude air and the entire contents of the flask were throughly mixed by inverting the flask 20-25 times.

When the precipitate had settled the contents were again thoroghly mixed in the same manner as above. After the precipitate had again settled the stopper was removed and 1 ml. of 40% sulphuric acid solution was added by running the acid down the side of the flask. The stopper was replaced and the contents mixed so as to dissolve the precipitate and release the iodine. After sufficient time had passed to allow the iodine to distribute evenly in the sample, a 20 ml. portion was drawn off using a 20 ml. pipette. The 20 mls. were titrated with a solution of sodium thiosulphate approximately 0.0025 N . Through a standardization technique described below the level of dissolved oxygen in the original sample could then be related to the volume of titrant used.

Standardization :

To standardize the dissolved oxygen analysis the following technique was employed. A sample of distilled water was saturated with air at a known temperature and pressure. Tables form the literature [40] provided equilibrium values of dissolved oxygen at specified temperatures and partial pressures of oxygen; these values were then corrected to the conditions of the standardization run. Six samples were collected in volumetric flasks and the procedure of analysis as outlined above was followed.

After titrating these known samples the volume of titrant used could then be related to the level of dissolved oxygen. This procedure was carried out about every 3-4 days during the course of the mass transfer work as only a litre of thiosulphate solution was prepared at a time. The reproducibility of the standardization technique was quite good as indicated by a typical run presented in table A.

Table A

Temperature - 22 C

Barometer - 752.3 mm Hg

Corrected D.O. - 8.70 mgm./l.

Flask No.	Ml. Titrant
#1	8.35
#2	8.35
#3	8.40
#4	8.45
#5	8.45
#6	8.40

Factor - 8.70/8.40 = 1.035 mgm./l. per ml. titrant

This figure for the factor was very consistent and often 4 and sometimes 5 flasks would give the same values for volume of titrant used.

Appendix 4-Analysis of Variance

Bartlett's test for homoscedacticity was carried out on the mass transfer data in order to determine its suitability for non-linear least squares analysis. On the tracer data Bartlett's test showed the data to be unsuited to non-linear least squares analysis and an iterative, weighted, linear least squares technique was used as previously outlined. Results of the test as applied to the mass transfer data are presented in table A. The pertinent formulae and discussion of the method are outlined by Himmelblau ("Process Analysis by Statistical Methods"; John Wiley & Sons, 1970).

Table A

Duplicate	Sampling Position	Variance	Test
#1	#1	0.042	
	#2	1.380	
	#3	2.080	
	#4	0.460	
	#5	0.990	4.75
#2	#1	0.340	
	#2	0.760	
	#3	1.020	
	#4	0.061	
	#5	0.300	3.04
#3	#1	0.900	
	#2	0.430	
	#3	0.870	
	#4	0.095	
	#5	0.170	2.78
#4	#1	0.470	
	#2	0.330	
	#3	1.160	
	#4	0.200	
	#5	0.150	2.23
#5	#1	1.110	
	#2	0.590	
	#3	1.110	
	#4	0.150	
	#5	1.200	1.89

Table A contd.

Duplicate	Sampling Position	Variance	Test
#6	#1	0.340	
	#2	0.300	
	#3	1.220	
	#4	0.730	
	#5	0.420	1.19

The hypothesis in each case was that the variances at each position were independent of their position. At the 95% level of confidence one accepts the hypothesis if the test value is found to be less than 9.48. This, as can be seen, is the case for each of the duplicates.

The same test was then applied over the experimental range by considering the pooled variances calculated from each of the duplicates and the degrees of freedom associated with each. The test value arrived at in this instance was 1.11 which was less than 11.07 and the hypothesis was accepted. Thus the property of homoscedacticity was assumed to apply throughout the experimental range and the non-linear least squares analysis procedure was justified.

Appendix 5-Error

Some mention of error has been made previously as regards the instrument used in the tracer experiments to measure concentrations of tracer. The manufacturers specs give :

Bausch & Lomb Spectronic 20

photometric accuracy - 2.5% of full scale
photometric reproducibility - 1% of full scale

In the section describing the tracer experimental setup, a run was described which indicated 15 minutes to be a reasonable length of time to allow for the attainment of steady-state. Assuming the average reading to be the true value an estimate of the error involved in sampling for the tracer experiments can be established.

average - 55.65 % transmission
max. % error (estimated) - 3.1 %

This value certainly seems to be reasonable in view of the specifications on the equipment used for analysis. The optical cells as mentioned previously proved to be very consistant; they were always within 0.5% at the worst when checked against each other.

Errors involved in measuring the pulsation velocity and setting the liquid and gas flow rates are common to both the tracer and mass transfer work. The gas flow was easily set to the desired setting and held that setting. The pulsations did not cause any noticeable disturbance in the flow meter. Regarding the liquid flow rate the most error here would be in setting up for the highest rate.

The flow rate was determined by measuring the time required to collect a litre of fluid and adjusting the pump accordingly.

Typical is : 16.6 0.2 sec./l.

Around a 2% error could be expexted in the setting of the liquid flow rate. In order to determine the frequency of pulsation the time taken for 10 cycles was measured using a stop watch and this was reproducible to within 0.1 sec. giving a maximum error here of about 2%. The worst error involved in measuring the stroke of pulsation would have to be in the measurement of the smallest stroke used with the measurement of progressively larger strokes showing improved accuracy. The largest error here would be 3/16 inches giving an error of no larger than 7%. The resulting error in the determination of the pulsation velocity should then be no larger than 10%. A summary thus far is given in table A.

Table A

Measurement	Error
tracer concentration	3%
gas flow rate	3%
liquid flow rate	2%
pulsation frequency	2%
pulsation stroke	7%

From the appendix on chemical analysis for dissolved oxygen it can be seen that the error involved is about 1% at 8.7 mgm./l. of dissolved oxygen. Naturally at higher levels the accuracy here could be expected to improve. One form of error in technique could have been the trapping of air bubbles in the sample; however great care was taken to

avoid this and the consistency of the standardization factors would seem to diminish this possibility; also the technique was exactly that used for the mass transfer experiments themselves.

Another point rather difficult to assess is the presence of air in the sampling lines. Care was taken before hand to remove air from the sampling lines. This could be achieved by tapping the lines and driving the air up to the needle valve where slow flow and continued tapping would drive the air out. Bleeding the line with slow flow proir to sampling purged it, and filled it with water representative of the water in the column at that particular point. The flow rate when sampling was adjusted so as not to entrain bubbles in the sampling line; the needle valve provided the control over the sampling flow rate. The time taken to add reagents was about a minute and no signifigant losses of dissolved oxygen were assumed to occur.

Using the repeated runs some feel for the overall experimental error can be established. These repeated runs were used for Bartlett's test for homoscedasticity. Using the position with the largest variance for each repetition an error can be worked out (Table B).

Table B

Duplicate	Position	Error
#1	3	5.2%
#2	3	1.9%
#3	1	2.9%
#4	5	2.0%
#5	5	2.9%
#6	3	2.4%

The assumption of the average being the true value in the case of two replicates may not be very good; however, if one assumes one value to be close to the true value and the other off a maximum overall error of around 10% is arrived at. This would appear to be a reasonable value in view of the other considerations.

In the few mass transfer runs which showed a relatively large residual sum of squares it can be seen that the outlet value of dissolved oxygen is lower than the value in the first sampling position. The model nevertheless forces the outlet value to be close numerically to the value at the first sampling position $dx/dz=0$ @ $z=1.0$. When this "inversion" takes place then the residual sum of squares rises quite high by virtue of this single point alone. In most cases of course there was no problem. It is felt that there are two prime suspects which could possibly account for the "inversions". There was the possibility that a pocket of air might not have been dislodged in the copper fittings at the outlet; the presence of such would no doubt have an effect on the dissolved oxygen levels. The 15-20 minute run time however seems to favor another explanation. The interfacing region between the mass transfer side of the apparatus and the pulsation side may have caused the "inversion". The mixing of the two sides would tend to enrich the pulsation arm with respect to dissolved oxygen while depleting the mass transfer side. The equilibrium value of the concentration was calculated without correcting for holdup. The maximum error involved in this simplification is estimated at 3-4 % using the holdup data of Baird and Garstang [3]. Tap water should have provided a reasonably consistent source of slightly surface-contaminated water and no signifigant effects were to be expected in this regard.

PLATES

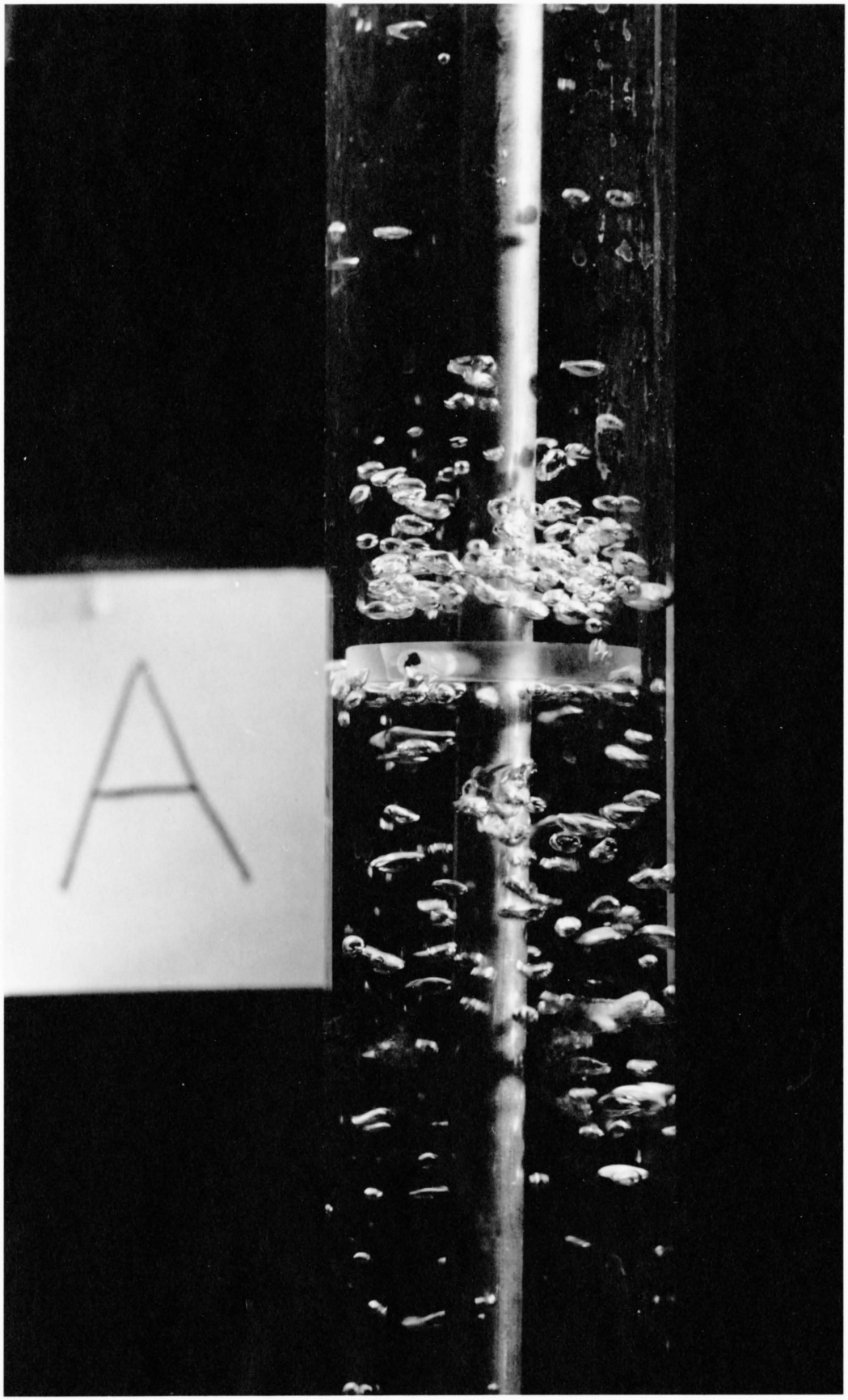

Plate A

Plate B

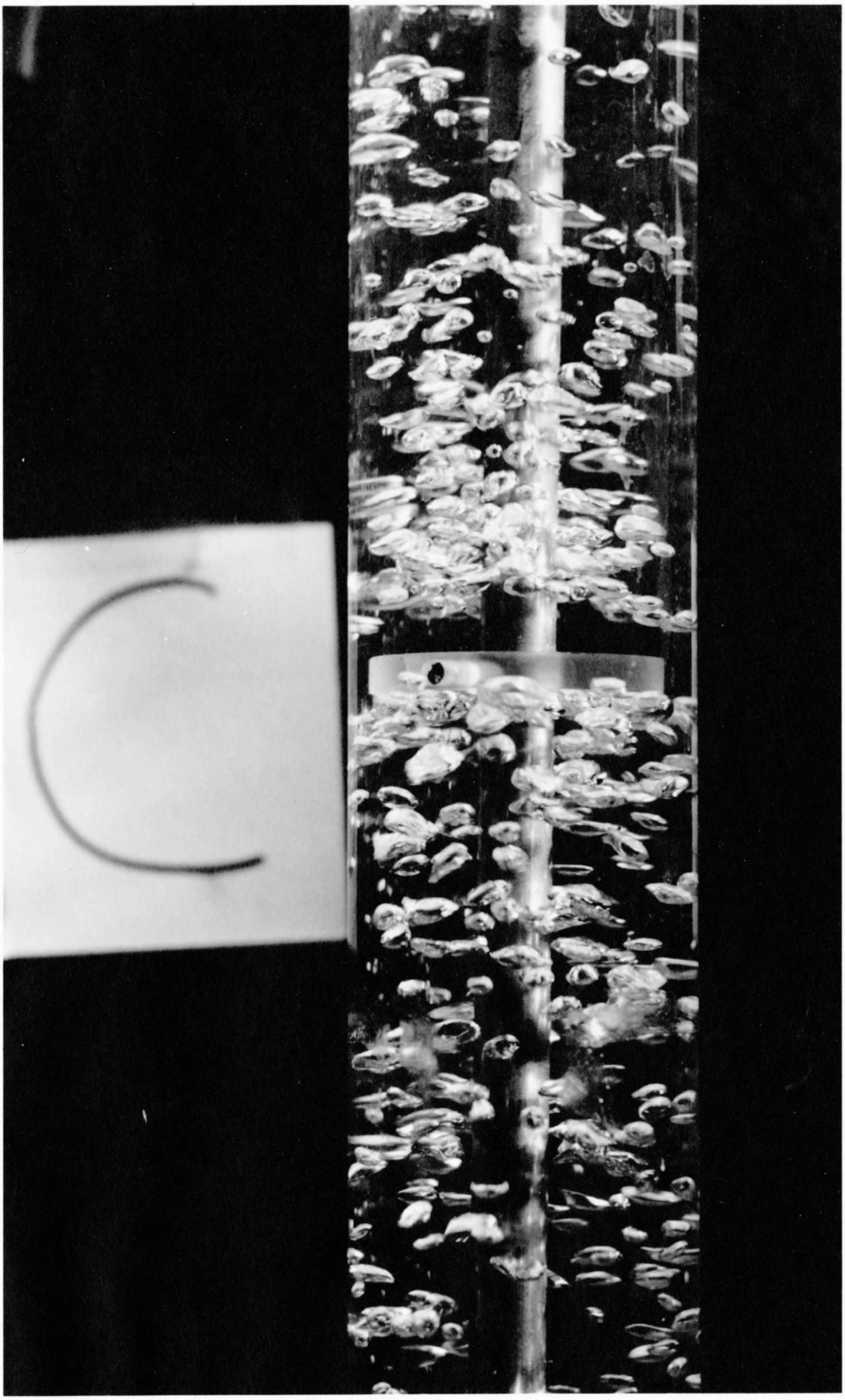

Plate C

Plate D

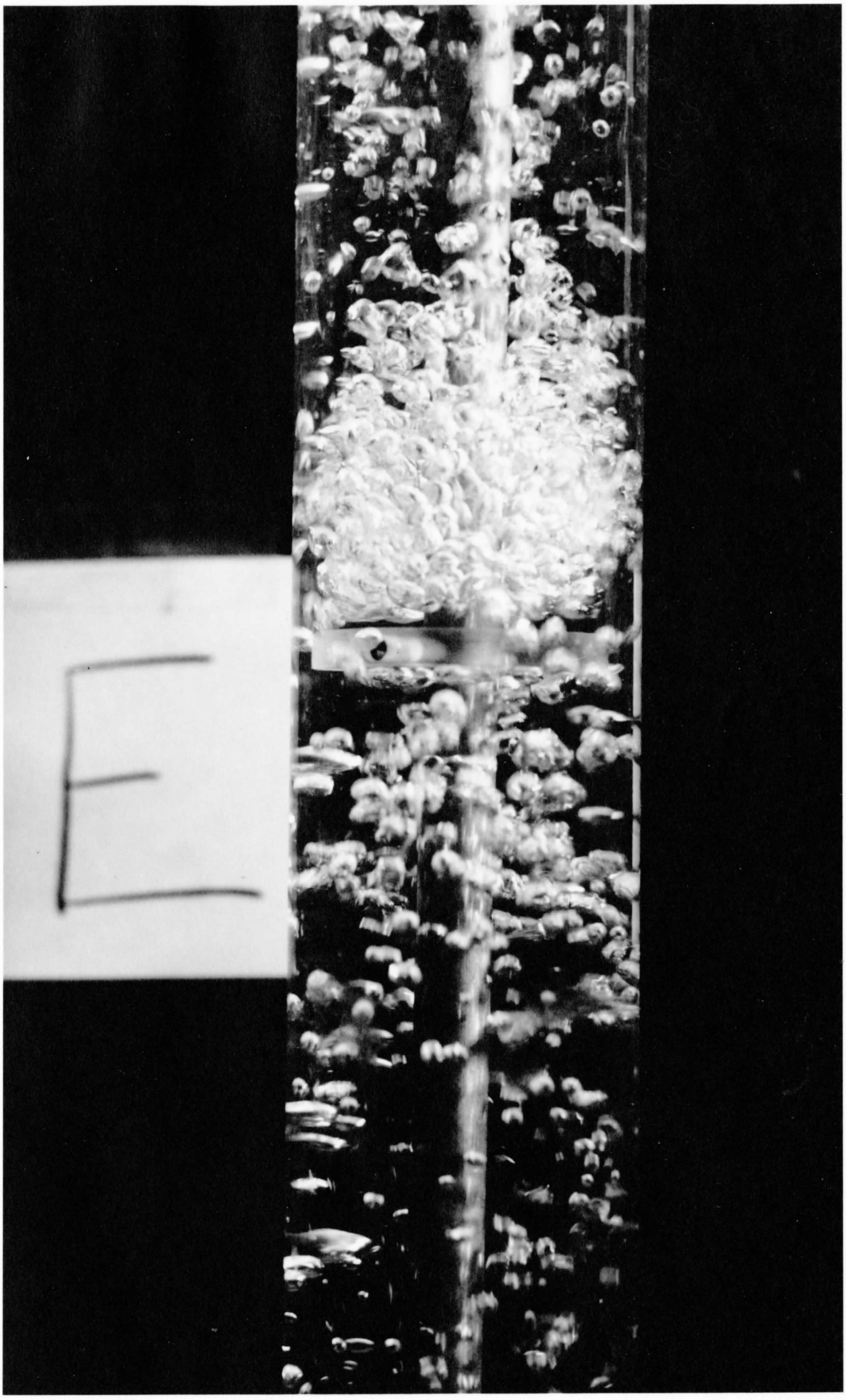

Plate E

Plate G

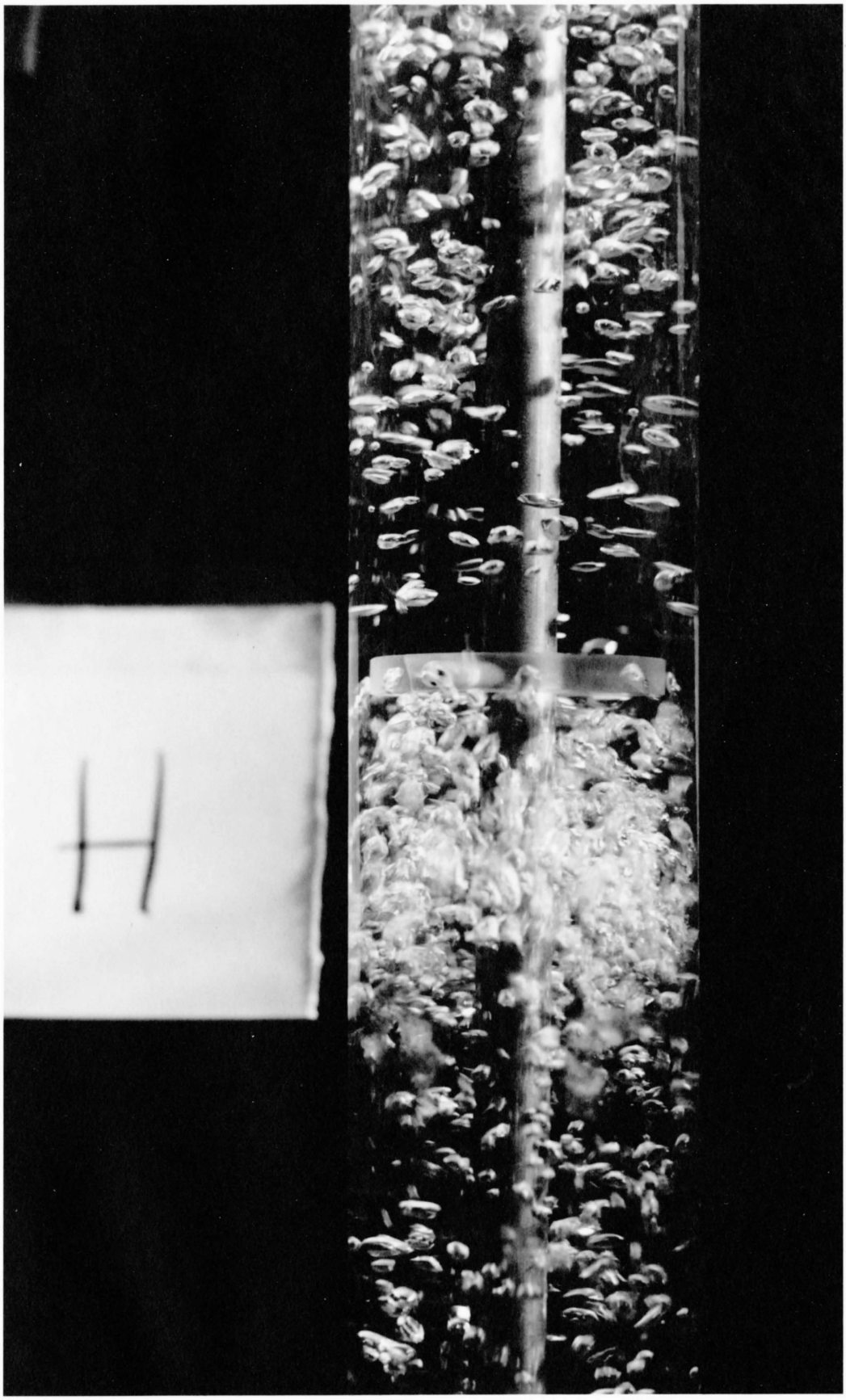

Plate H

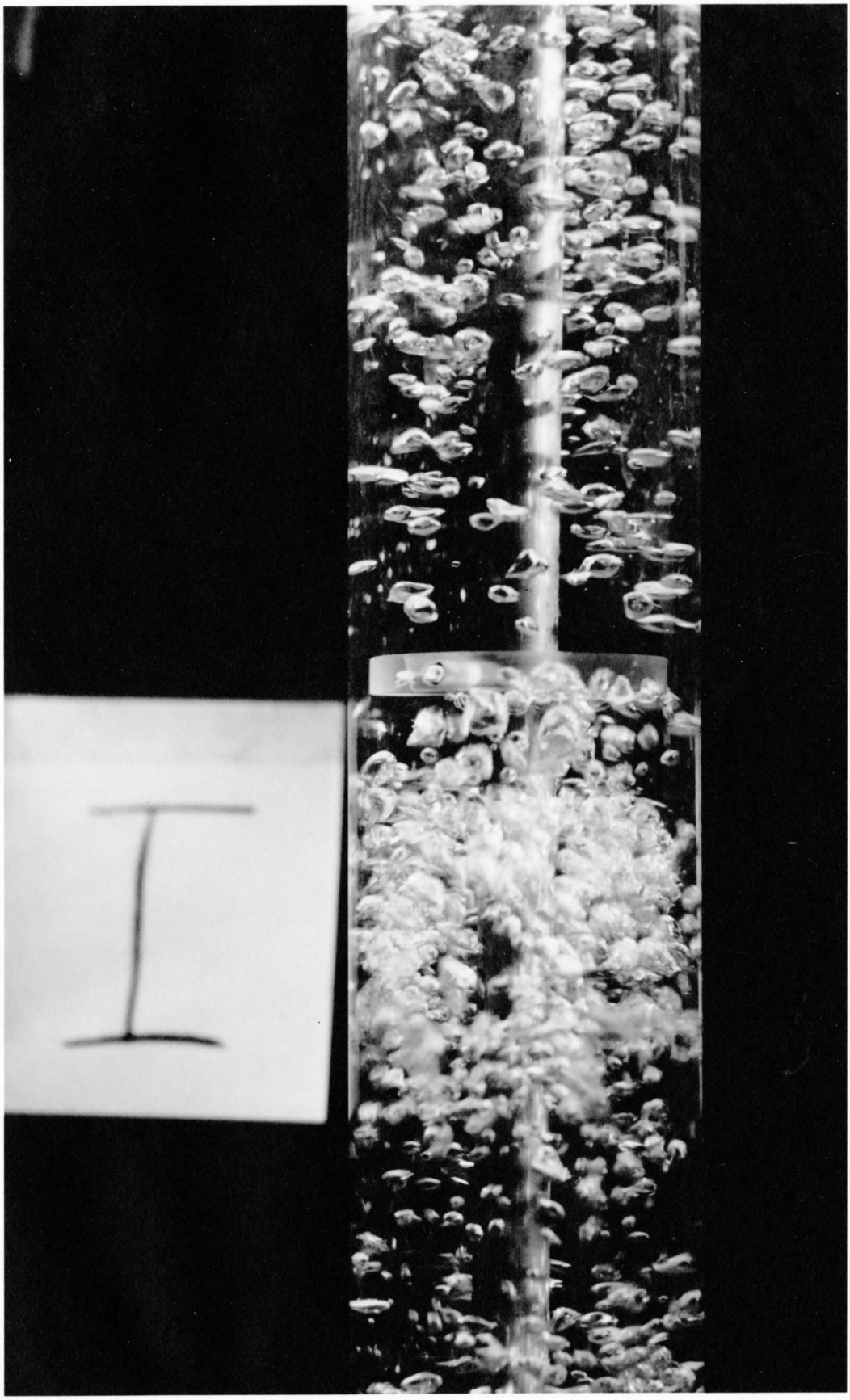

Plate I

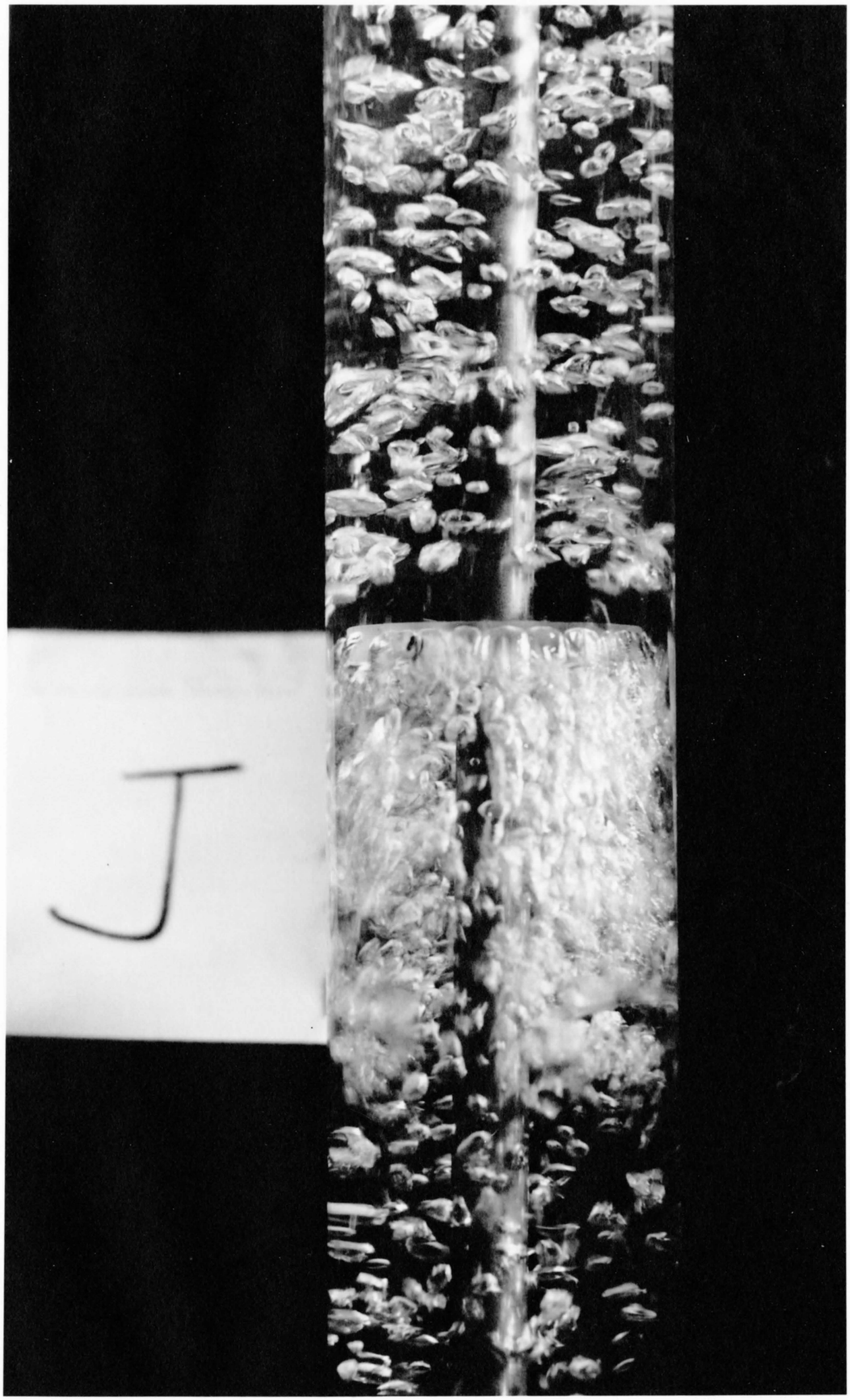

Plate J

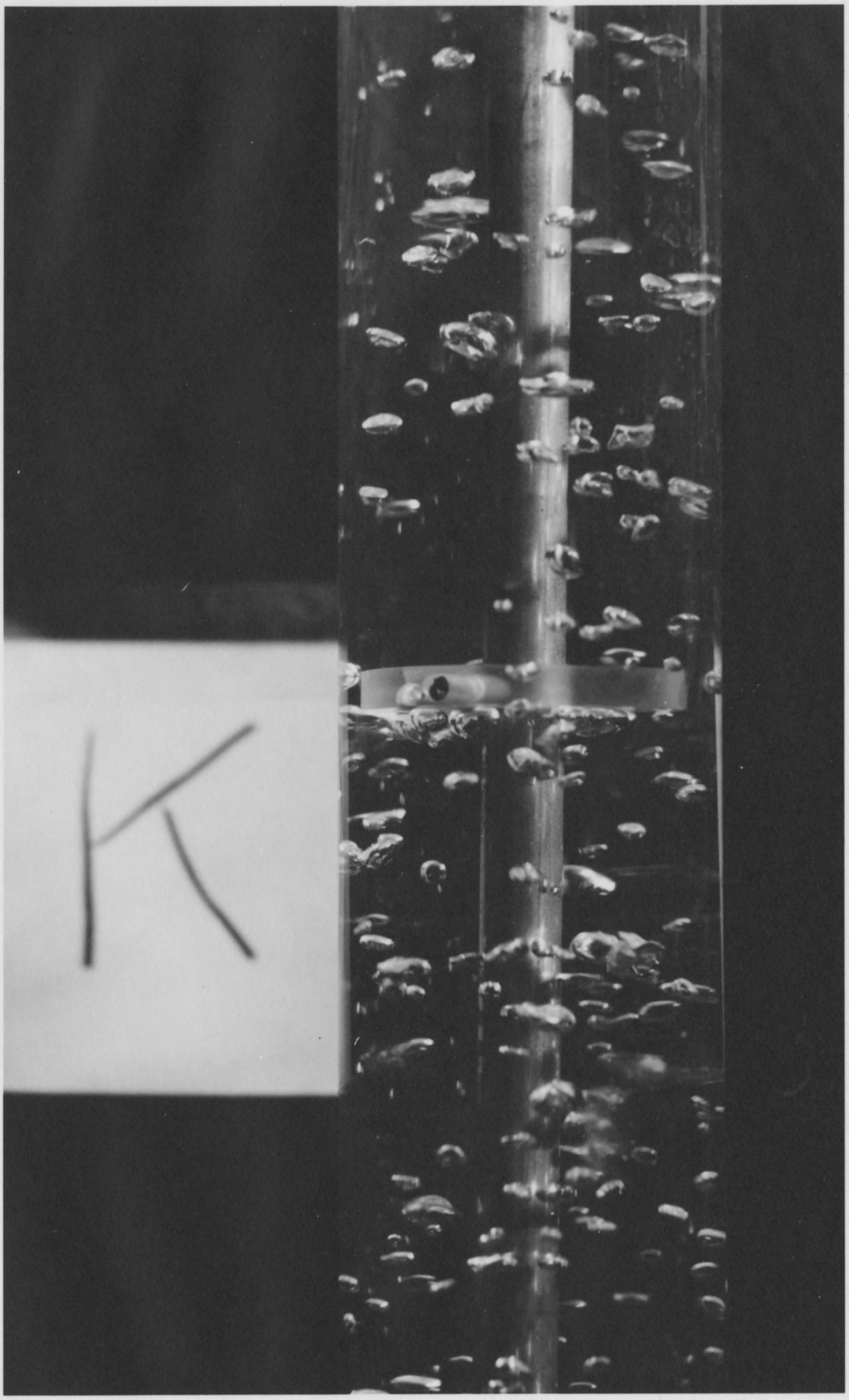

Plate K

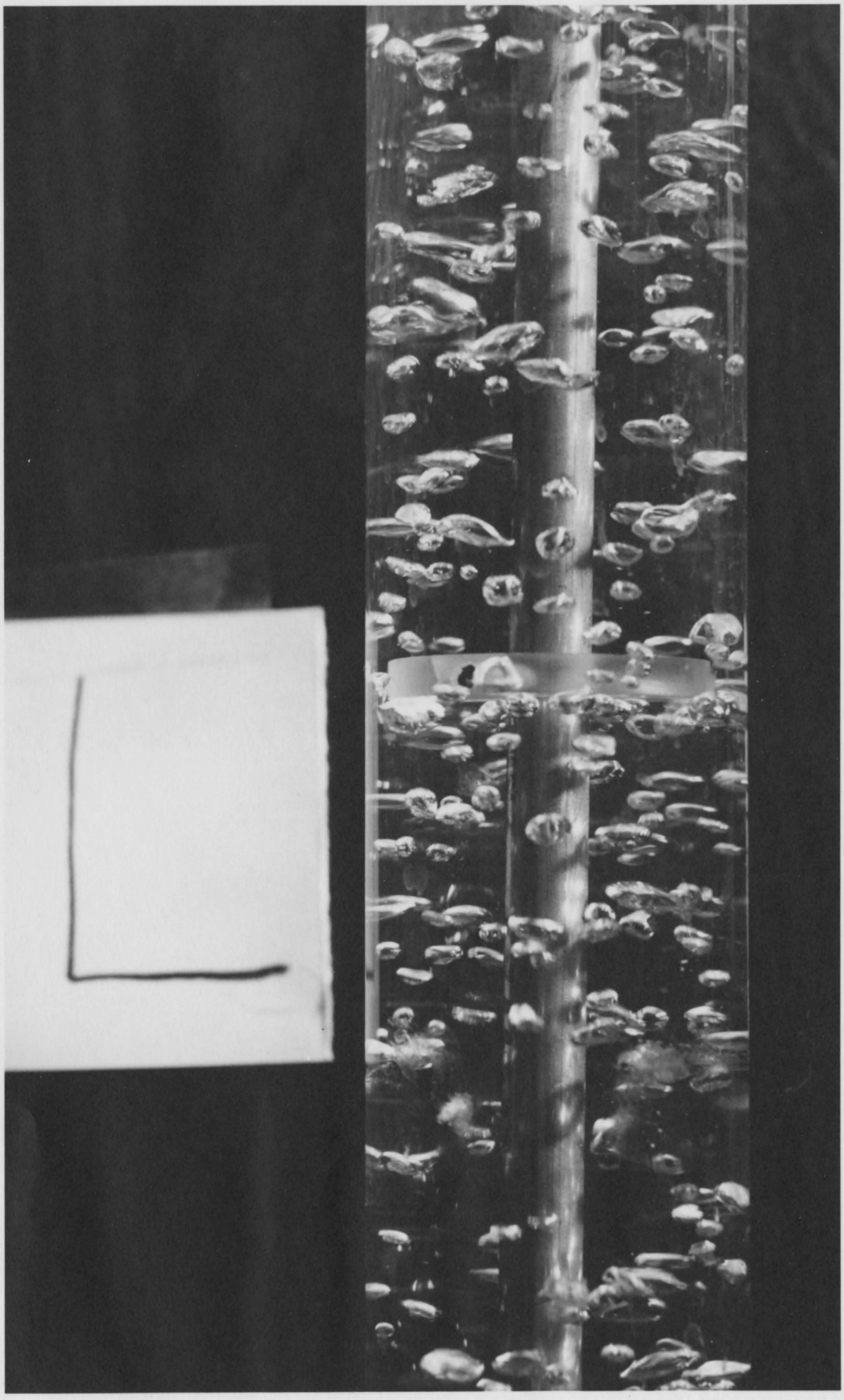

Plate L

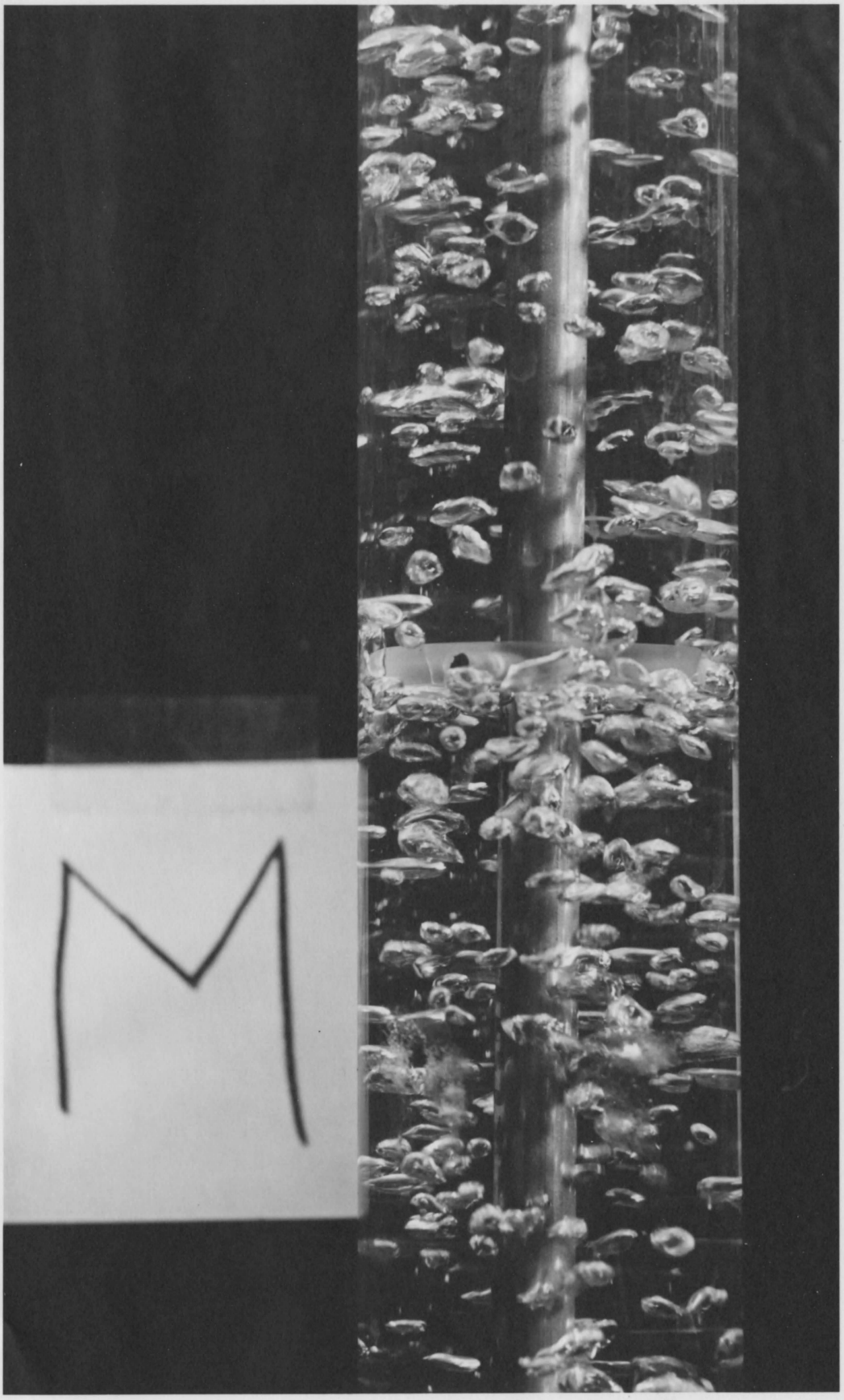

Plate M

TABULATED RESULTS

Run	Pulsation Velocity (cm./sec.)	Gas Velocity (cm./sec.)	Liquid Velocity (cm./sec.)	Oxygen inlet	Concentration Profile (mgm./l.) #1	#2	#3	#4	#5
1	27.0	0.388	1.0	8.26	22.30	31.40	37.90	42.00	44.00
2	39.0	0.388	1.0	8.55	27.40	36.50	41.10	43.60	42.20
3	27.0	0.388	1.0	8.67	22.59	29.74	35.86	41.04	42.59
4	39.0	0.650	1.6	8.52	32.46	37.40	42.69	46.00	46.31
5	27.0	0.388	1.0	8.27	20.00	27.81	35.56	37.47	39.95
6	27.0	0.650	1.6	8.27	26.26	34.01	40.11	43.00	43.31
7	27.0	0.388	1.6	8.27	23.62	29.05	34.01	38.04	38.87
8	27.0	0.650	1.0	7.70	29.13	33.29	39.23	42.97	43.80
9	39.0	0.388	1.0	8.32	26.43	35.69	39.58	42.97	43.91
10	39.0	0.650	1.0	8.22	30.90	38.39	41.51	44.32	45.05
11	39.0	0.388	1.6	7.83	26.52	34.81	39.62	42.08	42.49
12	49.0	0.388	3.0	8.04	21.09	32.25	37.16	39.92	40.24
13	49.0	0.650	3.0	8.24	24.98	34.09	38.90	41.67	41.16
14	49.0	1.165	3.0	8.59	29.23	35 52	40.24	43.51	43.92
15	49.0	0.388	1.6	8.59	26.41	34.90	40.45	43.70	44.20
16	39.0	0.650	1.6	8.28	29.66	37.83	40.76	43.49	43.70
17	49.0	1.165	3.0	8.37	28.40	36.30	41.80	42.30	43.00
18	27.0	0.388	3.0	8.33	20.80	25.80	28.10	34.80	35.60
19	49.0	1.165	1.6	8.23	31.44	38.14	42.13	42.65	43.07
20	27.0	1.165	1.6	8.20	30.00	36.02	38.82	41.84	42.25
21	49.0	0.650	1.0	8.27	27.80	36.25	38.95	41.80	42.20
22	39.0	1.165	1.6	8.25	30.94	37.84	40.49	42.87	43.08

Run	Pulsation Velocity (cm./sec.)	Gas Velocity (cm./sec.)	Liquid Velocity (cm./sec.)	Oxygen inlet	Concentration Profile (mgm./l.) #1	#2	#3	#4	#5
23	27.0	0.388	3.0	8.25	19.31	24.71	29.59	34.26	34.05
24	27.0	0.650	3.0	8.30	21.70	27.51	33.27	37.68	39.14
25	27.0	1.165	3.0	8.37	24.90	30.42	37.37	42.45	42.87
26	39.0	0.388	3.0	8.33	21.25	30.01	35.21	40.84	34.80
27	39.0	0.650	3.0	8.33	23.55	30.52	36.15	39.90	38.55
28	39.0	1.165	3.0	8.33	24.28	34.49	38.76	41.47	41.41
29	27.0	1.165	1.0	8.23	28.86	32.92	38.24	41.15	42.92
30	39.0	1.165	1.0	8.33	30.31	37.68	42.67	43.76	40.84
31	49.0	0.388	1.0	8.30	30.93	34.78	42.04	42.77	39.97
32	49.0	0.650	1.0	8.41	26.58	37.48	40.38	42.15	43.18
33	49.0	1.165	1.0	8.62	30.94	33.84	39.66	42.35	42.25
34	0.0	0.388	1.0	8.62	21.70	24.19	31.35	36.96	40.80
35	0.0	0.650	1.0	8.50	27.35	31.91	35.54	39.99	41.75
36	"	1.165	1.0	8.29	27.35	33.26	39.89	42.58	36.78
37	"	0.388	1.6	8.39	23.93	27.35	30.87	35.12	39.16
38	"	0.650	1.6	8.50	24.14	32.33	37.92	41.86	42.38
39	"	1.165	1.6	8.50	27.04	34.40	38.65	42.48	40.51
40	"	0.388	3.0	8.44	19.08	22.78	25.33	29.50	31.90
41	"	0.650	3.0	8.44	20.32	25.78	30.02	35.34	35.23
42	"	0.650	1.6	8.59	22.80	31.40	36.60	42.30	41.80

Run	$k_L a$ (sec^{-1})	E_L ($cm^2/sec.$)	Reflux Ratio	Residual Sum of Squares
1	0.0119 ± 0.0009	38.52 ± 52.43	0.105	0.220
2	0.0143 ± 0.0042	96.10 ± 65.30	-	7.330
3	0.0098 ± 0.0010	15.90 ± 58.80	0.270	0.384
4	0.0281 ± 0.0065	82.20 ± 303.6	0.257	0.885
5	0.0092 ± 0.0014	40.50 ± 31.80	-	3.140
6	0.0232 ± 0.0026	75.30 ± 44.60	-	1.080
7	0.0143 ± 0.0010	66.30 ± 87.60	0.293	0.155
8	0.0166 ± 0.0054	32.10 ± 257.3	0.736	1.910
9	0.0170 ± 0.0024	59.00 ± 32.10	0.520	1.260
10	0.0265 ± 0.0040	97.70 ± 47.20	-	0.876
11	0.0225 ± 0.0034	107.8 ± 70.20	-	1.910
12	0.0324 ± 0.0092	138.6 ± 168.3	-	7.530
13	0.0376 ± 0.0082	200.2 ± 176.7	-	4.480
14	0.0443 ± 0.0024	258.9 ± 146.4	0.018	0.078
15	0.0261 ± 0.0022	73.30 ± 28.70	-	0.478
16	0.0298 ± 0.0065	174.5 ± 122.0	-	2.690
17	0.0490 ± 0.0138	280.2 ± 269.7	-	5.240
18	0.0170 ± 0.0065	36.10 ± 635.5	0.424	4.150
19	0.0338 ± 0.0099	263.6 ± 213.5	-	3.750
20	0.0264 ± 0.0026	235.0 ± 71.70	-	0.600
21	0.0148 ± 0.0032	103.9 ± 75.90	-	3.370
22	0.0302 ± 0.0055	250.9 ± 133.0	-	1.760
23	0.0167 ± 0.0026	152,9 ± 355.8	0.065	0.947
24	0.0235 ± 0.0020	66.60 ± 155.3	0.239	0.256
25	0.0316 ± 0.0091	72.20 ± 564.8	0.186	2.930
26	0.0233 ± 0.0100	203.1 ± 403.3	-	28.37
27	0.0260 ± 0.0040	222.9 ± 143.2	-	3.140
28	0.0333 ± 0.0082	181.9 ± 204.5	-	6.820
29	0.0145 ± 0.0032	15.30 ± 151.3	0.827	0.859
30	0.0224 ± 0.0026		0.327	4.260
31	0.0171 ± 0.0087	162.3 ± 251.3	-	14.30
32	0.0167 ± 0.0064	64.30 ± 100.6	-	9.590
33	0.0147 ± 0.0060	82.60 ± 432.8	0.675	2.810

Run	$k_L a$ (sec^{-1})	E_L ($cm^2/sec.$)	Reflux Ratio	Residual Sum of Squares
34	0.0073	1.830	0.243	12.40
35	0.0114	1.600	0.826	0.477
36	0.0128 $\pm$ 0.0078	121.7 $\pm$ 248.9	-	28.10
37	0.0112	2.350	0.585	3.740
38	0.0198 $\pm$ 0.0015	71.50 $\pm$ 19.30	-	0.287
39	0.0219 $\pm$ 0.0052	153.5 $\pm$ 127.0	-	4.510
40	0.0123	2.290	0.501	0.787
41	0.0177 $\pm$ 0.0034	116.9 $\pm$ 400.2	0.184	1.320
42	0.0258 $\pm$ 0.0048	168.6 $\pm$ 453.8	0.066	1.250
43	0.0180 $\pm$ 0.0023	54.40 $\pm$ 44.30	-	1.950

Run	Pulsation Velocity (cm./sec.)	Gas Velocity (cm./sec.)	Liquid Velocity (cm./sec.)	c/c_o Profile #1	#2	#3
1	39.0	0.0	1.6	0.0102	0.0207	0.0154
2	0.0	0.388	1.0	0.0256	0.0256	0.0314
3	55.4	0.0	1.6	0.0155	0.0077	0.0005
4	55.4	0.388	1.6	0.0767	0.0077	0.0002
5	55.4	0.650	1.6	0.1103	0.0103	0.0009
6	55.4	1.165	1.6	0.1396	0.0144	0.0015
7	52.2	0.0	0.705	0.0880	0.0118	0.0059
8	51.0	0.388	0.705	0.1448	0.0232	0.0080
9	49.0	0.650	0.705	0.2226	0.0607	0.0403
10	49.0	1.165	0.705	0.2607	0.1273	0.1182
11	0.0	0.388	"	0.0434	0.0368	0.0315
12	0.0	0.650	"	0.1309	0.1401	0.1494
13	0.0	1.165	"	0.5270	0.1002	0.0148
14	0.0	0.388	1.0	0.0107	0.0132	0.0189
15	"	0.650	1.0	0.0782	0.0687	0.0734
16	39.0	0.388	1.0	0.0250	0.0005	0.0001
17	39.0	0.650	"	0.0685	0.0025	0.0001
18	39.0	1.165	"	0.1281	0.0144	0.0049
19	27.0	0.388	0.705	0.0706	0.0652	0.0619
20	27.0	0.650	0.705	0.1778	0.1819	0.1593
21	27.0	1.165	0.705	0.2559	0.2657	0.2800

Run	Pulsation Velocity (cm./sec.)	Gas Velocity (cm./sec.)	Liquid Velocity (cm./sec.)	c/c_o Profile #1	#2	#3
22	39.0	0.388	0.705	0.1617	0.2001	0.0049
23	39.0	0.650	"	0.1715	0.1513	0.1481
24	39.0	1.165	"	0.2840	0.0754	0.0200
25	49.0	0.0	"	0.0794	0.0098	0.0024
26	49.0	0.388	"	0.3902	0.0829	0.0169
27	49.0	0.650	"	0.2179	0.0550	0.0342
28	49.0	1.165	"	0.2537	0.1320	0.1226
29	"	0.388	"	0.0800	0.0025	0.0002
30	"	0.650	"	0.1129	0.0211	0.0140
31	"	1.165	"	0.2571	0.0990	0.0850
32	"	0.650	"	0.1897	0.0410	0.0386
33	"	0.0	"	0.1117	0.0048	0.0010
34	"	0.388	"	0.1410	0.0089	0.0049
35	"	0.650	"	0.1955	0.0454	0.0247
36	"	1.165	"	0.6863	0.3609	0.1073
37	"	0.650	"	0.2520	0.0814	0.0426
38	"	0.0	"	0.0932	0.0047	0.0002
39	"	0.388	"	0.4322	0.0913	0.0095
40	"	0.650	"	0.5901	0.1890	0.0345
41	"	1.165	"	0.2498	0.1068	0.0882
42	"	0.0	"	0.0861	0.0048	0.0003

Run	Pulsation Velocity (cm./sec.)	Gas Velocity (cm./sec.)	Liquid Velocity (cm./sec.)	c/c_o Profile #1	#2	#3
43	49.0	0.388	0.705	0.4631	0.0877	0.0098
44	"	0.650	"	0.6447	0.2229	0.0444
45	"	1.165	"	0.2886	0.1274	0.1120
46	"	0.0	"	0.0858	0.0044	0.0003
47	"	0.388	"	0.4553	0.1033	0.0149
48	"	0.650	"	0.2343	0.0599	0.0419
49	"	1.165	"	0.2877	0.1345	0.1186
50	27.0	0.0	"	0.0074	0.0074	0.0049
51	27.0	0.388	"	0.0937	0.0937	0.0997
52	27.0	0.650	"	0.1554	0.1554	0.1487
53	"	1.165	"	0.2431	0.2431	0.2684
54	"	0.388	"	0.0790	0.0736	0.0785
55	"	0.650	"	0.1642	0.1735	0.1642
56	"	1.165	"	0.2535	0.2681	0.2849
57	39.0	0.0	"	0.0711	0.0603	0.0657
58	39.0	0.388	"	0.0724	0.0237	0.0141
59	"	0.650	"	0.2017	0.1290	0.1511
60	"	1.165	"	0.2895	0.2600	0.2600
61	"	0.0	"	0.0550	0.0499	0.0578
62	"	0.388	"	0.1172	0.0445	0.0292
63	"	0.650	"	0.1750	0.1420	0.1582

Run	Pulsation Velocity (cm./sec.)	Gas Velocity (cm./sec.)	Liquid Velocity (cm./sec.)	c/c_o Profile #1	#2	#3
64	39.0	1.165	0.705	0.2651	0.2521	0.2481
65	0.0	0.388	"	0.0662	0.0761	0.0743
66	0.0	0.650	"	0.0906	0.0048	0.0002
67	"	1.165	"	0.8953	0.1887	0.0155
68	"	0.388	"	0.0990	0.0932	0.1048
69	"	0.650	"	0.1925	0.2113	0.1896
70	"	1.165	"	1.0000	0.2581	0.2609

Run	E_L ($cm^2./sec.$)	Reflux Ratio	Dispersion Number
1	11.70	0.016	1.44
2	12.50	0.029	1.52
3	31.55 ± 13.1	-	3.85
4	39.52 ± 0.82	-	4.80
5	42.57 ± 3.60	-	5.20
6	43.65 ± 3.93	-	5.30
7	16.94 ± 1.95	0.005	4.70
8	21.86 ± 1.05	0.005	6.10
9	23.56 ± 4.21	0.038	6.55
10	23.11 ± 3.23	0.139	6.45
11	6.0	0.039	1.68
12	8.0	0.163	2.24
13	30.73 ± 8.20	-	8.10
14	6.85	0.010	1.35
15	9.50	0.079	1.87
16	16.16 ± 1.07	-	3.18
17	20.67 ± 2.21	-	4.06
18	26.55 ± 2.23	0.004	5.25
19	6.50	0.072	1.82
20	8.10	0.210	2.26
21	9.50	0.300	2.65
22	23.73 ± 4.19	-	6.60
23	23.04 ± 10.5	0.179	6.40
24	32.83 ± 1.23	-	9.15
25	19.53 ± 4.67	-	5.45
26	31.92 ± 8.77	-	8.90
27	24.10 ± 3.69	0.031	6.75
28	28.02 ± 4.38	0.140	7.80
29	14.05 ± 2.63	-	3.90
30	18.51 ± 1.80	0.013	5.15
31	26.65 ± 4.04	0.086	7.45
32	17.60 ± 6.25	0.041	4.90

Run	E_L (cm^2/sec.)	Reflux Ratio	Dispersion Number
33	18.06 ± 4.50	-	5.05
34	19.08 ± 4.34	0.003	5.35
35	23.92 ± 2.60	0.021	6.66
36	41.38 ± 17.8	-	9.40
37	26.99 ± 11.2	-	7.55
38	16.38 ± 3.58	-	4.60
39	30.54 ± 12.8	-	8.50
40	42.82 ± 18.8	-	11.9
41	21.55 ± 6.13	0.095	6.00
42	15.13 ± 1.98	-	4.27
43	30.44 ± 12.9	-	8.50
44	46.68 ± 21.7	-	13.0
45	25.18 ± 5.83	0.122	7.00
46	15.12 ± 1.82	-	4.20
47	33.19 ± 13.1	-	9.70
48	23.23 ± 4.60	0.004	6.48
49	28.63 ± 5.80	0.125	7.00
50	4.70	0.020	1.35
51	7.05	0.105	2.00
52	9.50	0.180	2.65
53	9.90	0.336	2.77
54	6.70	0.084	1.87
55	8.35	0.200	2.33
56	10.4	0.368	2.90
57	6.50	0.071	1.82
58	18.61 ± 2.56	0.013	5.20
59	8.20	0.188	2.33
60	10.3	0.370	2.88
61	6.20	0.056	1.74
62	21.49 ± 3.18	0.028	5.80
63	8.20	0.190	2.30
64	6.75	0.086	1.90

Run	E_L (cm^2./sec.)	Reflux Ratio	Dispersion Number
65	10.0	0.342	2.80
66	16.29 $\pm$ 2.70	-	4.55
67	38.43 $\pm$ 23.3	-	10.7
68	7.15	0.110	2.00
69	8.90	0.246	2.50
70	45.01 $\pm$ 28.5	-	12.5

Nomenclature

A ..... amplitude
a ..... specific interfacial area
c ..... tracer concentration
c ..... concentration of a chemical species (intro)
c_i ..... inlet tracer concentration
c_o ..... outlet " "
c_Q ..... oxygen equilibrium concentration, atmospheric conditions
D_T ..... column diameter
E_L ..... axial dispersion coefficient
E ..... efficiency
f ..... freqency
h ..... column position
H ..... height between air stone and water level in column
J_T ..... total power dissapation per unit volume
k_L ..... liquid film mass transfer coefficient
k_La ..... volumetric mass transfer coefficient
NTU_L ..... number of transfer units
Q ..... volumetric flow rate
q ..... reflux superficial velocity
R ..... reflux ratio
S ..... column cross sectional area
s ..... slope of oxygen equilibrium line
T ..... transmittance
T_o ..... reference transmittance
U_L ..... superficial liquid velocity
U_G ..... " gas "
w ..... angular frequency
wA ..... pulsation velocity
x ..... oxygen concentration
x_i ..... inlet oxygen concentration
x_o ..... outlet " "

x^* ..... equilibrium oxygen concentration
x_p ..... particular integral equa. 5.4
x_c ..... complementry function " "
y ..... variable equa. 6.7, c/c_o - R/R+1
z ..... dimensionless column position